ETHANOL FROM PHOTOPERIOD-SENSITIVE SORGHUM: A STUDY ON BIOMASS STRUCTURE AND PROCESS OPTIMIZATION

by

FENG XU

B.S., JiangNan University, China, 2003
M.S., JiangNan University, China, 2006

AN ABSTRACT OF A DISSERTATION

submitted in partial fulfillment of the requirements for the degree

DOCTOR OF PHILOSOPHY

Department of Biological and Agricultural Engineering
College of Engineering

KANSAS STATE UNIVERSITY
Manhattan, Kansas

2012

Abstract

Cellulosic ethanol made from low cost lignocellulosic biomass has been considered as new generation transportation fuel with economic and environmental advantages. Photoperiod-sensitive (PS) sorghum, because of its high biomass yield (2.6 kg dry mass/m^2), about 18% of soluble sugar in dry mass, and drought tolerance, is a promising biomass for ethanol production. The overall goals of this study are to develop an efficient approach to convert PS sorghum to ethanol and to understand the structural characteristics of biomass. For increasing the efficiency of biomass conversion, an integrated method, using diluted sulfuric acid pretreatment, has been developed to utilize both the structural polysaccharide (cellulose) and the soluble sugar (sucrose, glucose, and fructose) for fermentation. Response surface methodology was employed to optimize the pretreatment condition for maximizing the cellulose-glucose conversion. Simultaneous enzymatic hydrolysis and yeast fermentation was used for ethanol production. The effects of the buffer concentration, the inoculation dosage and time, and the fermentation temperature were investigated for maximizing ethanol yield. A total conversion efficiency of 77.2% and an ethanol concentration of 2.3% (v/v) were obtained after 72 h fermentation. About 210 kg (~266 Liters) ethanol could be produced from one ton dry mass of PS sorghum under the optimized condition.

The structural features of the PS sorghum were studied using techniques including scanning electron microscopy and X-ray diffraction/scattering. Biomass at different botanic locations was investigated. Wide-angle X-ray diffraction (WAXD) study showed that the PS sorghum rind had oriented crystal peaks and the highest degree of crystallinity, whereas the crystalline structures of the inner pith and leaf were less ordered. The results from WAXD suggested that crystalline cellulose was melted at 120 °C before its significant degradation. Both the cellulose crystallinity and the crystal size at the dimension lateral to fiber direction increased as the temperature increased from 120 to 160 °C. The efficiency of enzymatic hydrolysis increased because the protective structure was damaged and most hemicellulose was removed, resulting in the increase in accessible area as suggested by small-angle X-ray scattering result of the increased length of microvoids. The results from WAXD also suggested a simultaneous hydrolysis and crystallization of cellulose by acid.

ETHANOL FROM PHOTOPERIOD-SENSITIVE SORGHUM: A STUDY ON BIOMASS STRUCTURE AND PROCESS OPTIMIZATION

by

FENG XU

B.S., JiangNan University, China, 2003
M.S., JiangNan University, China, 2006

A DISSERTATION

submitted in partial fulfillment of the requirements for the degree

DOCTOR OF PHILOSOPHY

Department of Biological and Agricultural Engineering
College of Engineering

KANSAS STATE UNIVERSITY
Manhattan, Kansas

2012

Approved by:

Co-Major Professor
Dr. Donghai Wang

Approved by:

Co-Major Professor
Dr. Yong-Cheng Shi

Copyright

Abstract

Cellulosic ethanol made from low cost lignocellulosic biomass has been considered as new generation transportation fuel with economic and environmental advantages. Photoperiod-sensitive (PS) sorghum, because of its high biomass yield (2.6 kg dry mass/m^2), about 18% of soluble sugar in dry mass, and drought tolerance, is a promising biomass for ethanol production. The overall goals of this study are to develop an efficient approach to convert PS sorghum to ethanol and to understand the structural characteristics of biomass. For increasing the efficiency of biomass conversion, an integrated method, using diluted sulfuric acid pretreatment, has been developed to utilize both the structural polysaccharide (cellulose) and the soluble sugar (sucrose, glucose, and fructose) for fermentation. Response surface methodology was employed to optimize the pretreatment condition for maximizing the cellulose-glucose conversion. Simultaneous enzymatic hydrolysis and yeast fermentation was used for ethanol production. The effects of the buffer concentration, the inoculation dosage and time, and the fermentation temperature were investigated for maximizing ethanol yield. A total conversion efficiency of 77.2% and an ethanol concentration of 2.3% (v/v) were obtained after 72 h fermentation. About 210 kg (~266 Liters) ethanol could be produced from one ton dry mass of PS sorghum under the optimized condition.

The structural features of the PS sorghum were studied using techniques including scanning electron microscopy and X-ray diffraction/scattering. Biomass at different botanic locations was investigated. Wide-angle X-ray diffraction (WAXD) study showed that the PS sorghum rind had oriented crystal peaks and the highest degree of crystallinity, whereas the crystalline structures of the inner pith and leaf were less ordered. The results from WAXD suggested that crystalline cellulose was melted at 120 °C before its significant degradation. Both the cellulose crystallinity and the crystal size at the dimension lateral to fiber direction increased as the temperature increased from 120 to 160 °C. The efficiency of enzymatic hydrolysis increased because the protective structure was damaged and most hemicellulose was removed, resulting in the increase in accessible area as suggested by small-angle X-ray scattering result of the increased length of microvoids. The results from WAXD also suggested a simultaneous hydrolysis and crystallization of cellulose by acid.

Table of Contents

List of Figures

List of Tables

Acknowledgements

First and foremost I want to thank my advisor, Dr. Donghai Wang. I appreciate his contribution of time, thoughtful guidance, and support for my Ph.D. research. I am so grateful for his idea and experience that motivated me during the study. As an excellent example of mentor, he taught me work in a professional way and gave me opportunities to attend those academic activities. It is his guidance and patience that help me through the tough time during the Ph.D. pursuit.

I also want to thank my co-advisor, Dr. Yong-Cheng Shi. I appreciate his idea and encouragement that enlightened me throughout my Ph.D. program. His enthusiasm stimulated me to keep thinking and searching.

I thank other professors of my supervisory committees, Dr. Ron Madl and Dr. Scott Staggenborg, for their precious time and valuable suggestions. I also want to thank Dr. Keith Hohn for being willing to serve as the chairperson of the examination committee.

I thank the faculty and staff in my department: Dr. Joseph P. Harner, Department Head; Dr. Naiqian Zhang, Graduate Program Director; Ms. Barb Moore, Mr. Randy Erickson, Mr. Darrel Oard, Ms. Lou Ann Claassen, and Ms Cindy Casper for their administrative assistance and technical support.

I thank Dr. Xiaorong Wu for providing so much suggestion and discussion during my research. I thank my other group members: Dr. Karnnalin Theerarattananoon, Dr. Liming Cai, Ms. Yanjie Bai, Ms. Leidy Pena Duque, Mr. Ningbo Li, Mr. Ke Zhang, Ms. Kristen, and Dr. Shuping Yan for their help during my research.

I would like to thank Drs. Jun Wang, Benjamin S. Hsiao, and Lixia Rong for their assistance in X-ray measurement in Brookhaven National Laboratory.

I thank the Center for Sustainable Energy for its support to this research.

I thank all the friends in my life, including my office-mates, and the international friends in K-State. It is those good friends that make my life splendid.

I am so grateful to K-state community for the excellent academic environment.

I wish to express deep appreciate to my family for their love and support.

Dedication

To my beloved family

To the People's Republic of China

Chapter 1 - Introduction

1.1 Background

1.1.1 Next generation biofuels from lignocellulosic biomass

Energy shortage and carbon dioxide emission have become serious issues to our sustainable economic development and environment (Fargione et al. 2008). Renewable fuels that are produced from plants and harvested annually could help ensure a more sustainable future and reduce carbon dioxide emissions. First-generation biofuels, including starch-based and sugar-based ethanol, are well developed and show good performance when mixed with gasoline. However, most substrates used for these biofuels are food resources, and the overuse of crop starch for ethanol will eventually result in competition with food and feed production for limited land (Tilman et al. 2006). Lignocellulosic biomass, with advantages of low-cost, renewable and abundant, has become a promising resource and has attracted much focus (Rubin 2008). Although corn stover has been considered as a major agricultural waste for biofuels production in the US, its annual yield (200 million tons) is not sufficient to meet the future demand (2022: 133 billion Liters) of biomass conversion without other biomass, such as sorghum biomass.

1.1.2 Photoperiod sensitive (PS) sorghum

Different alternative energy feedstocks have been used for studying the potential for biofuel production. Corn stover, one of the most important agricultural residues in the Corn Belt, can be harvested annually at a yield of 200 million tons, but only about 30% of this amount could be collected at a low cost without affecting soil quality (Graham et al. 2007). Sorghum is another important grain crop; it is a renewable resource that currently is grown on 6 to 10 million acres in the United States (data from National Agricultural Statistics Service, 2010). Sorghum is a tropical grass grown primarily in semiarid parts of the world. Sorghum cannot compete successfully with corn as a cereal crop in an agro-ecosystem with 900 mm of annual rainfall, but corn cannot compete with sorghum in areas that receive less than 900 mm of rainfall.

Photoperiod sensitive sorghum, which can grow in the semiarid area that is too dry for corn growth, is a high-energy sorghum, because it can accumulate increased levels of vegetative

dry mass with little or no grain production. Photoperiod sensitive sorghum produces much more dry mass per acre (80 Mg ha^{-1}, 65% moisture content) than corn (McCollum III et al. 2005), suggesting that PS sorghum biomass has great potential for cellulosic biofuel production. However, research on utilization of PS sorghum has barely been reported. Our recent studies showed that PS sorghum has another advantage: the significant amount of soluble sugar it contains could be converted to ethanol directly by fermentation. Thus, an integrated processing approach needs to be developed for efficiently converting both soluble and structural sugars to ethanol. One of the objectives of this research is to design and optimize the process from PS sorghum to ethanol.

1.1.3 Biomass structure

The natural structure of plant cell wall is excellently "designed". Functionally, the cell wall provides a rigid barrier that prevents the cell from outside erosion and allows turgor that is the motive force of cell expansion (Ray et al. 1972). The composition of cell wall varies in different biomass and even in different part of a certain biomass, which makes it possible to realize the different functions (Duguid et al. 2009). Primary and secondary walls are found to play different roles (Giddings et al. 1980). For example, primary wall, which contains about 1-10% of cellulose, allows cell expansion; while secondary wall provides a barrier against potential pathogens (Hernandez-Blanco et al. 2007). There are three main components in plant cell wall: cellulose, hemicellulose and lignin (Table 1.1). The complicated 3D structure of cell wall is not clarified yet (Monro et al. 1976). Since the cell wall naturally prevents attack from the environment, it could be one of the reasons why it is challenging to break up the cell and separate those components.

Cellulose, the main structure component in cell wall, is a long chain of more than hundreds of glucose molecules with β (1-4) glycosidic linkage (Kraessig 1993). The glucan chains usually are connected by hydrogen bonds to form microfibrils in cell walls. Most cellulose parts in plant cells have been considered as crystallite due to highly ordered repeating units, which make it possible to use XRD to analyze the crystalline structure. Since glucose degraded from the renewable cellulose source is an excellent substrate for most industrial microorganisms, cellulose becomes attractive for biofuel (ethanol) and polymer (polylactic acid) production (Gupta et al. 2007). Hemicellulose has different structural characteristics compared

with cellulose and is noncovalently connected with cellulose microfibrils with hydrogen bonds (Tolbert 1980). The bond is very strong, which makes it difficult to obtain purified cellulose from plant cell without cellulose loss (Haigler 1985). Hemicellulose is a complex of different polysaccharides (linked polymers of glucose, mannose and xylose, etc.) and the finer details of the structure of hemicellulose are still unknown. Hemicellulose in lignocellulosic biomass could be removed and degraded to mono-saccharides with acid treatment (Esteghlalian et al. 1997), and the mixture of pentose and hexose is a valuable sugar source for production of bioethanol and other bioproducts. Researchers in genetic and metabolic engineering already have enabled utilizing both hexose and pentose with one single strain of microbe (Ho et al. 1998). Lignin is amorphous phenolic polymers with molecular weight of about 11,000 (Barnett 1981). Both aliphatic and aromatic constituents are found in lignin. It is widely accepted that the biosynthesis of lignin stems from the polymerization of three types of phenylpropane units, also referred to as monolignols (Whetten et al. 1998). They are p-coumaryl alcohol, coniferyl alcohol, and sinapyl alcohol (El Mansouri and Salvadó 2007), which give rise to the p-hydroxyphenyl (H), guaiacyl (G), and syringyl (S) units of the lignin polymer, respectively. However, the exact native structure of lignin is still unknown. Lignin is a competitive inhibitor in cellulase hydrolysis because cellulase could be irreversibly absorbed by lignin (Palmqvist et al. 1996), which explain why lignin removal is a significant advantage of certain pretreatment approaches such as alkali treatment (Pavlostathis and Gossett 1985).

The compositional analysis has been conducted for various biomasses (Table 1.1), but the detailed structural information of plant cell wall is not clear yet. Without knowing the structural features of biomass, as well as structural changes during biomass processing, it is challenging to develop a high efficiency and low cost processing approach. One objective of this study is to reveal the structural features of sorghum biomass.

Table 1.1 Compositional analysis of various feedstocks.

Biomass[a] [b]	Cellulose (%)	Hemicellulose (%)	Lignin (%)
Corn stover	36.1 – 40.8	26 – 35	17.2 – 21
Switchgrass	32 – 36.6	21.5 – 26.6	18.5 – 21.4
Wheat straw	37.1 – 48.6	23.2 – 31.7	8.2 – 19.2
Hard wood	40 – 55	24 – 40	18 – 25
Soft wood	45 – 50	25 – 35	25 – 35
Sorghum stover	18.1	37.8	24.6

[a] Numbers do not sum to 100% because other minor components, such as ash, are not included.

[b] Data from sources (Alizadeh et al. 2005; Lloyd and Wyman 2005; Saha et al. 2005a; Sun and Chen 2008; Sun and Cheng 2002; Suryawati et al. 2008; Theerarattananoon et al. 2010; Xu et al. 2010; Zeng 2007; Zhao et al. 2009; Zhu et al. 2006a)

1.1.4 Biomass pretreatment: a critical step in biorefinery process

Lignocellulosic biomass biorefinery, including the sugar-ethanol platform, generally goes through feedstock harvest and storage, pretreatment (including physical and chemical), enzymatic hydrolysis, fermentation, and product recovery (Lee 1997) (Figure 1.1). Pretreatment is usually conducted before enzymatic hydrolysis to break up the tight structure of lignocellulosic biomass and expose polysaccharides for further digestion and recovery. Size reduction is an effective physical way to break up biomass chips, which increases the surface area of biomass for subsequent processing. Different pretreatment methods have been developed and the effects of these methods on structural change of lignocellulosic biomass are summarized in Table 1.2.

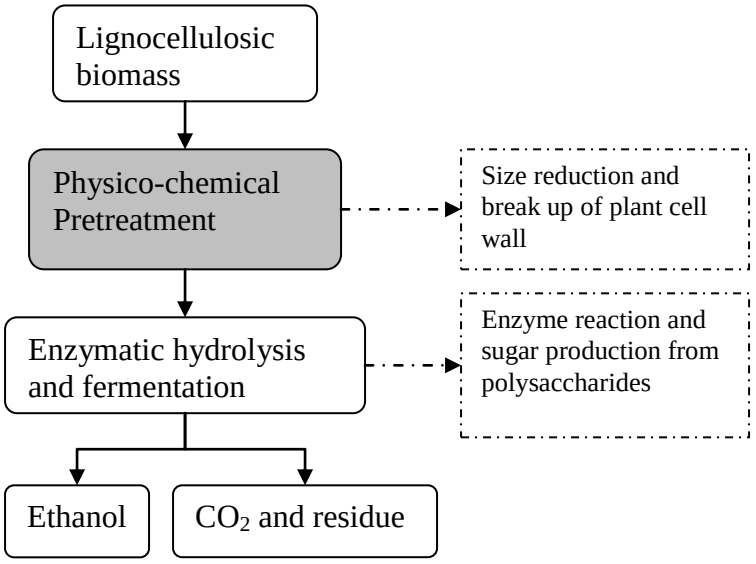

Figure 1.1 Flowchart of ethanol production from lignocellulosic biomass.

Table 1.2 Effects of pretreatment on biomass structure.

Pretreatment[a]	Mass loss	Change crystallinity[c]	Increases SSA	Removal of amorphous part
Diluted acid	●	+	●	●
Hot water	●	+	●	●
Alkali	●	+	●	●
AFEX	○[b]	○	●	○[b]
Steam explosion	●	+	●	●
Ionic liquids	●	-	●	●

[a] Data from sources (Balan et al. 2009; Lee et al. 2010; Li et al. 2011; Mosier et al. 2005b; Silverstein et al. 2007a; Sun et al. 2000; Thompson et al. 1992; Wu et al. 2011; Zeng et al. 2007; Zhao et al. 2008).
[b] Could become significant if a washing step is employed after pretreatment.
[c] Mass crystallinity summarized.
SSA: Specific surface area.
● Significant; ○ Insignificant; + Increased; - Decreased.

Acid (diluted and concentrated) treatment of biomass for carbohydrate recovery has been used to break plant cell walls (Teixeira 1999; Torget et al. 1991). Cellulose could be hydrolyzed to D-glucose under certain conditions because of its glycosidic linkage, which is susceptible to acid treatment (Atalla 1979). The branched structure makes hemicellulose more sensitive to acid treatment. Since a significant amount of hemicellulose could be hydrolyzed to mono-saccharides (xylose, arabinose, etc.) and other molecules, the increase in accessible surface area of cellulose and the mass loss of substrate is significant (Zeng et al. 2007). An increase in biomass crystallinity also was reported in most of the related research as a results of the removal of the amorphous part (Thompson et al. 1992), but the detail structural changes in crystalline domain is unknown. Liquid hot water pretreatment, without additional chemicals, has been used for pretreatment of some lignocellulosic biomass (Mosier et al. 2005b). Because liquid hot water at high temperature (about 200 °C) reacts with hemicellulose to form acids, which results in a decrease in pH in the reaction system, the whole process is comparable to acid pretreatment (Weil et al. 1997). To avoid the consequent degradation of mono-saccharides, pH control during liquid hot water pretreatment was employed (Mosier et al. 2005a).

Alkali pretreatment is also used for biomass pretreatment (Curreli et al. 1997; Silverstein et al. 2007a; Zhao et al. 2008). The glycosidic bonds in cellulose are generally considered stable toward alkali at low temperature (Johansson and Samuelson 1975), which enables a reduction in cellulose degradation during mild conditions. Alkali (such as sodium hydroxide) generally functionalized cellulose starting from the reduced terminal, which makes the cellulose with short chains dissolve at the beginning of treatment (Johansson and Samuelson 1975). Thus, the

decrease of polymerization (DP) may not be significant with this reaction. Amorphous parts were reported to be removed by alkali treatment (Sun et al. 2000). Delignification (Kim and Holtzapple 2006) and deacetylation (Kong et al. 1992) are other characteristics of alkali treatment, including lime treatment.

Steam explosion, in which biomass is treated with high temperature and high pressure followed by a sudden reduction of pressure, is another frequently used pretreatment method (Sassner et al. 2008). This method could cause hemicellulose removal and lignin transformation with an increase in pore surface area (Grous et al. 1986), and could limit cellulose loss under controlled conditions. Similar to steam explosion, ammonia fiber explosion/expansion (AFEX) utilizes both physical (high temperature and pressure) and chemical (ammonia) processes to change biomass structure and increase enzymatic digestibility (Foster et al. 2001). Delignification is one of the most important characteristics of this treatment because of the depolymerization of lignin (Mosier et al. 2005b). Although there is no significant mass (lignin and hemicellulose) loss during this process, some depolymerized lignin could be removed by a subsequent washing step (Balan et al. 2009). Worth mentioning is that this method has a limited effect on biomass with high lignin content (McMillan 1994). Although AFEX is considered to promote cellulose decrystallization (Balan et al. 2009; Gollapalli et al. 2002), the question whether the crystalline structure of lignocellulosic biomass changes during this treatment is debated (Lee et al. 2010), and the relationship between crystallinity and enzymatic digestibility remains uncertain.

Recently, ionic liquids (ILs) have emerged as a promising solvent for biomass pretreatment (Liu et al. 2006). By replacing the inter- and intra-molecular hydrogen bonds of cellulose with its anion, ILs become ideal solvents for dissolving cellulose (Maki-Arvela et al. 2010; Swatloski et al. 2002). Complete dissolution of biomass, such as corn stover and switchgrass, was reported to achieve high digestibility of cellulose at 160 °C for 3 h, and glucose recovery after hydrolysis was over 90% (Li et al. 2011). After dissolution, cellulose could be regenerated by adding water to ILs, and the natural structure of cellulose in biomass, cellulose I, was transformed to cellulose II accompanying a change of crystallinity (Wu et al. 2011). In addition, hemicellulose and lignin also could be extracted in ILs for a following fractionating.

It should be noted that the effects of some methods are material-dependent, which means the effectiveness of certain treatment could vary on different materials (Kumar et al. 2009a).

Furthermore, although the general goal of pretreatment is to break up the structure of plant cell walls for downstream processing at a low cost, pretreatment is still variable and objective dependent. For example, acid pretreatment under severe conditions may remove and break down hemicellulose (Schell et al. 2003), which is preferred for glucose-ethanol conversion but is not cost-effective for co-fermentation with both glucose and xylose because of an additional neutralization step.

1.1.5 Understanding biomass structure at a molecular level

Structural characteristic and change during processing have received attention (Wyman 2003). A large number of papers targeting different biomass with different methods have been published in the past 30 years (Bansal et al. 2012; Fan et al. 1980; Liu et al. 2005; Mansfield et al. 1999a; Sinitsyn et al. 1991). The basic structure of lignocellulosic biomass has been modeled (Somerville et al. 2004) although the detail structure varied from one type of biomass to another. Cellulose is considered to be the only contributor for the crystalline part, while hemicellulose and lignin are thought as amorphous parts. Structural changes of biomass vary depending on pretreatment methods and hydrolysis conditions on sugar platform. For example, sulfuric acid pretreatment is effective in hemicellulose removal (Saha et al. 2005a). Aqueous ammonia was used in corn stover pretreatment and performed well in lignin removal (Kim et al. 2003). The removal of those amorphous parts in biomass not only increases the specific surface area (SSA) of cellulose for the following enzyme treatment but also reduces possible inhibition to enzyme as reported earlier (Hidaka et al. 1984). One of the important structural factors is crystallinity which is generally referred to the ratio of crystal part to whole mass. The increase of mass crystallinity was found in many pretreatment processes, as a result of amorphous components removal. However, limited studies have been conducted on the structural changes of cellulose during processing. It is still not clear how cellulose, including crystalline and amorphous cellulose, and other polymers change during different pretreatment. Other factors, including substrate factors (eg. lignin distribution) and enzyme factors (eg. synergism), are also critical for biomass processing (Mansfield et al. 1999b).

1.1.6 Structural characterization techniques for biomass study

The study of cellulose structure has a long history (Liang and Marchessault 1959; Sisson 1935). The goals of the study include deduction of O-H bond orientation and providing

molecular models of cellulose in both crystalline and noncrystalline regions (Cael et al. 1975). However, it becomes much more complicated to study natural cellulose in lignocellulosic biomass than pure cellulose because of various cross-linkages and twists among cellulose, hemicellulose and lignin. For biomass conversion research in a sugar platform, there are a number of techniques available for structural determination. Several major techniques being frequently used are: scanning electron microscopy (SEM) (Zeng et al. 2007), transmission electron microscopy (TEM) (Donohoe et al. 2008), Raman spectroscopy (Sivakesava et al. 2001), confocal laser scanning microscopy (Bak et al. 2009), atomic force microscopy (Zhang et al. 2007), Fourier transform infrared spectroscopy (FTIR) (Schultz et al. 1985), nuclear magnetic resonance (NMR) (Haw et al. 1984), wide-angle X-ray diffraction (WAXD), small-angle X-ray scattering (SAXS), and small-angle neutron scattering (SANS) (Pingali et al. 2010b), etc. An example of synchrotron X-ray beamline used in this study has been illustrated in Figure 1.2.

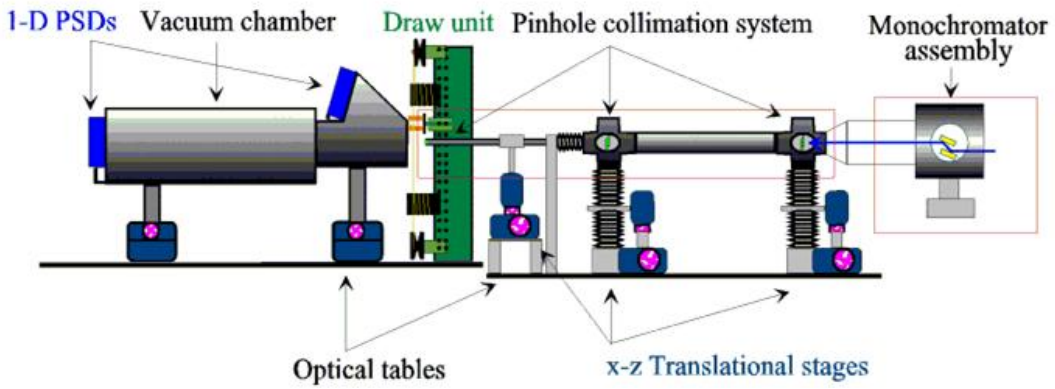

Figure 1.2 Schematics of simultaneous wide-angle X-ray diffraction and small-angle X-ray scattering setup. (X27C beamline, National Synchrotron Light Source, Brookhaven national laboratory, NY. Image courtesy of Drs. Lixia Rong and Benjamin S. Hsiao, Stony Brook University, Stony Brook, NY)

1.2 Research objectives

The goals of this study were to develop an effective conversion process for ethanol production using PS sorghum and to understand how the structure changes during processing. The detail objectives are as following:

a) To develop an effective and integrated processing method to convert PS sorghum to ethanol: including pretreatment, hydrolysis, and co-fermentation.

b) To optimize the processing system to achieve a higher conversion efficiency by investigating the processing conditions with statistical methods.

c) To understand the structural features and changes of PS sorghum at a molecular level during processing.

d) To understand the effect of structural changes during acid pretreatment on the subsequent enzymatic hydrolysis.

1.3 Related Current and Previous Research

1.3.1 Sulfuric acid pretreatment

Cellulosic materials are a complex mixture of cellulose, hemicellulose, and lignin. The cellulose of these materials in their original form is not readily available for hydrolysis, so pretreatment (both physical and chemical) is usually required. Much research, in which different pretreatment methods in the sugar platform are used, has been conducted to increase fermentable sugar yield (Fan et al. 1980; Hu and Wen 2008; Karimi et al. 2006; Saha and Bothast 1999; Zeng 2007). In this study, we will compare the cellulose conversion efficiency using different concentrations of diluted sulfuric acid. Much of the research conducted to date focused only on the efficiency of enzymatic hydrolysis (EEH) after pretreatment and failed to take into account the cellulose or hemicellulose loss during pretreatment (Ma et al. 2009; Zhu et al. 2006b; Zhu et al. 2004). Without considering this possible loss, even a high conversion rate during enzymatic hydrolysis cannot prove that the pretreatment method is successful. In this study, however, we address this issue by studying cellulose yield in both pretreatment and hydrolysis, and we also use total yield as an important parameter to assess the efficiency of pretreatment methods. A mass balance is also conducted.

1.3.2 Response surface methodology

Conventional optimization, in which factors in all combination are tested, provides a large amount of information. However, it is time consuming and fails to explain potential interactions between variables. Response surface methodology (RSM), with its advantage of efficient design, not only reduces experimental time and energy but also provides the regression

model and possible optimal combinations of variables. The interaction between factors could be visualized by RSM in software.

In this study, for a co-fermentation that uses substrates of soluble sugar and cellulose together, we will first investigate the relationship between pretreatment conditions and glucose yield using RSM. Fermentation conditions, including temperature, inoculation, and buffer concentration, will also be optimized.

1.3.3 Simultaneous saccharification and fermentation

Although sugar and starch based ethanol fermentation has been studied for long time (Inlow et al. 1988), these processes are different from cellulose based ethanol fermentation. Simultaneous saccharification and fermentation (SSF) has been accepted for most of biomass processing, since it saves energy and time and reduce end-product inhibition of enzyme hydrolysis (Wright et al. 1988). Simultaneous saccharification and fermentation also reduces equipment costs by performing the hydrolysis and fermentation in a single reactor. The limitation of lignocellulose loading, depending on material characteristics and pretreatment method, makes it difficult for cellulose based SSF to achieve a high ethanol concentration (more than 10 % (v/v)). Thus, for yeast fermentation with low sugar concentration and low ethanol concentration, substrate inhibition or end-product inhibition is not critical problem, because it was reported that ethanol begins to inhibit yeast fermentation at 25 g ethanol/L (Maiorella et al. 1983). Meanwhile, one of the current barriers preventing commercialization of lignocellulosic ethanol is a high processing cost. The optimization of cellulose based fermentation is then supposed to include a mechanism for lowering processing costs. It is well known that the optimal temperature for yeast fermentation is about 30 °C, which is significantly different from the temperature (50 °C) for enzymatic hydrolysis. Thus, it is a challenge to study how to make the two reaction work well in one system. In this research, the optimization of SSF will be conducted with consideration of ethanol yield and energy input.

1.3.4 WAXD and SAXS study of biomass structure

To date, the effects of treatment, with regard to changes at molecular level, have not been fully understood. Wide-angle X-ray diffraction has been used historically in studying crystalline structure of cellulose (Nishiyama et al. 2002). Recently, it was frequently used for the study of crystalline structure in biomass processing (Oh et al. 2005). Different methods for analysis of

diffraction patterns have been developed to calculate crystallinity depending on how to separate or model crystalline part and amorphous parts. One of the most frequently used methods is the Segal's method (Segal et al. 1959). The intensity of crystalline and amorphous peaks was considered an important factor in analyzing X-ray data in the mid-20th century (Goppel 1949; Krimm and Tobolsky 1951). Segal's method, which designated the term of "Crystallinity Index" to represent the relative degree of crystallinity, could be used easily to obtain general information about crystalline parts with limited information loss. A detailed comparison of mass crystallinity changes after pretreatment has been summarized (Table 1.3). As mention in Table 1.2, mass crystallinity increased after most of pretreatment as a result of the removal of amorphous components. The 1D curve integrated from 2D pattern could be analyzed easily to generate those factors needed in Segal's equation. However, the intensity loss is not negligible even for an entire crystalline substance due to thermal vibrations of atoms or lattice imperfections. For this reason, scientists started using separated diffraction peaks to obtaining crystalline information in the 1960s (Ruland 1961). It is assumed that Bragg peaks are sharp and splittable, which make it possible to construct crystalline peak that is partially diffused with amorphous diffraction. Amorphous sample (eg. lignin) is usually necessary for diffraction deduction in Ruland's method. Thus the results are highly dependent on the amorphous materials selected, which make it challenging to analyze samples from different sources. Another approach, peak fitting procedure (Rietveld 1967), was developed to refine and model those peaks with assumed functions such as Gaussian functions (Hult et al. 2003). Fundamentally understanding the knowledge of crystal structure is required for this refining process. Since this method accounts for the full convolution of cellulose and provides consistent results, it has been employed frequently in semicrystalline polymer studies (Bish and Howard 1988; McCusker et al. 1999; Stephens 1999).

Table 1.3 Mass crystallinity changes during pretreatments.

Pretreatments	Biomass	Crystallinity (%) change		References
		Before	After	
Diluted sulfuric acid	Corn stover	50.3	52.5	(Kumar et al. 2009c)
	Switchgrass	26.2	39.1	(Li et al. 2010)
	Hardwood	73.2	76.1	(Grethlein 1985)
	Hardwood	71.6	82.3	(Thompson et al. 1992)
	Sweet sorghum bagasse	32.6	56.1	(Theerarattananoon et al. 2010)
Ammonia fiber explosion (AFEX)	Coastal Bermuda grass	50.2	From 52.2 to 59.5	(Lee et al. 2010)
	Rice straw	40.7	From 18.7 to 42.9	(Gollapalli et al. 2002)
	Corn stover	50.3	36.3	(Davison et al. 2005)
Liquid hot water	Hardwood	71.6	85.8	(Thompson et al. 1992)
Subcritical water	Switchgrass	51.6	64.3	(Kumar and Gupta 2009)
Steam explosion	Wood	Increased about 1.5 times		(Tanahashi et al. 1983)
CO_2 explosion	Wheat straw	35	56	(Puri 1984)
Lime	Corn stover	43	60	(Kim and Holtzapple 2006)
Hydrogen peroxide	Rice straw	77.0	90.7	(Wei and Cheng 1985)
Zinc chloride	Textile cotton wastes	Decreased*		(Focher et al. 1984)
Ammonia recycled percolation	Corn stover	~60	~75	(Kim et al. 2003)
1-ethyl-3-methylimidazolium acetate	Switchgrass	26.2	2.6	(Li et al. 2010)
Ethylene glycol	Wheat straw	69.6	55.0	(Gharpuray et al. 1983)
Buffer	Cotton linter	74, 63, and 32	76, 64 and 45	(Bertran and Dale 1985)
Ball milling	Wheat straw	~80	26.3	(Christakopoulos et al. 1991)

* Calculation of crystallinity is a use of peak comparison.
Segal's method was employed if not specified. This table is not meant to be exhaustive.

Crystal (crystallite) size, unlike particle size, is defined depending on the method used. Scherrer's equation, which was developed almost 100 years ago, is the classic method for crystallite size calculation (Langford and Wilson 1978). The factor of full width at half maximum could be obtained after peak analysis. Since many factors may affect the peak width in XRD pattern and sometimes the peak deconvolution approaching may introduce artifacts, this method is not precise, especially for a crystalline complex with different sizes. The Scherrer constant K should be used cautiously because it depends on how the width and the crystal shape are determined. A K-value of 0.89, which works well for spherical crystals without cubic symmetry (Langford and Wilson 1978), was employed in most of the research related to crystal

size. Although this method is an estimate on average, it still was used frequently in polymer studies (Marchisio 2009; Shivakumara and Bellakki 2009). For instance, a study on cellulose fibril in wood using both WAXD and SAXS showed the crystal size of sprucewood is close to 2.2 nm (Jakob et al. 1995). The crystalline structure information of cellulose in corn stalk has been reported, and the crystal size was found as 3.8 nm (Reddy and Yang 2005). In a study of the enzymatic hydrolysis of pretreated wood samples, both crystallinity and crystal size of peroxide-treated samples decreased gradually during hydrolysis, but those of full bleached samples did not change significantly (Ramos et al. 1993). In contrast, crystal size, as well as crystallinity index, was found to increase after cellulase hydrolysis in study of the effect of enzymatic hydrolysis on biomass (softwood, hardwood and linter) structure (Cao and Tan 2005). For sizes changes during biomass pretreatment, however, the study was limited. One example is that the crystal size of wood increased from about 3 to 6.3 nm after steam explosion (Tanahashi et al. 1983). More fundamental studies on crystalline structure of biomass are suggested.

SAXS has been applied to the study of polymer ultrastructure (Chu and Wang 1988; Ivan Krakovský 1997; Waigh et al. 1999). However, for lignocellulosic biomass, SAXS study is limited to a few biomass, such as wood fiber (Lichtenegger et al. 1999). For example, the diameter of cellulose fibrils was reported as 2.5 nm in sprucewood (*Picea abies*) with SAXS study (Jakob et al. 1994). The spiral angles of the fibrils in earlywood and latewood were found to be significantly different (Jakob et al. 1995; Reiterer et al. 1998). In addition, the SAXS study on individual components, including cellulose and lignin, were reported frequently (Astley and Donald 2001; Canetti et al. 2006; Nishiyama et al. 2002; Vickers et al. 2001). For instance, lignin from pine wood was reported to have a SSA of 34 m^2/g and show characteristic of surface fractal (Vainio et al. 2004). It is well known that the structure information could be accessed at both the length scales larger than the separation between crystal planes and on the spacing between the regular stacks of lamellae using SAXS (Chu and Hsiao 2001). SAXS possibly could be used for structure analysis of both crystalline and amorphous parts, such as lignin. Thus, SAXS, complementary to WAXD, is a powerful tool for study of biomass structure (Crawshaw et al. 2002). Interesting results about biomass structural changes at submicrometer-length scales during diluted acid pretreatment with small-angle neutron scattering have been reported recently (Pingali et al. 2010b). Although a complete structural model was not provided in this article, the results are important for strategic development of biomass pretreatment.

Chapter 2 - Diluted sulfuric acid pretreatment and enzymatic hydrolysis of photoperiod-sensitive sorghum for ethanol production: Method development[1]

2.1 Abstract

Photoperiod-sensitive sorghum, with high soluble sugar content, high mass yield and high drought tolerance in dryland environments, has great potential for bioethanol production. The effect of diluted sulfuric acid pretreatment on enzymatic hydrolysis was investigated. Hydrolysis efficiency increased from 78.9 to 94.4% as the acid concentration increased from 0.5 to 1.5%. However, the highest total glucose yield (80.3%) occurred at the 1.0% acid condition because of the significant cellulose degradation at the 1.5% concentration. Synchrotron wide-angle X-ray diffraction was used to study changes of the degree of crystallinity. With comparison of cellulosic crystallinity and adjusted cellulosic crystallinity, the crystalline cellulose decreased after low acid concentration (0.5%) applied, but did not change significantly as the acid concentration increased. Scanning electron microscopy was also employed to understand how the morphological structure of PS sorghum changed after pretreatment. Under current processing conditions, the total ethanol yield is 74.5% (about 0.2g ethanol from 1g PS sorghum). A detail mass balance was also provided.

2.2 Introduction

Energy shortage and carbon dioxide emission have become serious issues (Fargione et al. 2008). Renewable fuels that are produced from plants and harvested annually could help ensure a more sustainable future and reduce carbon dioxide emissions. First-generation biofuels, including starch-based and sugar-based ethanol, are well developed and show good performance when mixed with gasoline. However, most substrates used for these biofuels are food resources, and the overuse of crop starch for ethanol will eventually result in competition with food production for limited land (Tilman et al. 2006). Lignocellulosic biomass, which is advantageous

[1] This chapter has been published as a peer-reviewed research paper in the Journal of Bioprocess and Biosystems Engineering. 2011. 34(4):485-492. The original publication is available at www.springerlink.com.

because it is a low-cost, renewable and abundant material, has become a promising resource and has attracted much focus (Rubin 2008). Recent legislation calls for the United States to annually produce 36 billion gallons of renewable fuel by 2022 to help offset impending concerns over climate change and energy security, The U.S. Department of Energy and U.S. Department of Agriculture projected that U.S. biomass resources could provide approximately 1.3 billion dry tons of feedstock, which could produce up to 100 billion gallons of biofuel. Corn stover, one of the most important agricultural residues in the Corn Belt, can be harvested every year at a yield of 200 million tons, but only about 30% of this stover could be collected at a low cost without affecting soil quality (Graham et al. 2007). Energy sorghum such as forage sorghum and sorghum stover is another important source of biomass; it is a renewable resource that currently is grown on 6 to 10 million acres in the United States (data from National Agricultural Statistics Service, 2010). Sorghum is a tropical grass grown primarily in semiarid parts of the world, especially in areas too dry for corn. Sorghum cannot compete successfully with corn as a cereal crop in an agro-ecosystem with 900 mm of annual rainfall, but corn cannot compete with sorghum in areas that receive less than 900 mm of rainfall. Sorghum also produces 33% more dry mass than corn in dryland conditions. Photoperiod-sensitive (PS) sorghum, like many other types of sorghum, has high water use efficiency (Rai et al. 1999). Photoperiod-sensitive sorghum, as a high-energy sorghum, does not initiate reproductive flowering stages and accumulates increased levels of vegetative dry mass with no grain production at most latitudes in the continental United States. PS sorghum produces much more dry mass per acre (80 Mg ha^{-1}, 65% moisture content) than corn (McCollum III et al. 2005 at Plains Nutrition Council), suggesting that PS sorghum biomass has great potential for cellulosic biofuel production.

The challenge in producing ethanol from cellulose is the difficulty in breaking down cellulosic matter to sugars. Cellulosic materials are a complex mixture of cellulose, hemicellulose, and lignin. The cellulose of these materials in their original form is not readily available for hydrolysis, so pretreatment (both physical and chemical) is usually required. Much research, in which different pretreatment methods in the sugar platform are used, has been conducted to increase fermentable sugar yield (Fan et al. 1980; Hu and Wen 2008; Karimi et al. 2006). In the present study, we compared the cellulose conversion efficiency of different concentrations of diluted sulfuric acid used to process PS sorghum. Much of the research conducted to date focused only on the efficiency of enzymatic hydrolysis (EEH) after

pretreatment and failed to take into account the cellulose or hemicellulose loss during pretreatment (Ma et al. 2009; Zhu et al. 2006b; Zhu et al. 2004). Without considering this possible loss, even a high conversion rate during enzymatic hydrolysis cannot prove that the pretreatment method is successful. In the present study, however, we addressed this issue by studying cellulose yield in both pretreatment and hydrolysis, and we also used total yield as an important parameter with which to assess the efficiency of pretreatment methods. Simultaneous saccharification and fermentation (SSF) has shown good performance in biomass conversion (Öhgren et al. 2007). In this research, SSF was used to evaluate the potential of PS sorghum for ethanol production.

Wide-angle X-ray diffraction (WAXD) and SEM were employed to study the structural changes during processing. The crystalline structure of cellulosic compound has been studied for a long time and is becoming a popular topic because of the dramatic developments in renewable biofuels (Chang and Holtzapple 2000). The classic method of obtaining degree of crystallinity (%) takes into account the crystalline part based on the whole biomass, provides direct value about crystallinity and has been used in many studies. However, direct use of this method, as well as the Segal's method (Segal et al. 1959), results in large variance for biomass sample, especially when comparing crystallinity changes during the treatments in which significant cellulose loss occurs. In this research, degree of cellulosic crystallinity (CCr), taking account into the cellulose composition, was used to balance the possible mass loss, including both crystalline and amorphous parts. Both relative crystallinity (based on total biomass) and CCr were provided to study crystallinity change. Synchrotron beamline, with its high energy and focusing accuracy, was applied in this research to study the crystallinity of cellulose.

The objectives of this research were to study the structural changes of PS sorghum during sulfuric acid pretreatment and their effects on enzymatic hydrolysis as well as SSF, and to develop an integrated method for utilizing the soluble sugar and the cellulose in PS sorghum.

2.3 Materials and methods

2.3.1 Materials

The PS sorghum (1990/AC791) used in this research was harvested from the Kansas State University Agronomy Research Farm in Manhattan, Kansas, from 2007 to 2009. After being ground with a cutting mill (SM 2000, Retsch Inc., Newtown, PA) to <1 mm particle size,

the sample with moisture content of 7% was stored at room temperature. The chemical composition of PS sorghum was determined by following NREL procedure (Sluiter et al. 2004) as shown in Table 2.1. In the NREL procedure, sulfuric acid hydrolysis at 121°C was used to degrade cellulose and hemicellulose to monosacchrides which were further tested by HPLC, while acid soluble lignin was tested by UV spectrophotometer. Before sulfuric acid pretreatment, the sample was washed with distill water to separate soluble sugar and was analyzed again for chemical composition. All chemicals used in this research were of analytical grade and purchased from Sigma (Sigma-Aldrich, Inc., St. Louis, MO, USA).

2.3.2 Sulfuric acid pretreatment

A reactor (Swagelok, Kansas City Valve & Fitting Co., KS) made from 316L stainless steel with a measured internal volume of 75 mL (outside diameter of 38.1mm, length of 125 mm, and wall thickness of 2.4mm) was used for this study. A working volume of 50mL was used to allow space for expanding liquid water at high temperature during pretreatment. The loading of the prewashed PS sorghum was 6.1% (w/v, 3.07 g dry mass in 50ml water). A sandbath (Techne, Inc., Princeton, NJ) with a temperature controller was used for increasing and controlling temperature. After the sand was increased to 160°C, the reactor was submerged in heated sand for 40 min. Then the reactor was immediately transferred to room-temperature water to decrease the internal temperature to below 50°C in 2 min. All slurry removed from the reactor was washed and separated by filtration. Part of the solid mass after filtration was used for enzymatic hydrolysis, and a small part was then oven dried at 40°C for structural analysis. The remaining part and the liquid part were used for composition analysis. Cellulose recovery in the residues after pretreatment was defined as shown in the calculation below.

$$Y_{REC} = \frac{M_{pret} \times C_{pret}}{M_{OR} \times C_{OR}} \times 100\% \quad \textbf{[Equation 2-1]}$$

where M_{pret} is dry mass weight after pretreatment, M_{OR} is original dry mass weight, C_{pret} is the cellulose percentage of the solid part after pretreatment, and C_{OR} is percentage of the cellulose in original dry mass.

2.3.3 Enzymatic hydrolysis

Accellerase 1500, an enzyme complex including cellulase and β-glucosidase (Endoglucanase activity: 2200-2900 CMC U/g, one CMC U unit of activity liberates 1 μmol of

reducing sugars [expressed as glucose equivalents] in one minute under specific assay conditions of 50°C and pH 4.8), was generously provided by Genencor (Rochester, NY) and used in this study at the recommended dosage (0.5 mL per gram cellulose). Enzymatic hydrolysis was conducted with the sample after pretreatment at 4% solids concentration (grams dry weight per 100 mL) in 50 mM sodium acetate buffer (pH 5.00) with addition of 40 µg/mL tetracycline and 30 µg/mL cycloheximide. Flasks were incubated in a water bath at a constant temperature of 50°C and agitation of 140 rpm. Total sugar analysis was conducted at the end of hydrolysis (72h) on supernatants by high-performance liquid chromatography (HPLC) described below. The conversion efficiency of enzymatic hydrolysis (EEH) was defined as shown in the calculation below.

$$EEH = \frac{G_{EH} \times 0.9}{M_{EH} \times C_{pret}} \times 100\% \quad \textbf{[Equation 2-2]}$$

where M_{EH} is the weight of dry mass used in enzymatic hydrolysis (or SSF), G_{EH} is glucose content after hydrolysis ($C_{EH} = G_{EH} * 0.9$), and 0.9 is the mass coefficient of glucose to cellulose (g/g). Total product (glucose) yield was defined as the product of cellulose percentage in the solid part after pretreatment and EEH.

$$Y_P = \frac{EEH \times Y_{REC}}{100\%} \quad \textbf{[Equation 2-3]}$$

2.3.4 Simultaneous saccharification and fermentation

The same enzyme and buffer system were used in SSF as in enzymatic hydrolysis without antibiotics. Yeast (Ethanol Red, Lesaffre Yeast Corp., Milwaukee, WI) was prepared following the method reported by Wu et al (Wu et al. 2010). Both concentrated washing juice and pretreated solid were added together (the ratio of the soluble sugar amount to the cellulose in solid was based on data in Table 1), and the initial fermentation system contained 4% (w/v) solids. A synthetic juice containing the same amounts of sugars as the washing juice was also prepared for comparison. The SSF was conducted in an incubator shaker (Model I2400, New Brunswick Scientific Inc., Edison, NJ) at 38°C and 150 rpm. HPLC was used to analyze the ethanol concentration and other end products. An integrated method to process PS sorghum for ethanol production was depicted in Figure 2.1. Fermentation yield (Y_{SFF}) and total ethanol yield (Y_{ETH}) for the biomass-ethanol production were calculated using the following equations:

$$Y_{SSF} = \frac{M_{EP}}{\left(M_{EH} \times C_{pret} \times 1.11 + M_{Hex}\right) \times 0.511} \times 100\% \quad \textbf{[Equation 2-4]}$$

$$Y_{ETH} = \frac{M_{EP}}{M_{TEP}} = \frac{M_{EP}}{\left(M_{OR} \times C_{OR} \times 1.11 + M_{Hex}\right) \times 0.511} \times 100\% \quad \textbf{[Equation 2-5]}$$

where M_{EP} is mass of ethanol after SSF; M_{TEP} is the theoretical value calculated from cellulose and soluble sugar, M_{Hex} is the total amount of soluble sugar (expressed as glucose equivalents), 0.511 is the mass coefficient of glucose to ethanol (g/g), and 1.11 is the mass coefficient of cellulose to glucose (g/g).

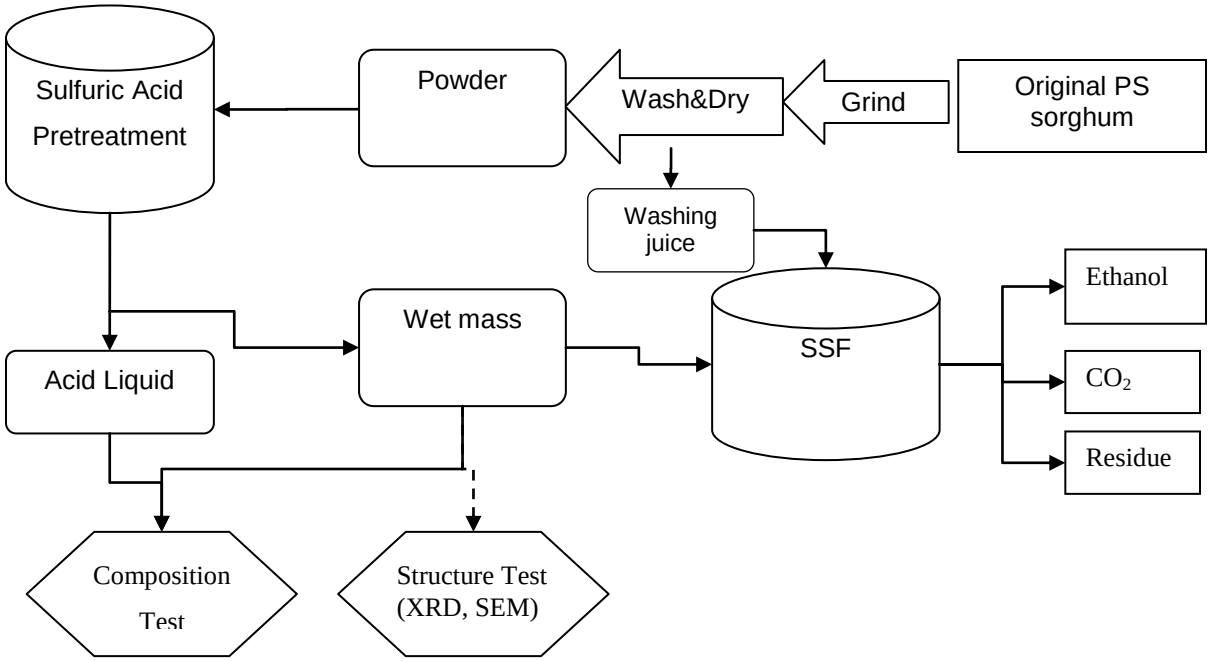

Figure 2.1 Flowchart of photoperiod-sensitive sorghum processing.

2.3.5 Wide-angle X-ray diffraction

Wide-angle X-ray diffraction was carried out at the advance polymers beamline (X27-C) at the National Synchrotron Light Source (NSLS), Brookhaven National Laboratory (Upton, NY). Details on the beamline system set up have been reported elsewhere (Chu and Hsiao 2001). The wavelength used was 0.1371 nm. CCr and adjusted cellulosic crystallinity (ACCr) were calculated using the following equations:

$$CCr = \frac{RCr}{C_{pret}} \times 100\% \quad \textbf{[Equation 2-6]}$$

$$ACCr = \frac{CCr \times M_{pret} \times C_{pret}}{M_{OR} \times C_{OR}} \quad \textbf{[Equation 2-7]}$$

where RCr is relative crystallinity, which is defined as the crystal percentage of total mass and is calculated as the ratio of total crystal peak intensity to total diffraction intensity; CCr is cellulosic crystallinity, which is defined as the crystal percentage of cellulose and is equal to the ratio of relative crystallinity (RCr) to variable cellulose content of the solid with different conditions; and ACCr is adjusted cellulosic crystallinity, which presents the ratio of crystalline part amount to initial cellulose content.

2.3.6 Scanning electron microscopy

The morphological test was conducted with a scanning electron microscope (S-3500N) and an absorbed electron detector (S-6542, Hitachi Science System, Ltd., Hitachinaka, JP) operating at 5kV. Samples were mounted on a specimen stub with adhesive tape, followed by sputter-coating (Desk II Sputter/Etch Unit, Denton Vacuum, LLC., NJ, USA) with a mixture of 60% gold and 40% palladium before observation.

2.3.7 Sugar and ethanol analysis

The monosaccharide and ethanol was analyzed by using an HPLC with a Rezex RPM-monosaccharide column (300*7.8 mm; Phenomenex, CA) and a refractive index detector (RID - 10A, Shimadzu, MD). The column was eluted with double-distilled water at a flow rate of 0.6 mL/min. The temperature of the chromatograph column was maintained at 80 °C. The chemical composition test of solid after pretreatment and the potential oligosaccharide analysis were determined by the NREL procedure (as mentioned 2.3.1 Materials).

2.3.8 Statistics

Analysis of variance and Tukey's studentized range (HSD) test were employed to analyze data with SAS (SAS Institute, Inc. Cary, NC, USA). Mean values from the duplicated experiments are reported.

2.4 Results and discussion

2.4.1 Composition comparison of PS sorghum and other biomass

The chemical composition of PS sorghum was compared with that of corn stover, wheat straw and switchgrass which are currently used for research on bioethanol production (Table 2.1). Photoperiod sensitive sorghum naturally contains a significant amount of soluble sugars (including sucrose, glucose, and fructose), which were not reported in other major lignocellulosic biomass for ethanol production with significant amount. It is well known that these soluble sugars can be easily used for fermentation without additional treatment. These free sugars could be extracted for fermentation or high-value coproducts before pretreatment. Therefore, PS sorghum is an excellent feedstock for production of ethanol and high-value coproducts. Meanwhile, lignin, an important structural component of plant, has been reported to be the barrier that makes pretreatment more expensive (Mosier et al. 2005b). A low ratio of lignin to cellulose probably suggested that PS sorghum could be a promising source for biofuel production and have a reduced processing cost, which is the most important issue affecting the commercialization of cellulosic ethanol production.

Table 2.1 Composition comparison of photoperiod-sensitive sorghum and other major biomass sources (dry weight).

Biomass	Cellulose (%)	Hemicellulose (%)	Lignin (%)	Soluble Sugar (%)
PS sorghum[a]	32.5±0.8	19.8±0.8	11.7±0.2	17.5±0.5
Corn Stover[b]	36.1 – 40.8	26 – 35	17.2 – 21	NR[e]
Switchgrass[c]	32 – 36.6	21.5 – 26.6	18.5 – 21.4	NR
Wheat straw[d]	37.1 – 48.6	23.2 – 31.7	8.2 – 19.2	NR

[a]Numbers do not sum to 100% since other minor components, such as ash, are not included.
[b] (Lloyd and Wyman 2005; Zeng 2007; Zhao et al. 2009)
[c] (Alizadeh et al. 2005; Suryawati et al. 2008; Xu et al. 2010)
[d] (Saha et al. 2005a; Sun and Chen 2008; Zhu et al. 2006b)
[e]NR: not reported.

2.4.2 Diluted acid pretreatment of PS sorghum

The prewashed sample contained 40.5% cellulose. Figure 2.2 shows the percentage distribution of cellulose after it was treated with different concentrations of acid. As sulfuric acid concentration increased, the cellulose in the solid part decreased from 92.0% to 80.7%, which

suggests that some cellulose could be degraded to glucose as well as other molecules. The reason for the decrease in cellulose could be that the structure of PS sorghum was changed as hemicellulose was removed, making the cellulose component more susceptible to acid. Cellulose loss increased from 0.3% to 4.4% with an increase in acid concentration, indicating that glucose degradation become more significant in harsher conditions. Other researchers have reported similar results (Bienkowski et al. 1987; Xiang et al. 2004). With an increase in temperature or acid concentration, not only did cellulose loss increase, but many other small molecules (such as hydroxymethylfurfural) were generated, some of which are considered fermentation inhibitors. Compared with the original composition of PS sorghum, more than 90% of the hemicellulose was removed from the solid part, indicating sulfuric acid is a powerful agent for removing hemicellulose in the concentration range used in this experiment (Mosier et al. 2005b). Final hemicellulose content in the solid part after pretreatment ranged from 1% to 2% (dry basis) as sulfuric acid concentration decreased from 1.5% to 0.5%.

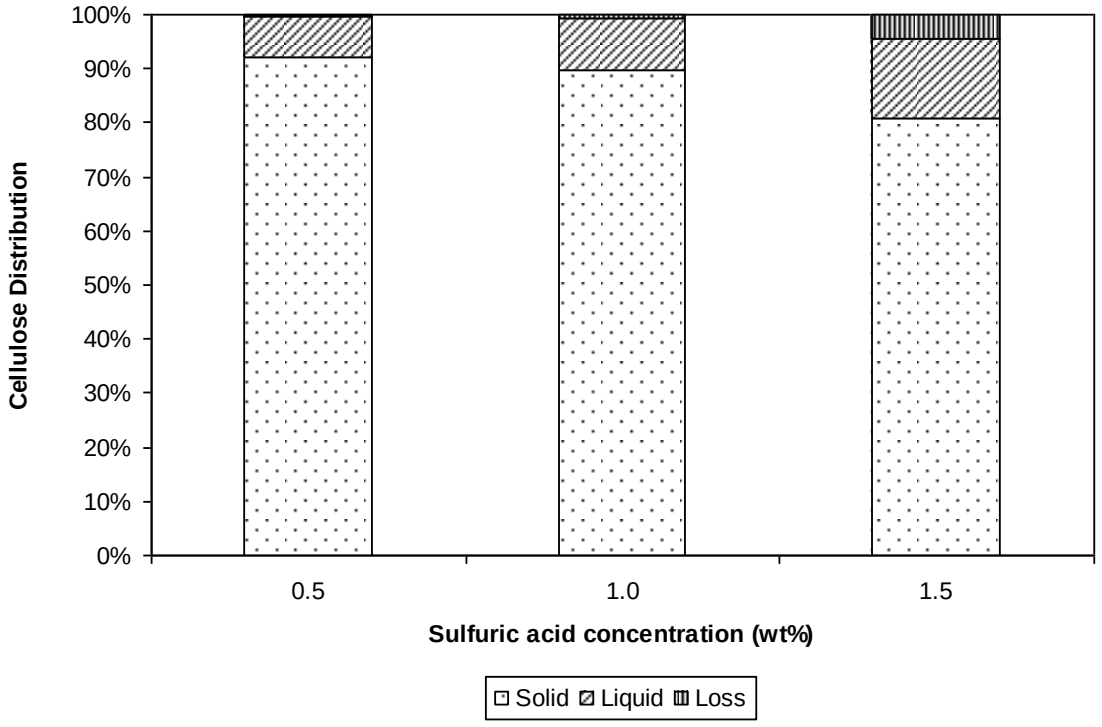

Figure 2.2 Cellulose (glucan) distributed in solid, liquid and loss parts, after pretreatment at 160 °C, for 40 min with different concentration of sulfuric acid.

2.4.3 Enzymatic hydrolysis

The EEH of the control sample without pretreatment was 20.9%, which was found in previous experiments. With the acid pretreatment, EEH increased from 78.9% to 94.4% as the acid concentration increased from 0.5% to 1.5% (Figure 2.3). Chum et al. (1990) defined a severity factor, which increased with the increase of acid concentration, reaction time and temperature, to describe the harsh level of acid pretreatment. It was also found that EEH was higher in a harsher condition (data not shown). A possible reason could be that the enzyme-accessible surface area of cellulose increased in harsher conditions, as a result of hemicellulose removal. Another possible reason is the partial removal of lignin, since lignin was reported as an inhibitor of cellulase activity (Berlin et al. 2005; Hidaka et al. 1984; Zheng et al. 2008).

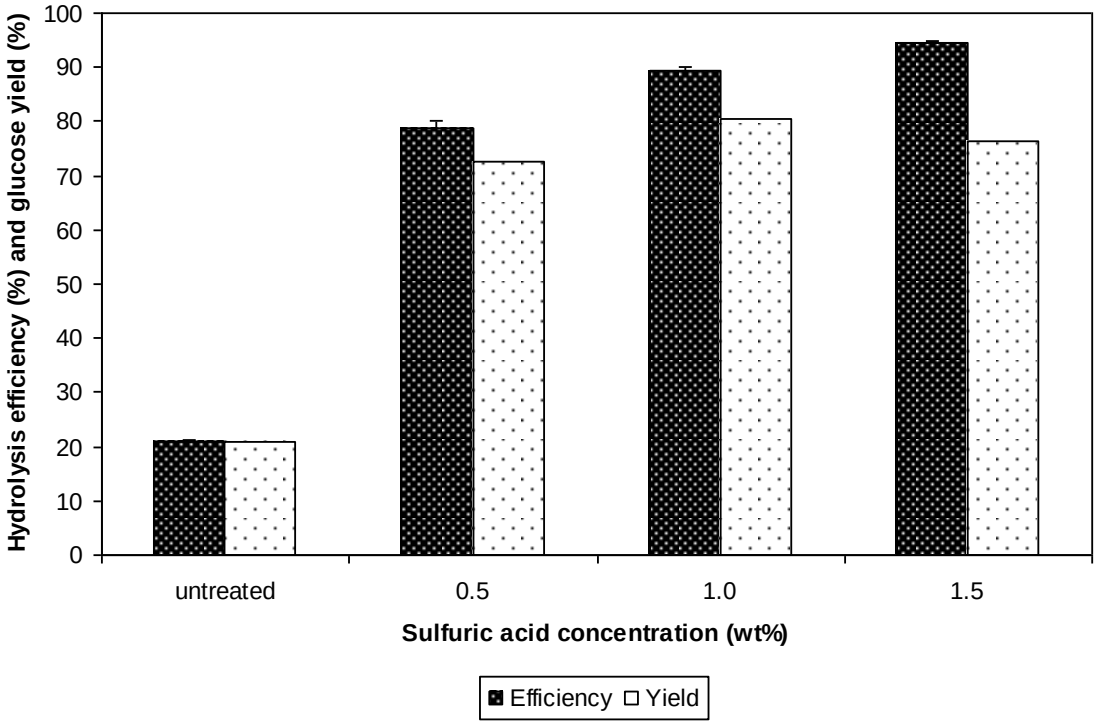

Figure 2.3 Efficiency of enzymatic hydrolysis and glucose yield, based on the solid part, after pretreatment at 160 °C for 40 min with different concentrations of sulfuric acid.

Although the EEH increased in harsher pretreatment conditions, the lignocellulosic structure was irreversibly damaged, and cellulose loss became an issue (e.g. about 4.4% with 1.5% of sulfuric acid used) as a result of glucose degradation. Since the value of EEH only takes

into account the cellulose conversion rate based on the solid part after pretreatment but does not include cellulose loss during pretreatment, the product yield (Yp) , based on solid part, is used to evaluate the total glucose yield of both pretreatment and hydrolysis. The glucose yield was 72.6%, 80.3% and 76.5% at the acid concentrations of 0.5%, 1.0% and 1.5%, respectively (Figure 2.3). The highest yield was found at 1.0% but not 1.5% of acid concentration because of the relatively high recovery of cellulose in the solid part at 1.0% acid concentration and the conversion of cellulose into degradation products at 1.5% acid concentration (Figure 2.2).

2.4.4 Crystallinity change during pretreatment

A synchrotron beamline, which provides a better signal-to-noise ratio than traditional methods, was used to conduct WAXD analysis for the PS sorghum sample. As shown in Figure 2.4, RCr increased after sulfuric acid pretreatment, as reported elsewhere (Kumar et al. 2009b). However, the discrepancies of RCr in the different acid conditions were not significant according to Tukey's studentized range test (detail not shown). We attributed the increase of relative crystallinity to removal of the amorphous part of biomass.

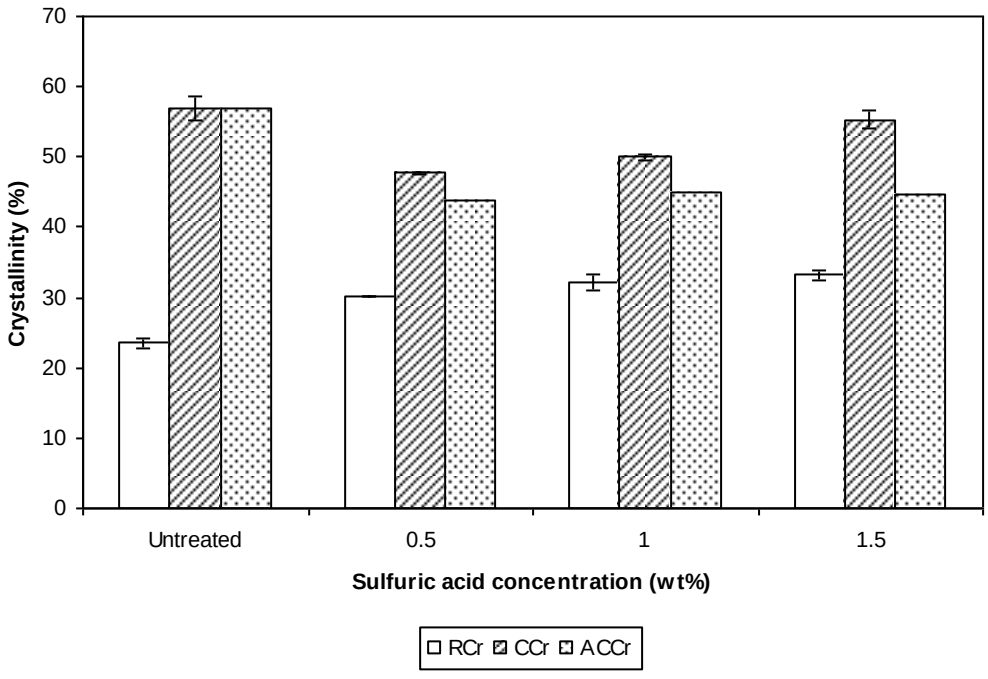

Figure 2.4 Comparison of crystallinity with different acid conditions (RCr, %: relative crystallinity based on whole dry mass; CCr, %: cellulosic crystallinity based on cellulose content; ACCr, %: adjusted crystallinity based on original cellulose content)

However, RCr failed to provide the detailed structure information about cellulose component, since the cellulose content, which is considered the only crystal contributor (Andersson et al. 2004), increased to about 65% after pretreatment (Figure 2.4). Thus, CCr was used to study the detailed structural change of crystalline cellulose. It was found that the CCr decreased after PS sorghum was treated with 0.5% acid (Figure 2.4). As shown in Figure 2.2, some cellulose was degraded to glucose. Thus, the decrease of CCr could be a result of change in crystalline cellulose. By calculating the change in both crystalline and amorphous parts with 0.5% acid treatment, it was found the decreased amount of crystalline cellulose (about 11.8% of initial cellulose content) was much more than that of degraded cellulose (about 7.68% of initial cellulose content) and the amorphous part increased at the same time, suggesting that some crystalline cellulose was changed to amorphous cellulose and was degraded to glucose simultaneously. Meanwhile, as acid concentration increased, CCr increased. According to the results from Figure 2.2, in which the percentage of degraded cellulose increased up to 4.4%, it is possible that the increase of CCr is the result of removal of amorphous cellulose in the solid part. To verify this assumption, ACCr was employed as mentioned in methods section. After pretreatment with 0.5% acid, the ACCr decreased from 57.0%, but it did not change significantly ($44.3 \pm 0.5\%$) as the acid condition changed (Figure 2.4). This finding suggests that the change of acid concentration from 0.5 to 1.5% did not change the crystalline structure of cellulose itself, but rather partially degraded the amorphous cellulose. Thus, the increase of EEH as acid concentration increased was not a result of the structural change of crystalline cellulose, but rather a result of the entire structural change of PS sorghum, including the removal of hemicellulose and lignin.

2.4.5 Morphological change of the PS sorghum

Unlike the structure of the pretreated sample (Figure 2.5c), the structure of the untreated sample was almost intact, excluding a few fractures that were considered as the result of grinding (Figure 2.5a and b). After pretreatment, many breaks were observed (Figure 2.5c), which suggests the lignocellulosic structure was highly disrupted. One possible reason for this result is that lignin, a main structural component in PS sorghum, was removed during acid treatment (data not shown). In addition, about 20% of the cellulose (Figure 2.2) was degraded at 1.5% acid concentration, which could be another reason for the disrupted structure. The presence of those

breaks made hemicellulose, which is generally buried in the lignin structure, more amenable to acid reaction. Composition test after pretreatment also showed that more than 90% of the hemicellulose was removed during pretreatment. Meanwhile, hollow areas, a result of removal of the inner parts of the plant cell wall, were observed. The significant amount of hollow areas suggests that enzyme-accessible surface area of cellulose increased, which could result in the relatively high EEH shown in Figure 2.3.

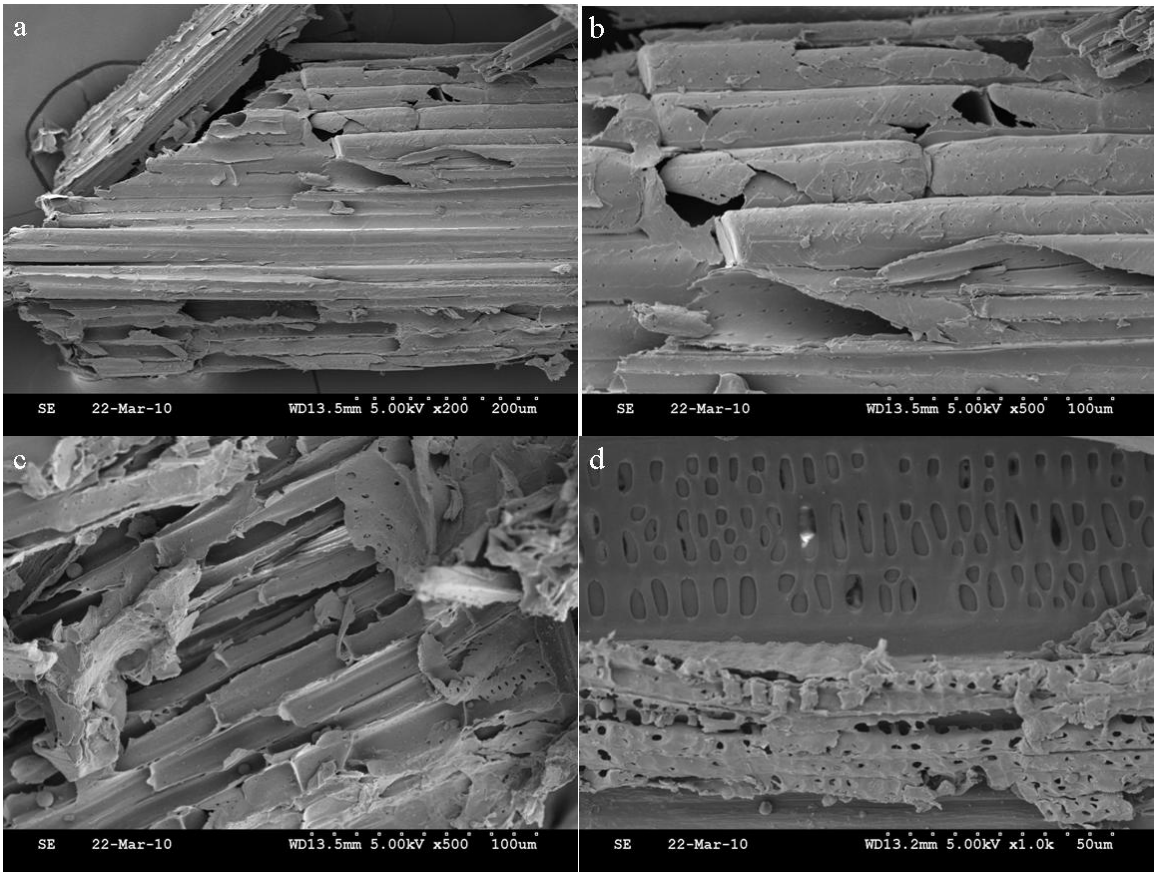

Figure 2.5 Scanning electron microscopy images of untreated (a, 200×; b, 500×) and acid treated (1.5%) samples (c, 500×; d, 1,000×).

2.4.6 Ethanol production with SSF

A SSF experiment was conducted to convert PS sorghum treated with the above optimal condition (160°C, 40min, 1% acid). As mentioned before, utilization of the soluble sugars in the PS sorghum is important for ethanol production. Thus, these soluble sugars in washing juice

were used proportionally for fermentation with pretreated PS sorghum, as shown in the flowchart (Figure 2.1). It was found that there was no significant difference in ethanol yield by comparing the effects of washing juice and synthetic juice on SSF. An 80% of ethanol yield during SSF could be reached by both approaches. The reason could be that those possible inhibitors (such as tannins and phenolic compounds) counteracted the positive effects of those nutrients (such as trace elements) in washing juice (Larsson et al. 2001; Pasha and Reddy 2005). Further study was needed to understand the effect of washing juice on yeast fermentation. The ethanol yield of SSF was about 90% in 72h assuming the same EEH (89.4%) was obtained. Glycerol, one of the byproducts, was found in fermentation broth as reported (Yazdani and Gonzalez 2007). This is one of the reasons why those sugar sources were not thoroughly converted to ethanol. The final ethanol yield was about 74.5% based on all available sugar sources (cellulose and soluble sugar) in original PS sorghum, which means that about 0.20 g ethanol could be produced from 1g PS sorghum under current processing conditions. A detail mass balance was provided as shown in Figure 2.6.

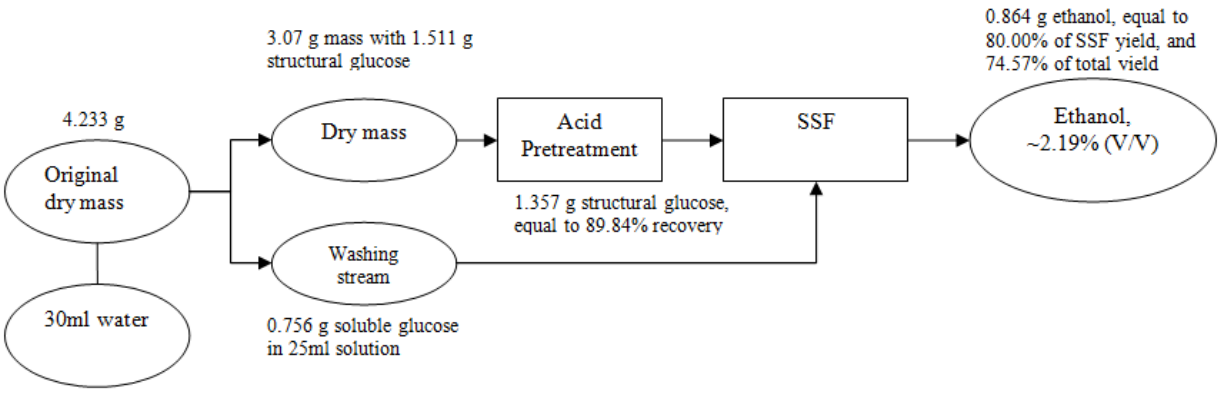

Figure 2.6 Mass balance of photoperiod-sensitive sorghum processing for ethanol production.

2.5 Conclusions

The composition of PS sorghum was determined for the first time, and the significant amount of soluble sugar as well as the low ratio of lignin to cellulose suggests PS sorghum has great potential for ethanol production. As determined by WAXD, the amount of crystalline

cellulose decreased after treatment with 0.5% acid. Further increase of acidic concentration did not change the amount of crystalline cellulose significantly but decreased the amount of amorphous cellulose. Scanning electron microscopy image suggested increase of surface area after pretreatment. SSF further showed a high conversion rate and ultimately produced about 0.20 g ethanol from 1 g PS sorghum.

Chapter 3 - Process optimization for ethanol production from photoperiod-sensitive sorghum: Focus on cellulose conversion[2]

3.1 Abstract

Photoperiod-sensitive sorghum, as a competitive biomass for ethanol production, was investigated to develop an integrated process for improving ethanol yield. Response surface methodology was employed to study the relationship between pretreatment variables (including temperature, sulfuric acid concentration, and reaction time) and cellulose recovery, as well as efficiency of enzymatic hydrolysis (EEH) in the solid part. Recovery yield decreased and EEH increased as the pretreatment temperature, acidic concentration, and reaction time increased. A model was successfully developed to predict total glucose yield with a maximum value of 82.2%. Conditions of co-fermentation were also optimized, and the optimal ethanol yield was obtained with constant-temperature simultaneous saccharification and fermentation (SSF) at 38°C. Acetate buffer at a concentration of 50 mM was found helpful for increasing efficiency of enzymatic hydrolysis, as well as ethanol yield. The maximum ethanol yield was 0.21 g ethanol per dry mass at the conditions of 38°C, 0.05 g yeast/L, and 50 mM acetate buffer. A complete cellulose balance was provided for the whole process.

3.2 Introduction

Production of ethanol from lignocellulosic biomass can effectively reduce the risk of food price increase because of sugar- or starch-based bioethanol production (Fargione et al. 2008; Tilman et al. 2006). Although corn stover has been studied for ethanol production (Zhu et al. 2009), the available amount of corn stover is not sufficient to support biorefineries with an annual production of 36 billion gallons of ethanol in 2022 (Graham et al. 2007). Photoperiod-sensitive (PS) sorghum, which can grow in semiarid parts of the world and especially in areas too dry for corn, contains a significant amount of soluble sugar and a low ratio of lignin to cellulose. These advantages make PS sorghum an excellent source for bioethanol production.

[2] This chapter has been published as a peer-reviewed research paper in the Journal of Industrial Crops and Products. 2011. 34(1):1212-1218.

Many studies about the effects of diluted sulfuric acid pretreatment on enzymatic hydrolysis of cellulose have been reported in which the acid pretreatment was proven effectively in removing most of the hemicellulose and some lignin component (Schell et al. 2003; Zhu et al. 2004). According to previous study on PS sorghum (Xu et al. 2011a), a harsher condition of pretreatment should be applied to make cellulose easily degradable, thus achieving a high efficiency (more than 90%) of enzymatic hydrolysis (EEH). Cellulose degradation during high temperature and diluted sulfuric acid pretreatment could be described as following. First, hydrogen bonds between glucan units are broken and cellulose is degraded to cellobiose and glucose, and cellobiose is not stable at acid condition and will be degraded to glucose. Glucose will further be degraded to form degradation products (Mosier et al. 2002), some of which are considered inhibitors to yeast fermentation (Klinke et al. 2004). Thus, it is more important to study the relationship between cellulose (glucose) recovery and EEH than to focus only on a high EEH because cellulose loss is not negligible even for mild pretreatment conditions (e.g., 143.2 °C, 0.4% sulfuric acid concentration and 30 min) (Bienkowski et al. 1987).

A previous study on diluted sulfuric acid pretreatment of PS sorghum has shown promising results: about 74% of the sugar source, including cellulose (structural glucose) and soluble sugar (sucrose, glucose, and fructose), could be converted to ethanol (Xu et al. 2011a). Thus, an in-depth investigation of how to maximize glucose yield is necessary to reveal the relationship between pretreatment conditions and total glucose yield from enzymatic hydrolysis. Response surface methodology (RSM) with the advantage of efficient design was employed in this study. Since PS sorghum contains a significant amount (about 17.5%) of soluble sugar, which can be easily degraded at high temperature and in acid conditions, a direct pretreatment will result in significant sugar loss. An integrated method was designed in this research to solve this problem: this method separates soluble sugar by washing the ground sample before pretreatment. The washing juice containing soluble sugar was then added to the pretreated sample for co-fermentation (Figure 3.1).

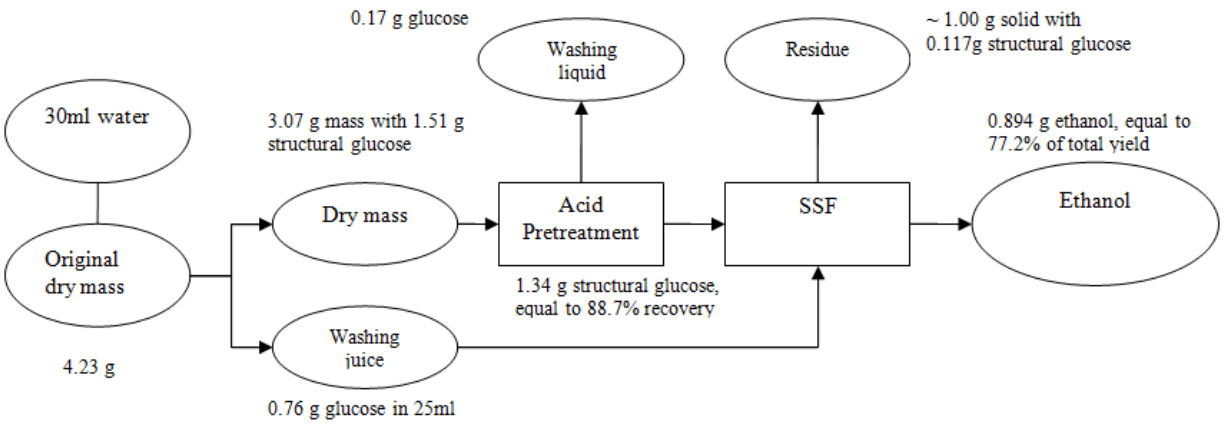

Figure 3.1 Cellulose balance of pretreatment and simultaneous saccharification and fermentation for ethanol production.

Although sugar- and starch-based ethanol fermentation has been studied for a long time (Inlow et al. 1988), these processes are different from cellulose-based ethanol fermentation. Simultaneous saccharification and fermentation (SSF) has been accepted in most biomass processing, since it saves energy and time and reduces end-product inhibition of enzyme hydrolysis (Wright et al. 1988). The low biomass loading, which varies depending on material characteristics and pretreatment method, makes it difficult for cellulose-based SSF to achieve a high ethanol concentration (more than 10 % (v/v)). Thus, for yeast fermentation of low sugar concentration and low ethanol concentration, substrate inhibition or end-product inhibition is not critical, because it was reported that ethanol begins to inhibit yeast fermentation at 25 g ethanol/L (Maiorella et al. 1983). Meanwhile, one of the current barriers preventing commercialization of lignocellulosic ethanol is its high processing cost. The optimization of cellulose-based fermentation is consequently supposed to include a mechanism for lowering processing cost. In this research, the optimization of SSF was balanced between ethanol yield and processing cost.

The objective of this study was to optimize the processing method, including both pretreatment and co-fermentation (SSF), for maximizing the ethanol yield from PS sorghum.

3.3 Materials and Methods

3.3.1 Material preparation and chemicals

The PS sorghum (1990/AC791) used in this research was harvested from the Kansas State University Agronomy Research Farm in Manhattan, Kansas, from 2007 to 2009. After being ground with a cutting mill (SM 2000, Retsch Inc., Newtown, PA) to less than 1 mm particle size, the sample with moisture content of 7% was stored at room temperature. The chemical composition of PS sorghum, analyzed by using the NREL procedure (Sluiter et al. 2004), is 32.5%, 19.8%, 11.7% and 17.5% for cellulose, hemicellulose, lignin, and soluble sugar, respectively. Before sulfuric acid pretreatment, the sample was washed with distilled water to separate soluble sugar and analyzed again for chemical composition. All chemicals used in this research were purchased from Sigma (Sigma-Aldrich, Inc., St. Louis, MO, USA).

3.3.2 Sulfuric acid pretreatment

A reactor (Swagelok, Kansas City Valve & Fitting Co., KS, USA) made from 316L stainless steel with a measured internal volume of 75 mL (outside diameter of 38.1mm, length of 125 mm, and wall thickness of 2.4 mm) was used for this study. A working volume of 50mL was used to allow space for expanding liquid water at high temperature during pretreatment. The loading of the prewashed PS sorghum was 6.1% (equal to 8.5% of original dry mass).

A sandbath (Techne, Inc., Princeton, NJ) with a temperature controller was used. After the sand was increased to a certain temperature, the reactor was submerged in boiling sand for different during according the experimental design presented in Table 3.1. Then the reactor was immediately transferred to room-temperature water to decrease the internal temperature to below 50°C in 2 min. All slurry removed from the reactor was washed, and the solid part was separated by filtration. Part of the solid mass from filtration was used for enzymatic hydrolysis, and the remaining part and the liquid part were used for composition analysis. Cellulose recovery yield (Y_{REC}) was defined as shown in Equation 3-1.

$$Y_{REC} = \frac{M_{pret} \times C_{pret}}{M_{OR} \times C_{OR}} \times 100\% \quad \textbf{[Equation 3-1]}$$

where M_{pret} is the dry mass weight after pretreatment, M_{OR} is the original dry mass weight, C_{pret} is the cellulose percentage of the solid part after pretreatment, and C_{OR} is the percentage of the cellulose in original dry mass.

Table 3.1 Experimental design with response surface methodology.

Trials	Temperature	Time	Concentration	EEH (%)[a]	Y_{REC} (%)[b]	Y_p (%)[c]
1	180	40	0.5	94.32	67.77	63.92
2	160	50	1.5	92.17	84.91	78.25
3	160	40	1	90.47	89.54	81.01
4	180	30	1	94.2	61.82	58.24
5	180	50	1	98.86	42.62	42.14
6	160	40	1	91.57	89.86	82.28
7	160	50	0.5	89.84	88.66	79.65
8	160	30	1.5	92.12	84.84	78.16
9	140	40	0.5	42.66	94.84	40.46
10	140	50	1	57.71	94.94	54.79
11	180	40	1.5	94.88	32.8	31.13
12	140	40	1.5	58.85	95.39	56.13
13	160	40	1	88.98	90.11	80.17
14	160	30	0.5	72.76	95.71	69.63
15	140	30	1	48.89	94.09	46

[a]EEH: Efficiency of enzymatic hydrolysis.
[b]Y_{REC}: Cellulose recovery yield during pretreatment at the solid part.
[c]Y_p: Total glucose yield during both pretreatment and hydrolysis.

3.3.3 Enzymatic hydrolysis

Accellerase 1500©, an enzyme complex including cellulase and β-glucosidase (Endoglucanase activity: 2200-2900 CMC U/g, one CMC U unit of activity liberates 1 μmol of reducing sugars [expressed as glucose equivalents] in 1 min under specific assay conditions of 50°C and pH 4.8), was generously provided by Genencor (Rochester, NY). The enzyme complex was used in this study at the recommended dosage (0.5 mL per gram cellulose). Enzymatic hydrolysis was conducted with the sample after pretreatment at 4% solids concentration (grams dry weight per 100 mL) in 50 mM sodium acetate buffer (pH 5.00) with addition of 40 μg/mL tetracycline and 30 μg/mL cycloheximide. Flasks were incubated in a water bath at 50°C and 140 rpm. Total monomer sugar analysis was conducted at the end of hydrolysis (72h) on supernatants using high-performance liquid chromatography (HPLC). EEH was defined as shown in the following calculation:

$$EEH = \frac{G_{EH} \times 0.9}{M_{EH} \times C_{pret}} \times 100\% \quad \textbf{[Equation 3-2]}$$

where M_{EH} is the weight of dry mass used in enzymatic hydrolysis (or SSF), G_{EH} is the glucose content after hydrolysis, C_{pret} is the cellulose percentage of the solid part after pretreatment, and

0.9 is the mass coefficient of glucose to cellulose (g/g). Total glucose yield (Y_p) was defined as the product of cellulose percentage in the solid part after pretreatment and EEH.

$$Y_P = \frac{EEH \times Y_{REC}}{100\%} \quad \textbf{[Equation 3-3]}$$

3.3.4 Simultaneous saccharification and fermentation

The same enzyme and buffer system were used in SSF as in enzymatic hydrolysis without antibiotics. Yeast (Ethanol Red, Lesaffre Yeast Corp., Milwaukee, WI) was prepared following the method reported elsewhere (Wu et al. 2010). Both concentrated washing juice and the pretreated solid were added together, and the initial fermentation system contained 4% (w/v) solids in 50 mL buffer solution (Figure 3.1). The constant-temperature (CT) SSF was conducted in an incubator shaker (Model I2400, New Brunswick Scientific Inc., Edison, NJ) at 38°C and 150 rpm, whereas the variable-temperature (VT) SSF was first conducted in a water bath for 6h at 50°C and then conducted in an incubator shaker at 30°C with inoculation for fermentation. Both CT-SSF and VT-SSF were conducted with 50 mM of acetate buffer. An HPLC was used to analyze the ethanol concentration and other end products. Fermentation yield (Y_{SFF}) and total ethanol yield (Y_{ETH}) for the biomass-ethanol production were calculated using the following equations (Equation 3-4 and 3-5):

$$Y_{SSF} = \frac{M_{EP}}{\left(M_{EH} \times C_{pret} \times 1.11 + M_{Hex}\right) \times 0.511} \times 100\% \quad \textbf{[Equation 3-4]}$$

$$Y_{ETH} = \frac{M_{EP}}{M_{TEP}} = \frac{M_{EP}}{\left(M_{OR} \times C_{OR} \times 1.11 + M_{Hex}\right) \times 0.511} \times 100\% \quad \textbf{[Equation 3-5]}$$

where M_{EP} is mass of ethanol after SSF, M_{TEP} is the theoretical value calculated from cellulose and soluble sugar, M_{Hex} is the total amount of soluble sugar (expressed as glucose equivalents), 0.511 is the mass coefficient of glucose to ethanol (g/g), M_{OR} is the original dry mass weight, C_{OR} is percentage of the cellulose in original dry mass, and 1.11 is the mass coefficient of cellulose to glucose (g/g).

3.3.5 Sugar and ethanol analysis

Monosaccharide and ethanol concentration were analyzed by using an HPLC with a Rezex RPM-monosaccharide column (300*7.8 mm; Phenomenex, CA) and a Refractive Index Detector (RID -10A, Shimadzu, MD). The column was eluted with double-distilled water at a

flow rate of 0.6 mL/min. The temperature of the chromatograph column was maintained at 80 °C.

3.3.6 Response surface methodology

Box–Behnken design was employed to optimize the processing conditions of pretreatment and hydrolysis. Three coded levels were used for those conditions: concentration of sulfuric acid, pretreatment time and temperature. The behavior of the system was explained by the following equation:

$$Y = \beta_0 + \sum \beta_i x_i + \sum \beta_{ij} x_i x_j + \sum \beta_{ij} x_i^2 \quad \textbf{[Equation 3-6]}$$

where β represents the coefficient for each term and x represents condition parameter. According to the results of previous experiments, the optimal condition for acquiring the highest total glucose yield (Y_p) could be in the range of 140 to 160°C, 30 to 50 min, and 0.5 to 1.5% for temperature, time and acid concentration, respectively. Table 1 shows the experiment design and corresponding results of EEH, Y_{REC}, and Y_p. Fifteen trials were performed in random order.

3.3.7 Statistics and softwares

Data were analyzed by using analysis of variance (ANOVA) and Tukey's studentized range (HSD) test in SAS (SAS Institute, Inc. Cary, NC, USA). RSM results were analyzed with Design Expert (Stat-Ease, Inc. Minneapolis, MN, USA). Mean values from the duplicated experiments were reported.

3.4 Results and discussion

3.4.1 Optimization of pretreatment and hydrolysis by RSM

Through analysis and optimization in Design Expert, three different models were obtained corresponding to the three response values. ANOVA was then conducted to remove insignificant terms. Finally, the three reduced models for EEH, Y_{REC}, and Y_p were obtained as shown (Equations 3-7, 3-8 and 3-9). The ANOVA for EEH showed that the model is highly significant (p-value < 0.0001), and the value of R-squared was 0.9877, indicating the regression model could provide good prediction. Lack-of-fit test was used to measure the failure of the model by representing data in the experimental domain at the points that are not included in the regression (Rastogi and Rashmi 1999). In this study, the test implied that lack-of-fit was

insignificant, which suggested the model fit the experimental data. The reduced model (Equation 3-7) for EEH suggested that the EEH increased as the variables (temperature, time and concentration) increased. During sulfuric acid pretreatment, the main structure was supposed to be disrupted (Zeng 2007), and most of the amorphous parts (hemicellulose and lignin) of PS sorghum were degraded or dissolved under certain conditions (Xu et al. 2011a). This could result in an increase of surface area of cellulose that was considered as an important parameter during enzyme hydrolysis (Fan et al. 1980). Many studies also have reported that EEH increased with surface area (Paakkari and Serimaa 1984; Puri and Pearce 1986), which could explain why EEH increased with those variables. The 3-D response surface image (Figure 3.2) suggested that the interaction between temperature and concentration was significant and the EEH would increase up to 100%, although the mass loss and/or cellulose loss would be significant (Table 3.1).

$$EEH = -1064.5 + 12.47 \times A + 0.2951 \times B + 103.3 \times C - 0.3908 \times A \times C - 0.03435 \times A^2 - 14.73 \times C^2$$ **[Equation 3-7]**

where A represents temperature, B represents time, and C represents acidic concentration.

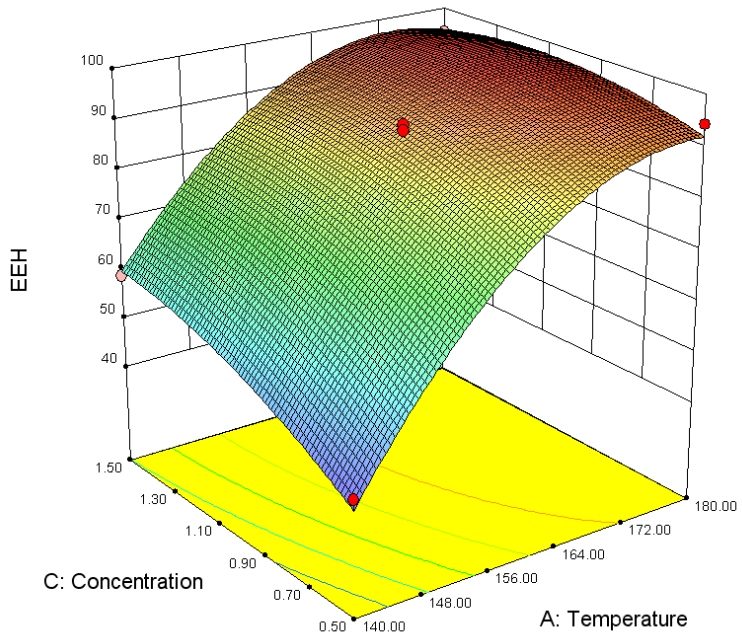

Figure 3.2 3-D response surface of the efficiency of enzymatic hydrolysis (EEH) in relation to temperature and concentration.

Although the glucose in the acid solution after pretreatment can be recovered by neutralization, the further degradation of glucose under harsher conditions would not only increase glucose (cellulose) loss, but also generate a significant amount of degradation by-products (such as hydroxymethylfurfural), some of which are considered inhibitors of yeast fermentation (Liu et al. 2004). Therefore, it may cost too much to recover either glucose or water in industry. For this consideration, it is important to limit cellulose loss and glucose degradation. Another reduced model was then obtained to study the cellulose recovery yield (Y_{REC}) (Equation 8). The ANOVA showed the model is highly significant. The lack-of-fit is insignificant and the R-squared value is 0.9849, indicating the regression model well represents the real relationships among those variables. The interaction between time and concentration was insignificant, whereas the interactions between temperature and time and the interaction between temperature and concentration were significant. From this model, Y_{REC} was found to decrease as those variables increased, which is entirely different from the case of EEH. This could be explained by understanding structural change during acid pretreatment. With pretreatment under mild conditions, the lignocellulosic structure was slightly disrupted and amorphous parts were partially removed; cellulose degradation to glucose is not significant since cellulose is embedded in the cell wall. With a strong pretreatment condition, the outside structure was seriously damaged, and cellulose loss or degradation increased with the increasing variables. Furthermore, as a result of cellulose degradation, glucose is amenable especially in low-pH, high-temperature conditions (Xiang et al. 2004), resulting in the decrease of cellulose recovery (including solid and liquid parts) during pretreatment.

$$Y_{REC} = -1041.8 + 13.65 \times A + 3.693 \times B + 129.8 \times C - 0.02506 \times A \times B - 0.888 \times A \times C - 0.04014 \times A^2$$ **[Equation 3-8]**

For yeast-ethanol fermentation, it is critical to obtain as high sugar (glucose) yield as possible. A high EEH without acceptable $Y_{REC,}$ and vice versa, could not be considered for application. Thus, the model for total glucose yield (Y_p) was generated to predict the best yield after pretreatment and hydrolysis. Since the experimental data for Y_p are calculated by multiplying EEH and Y_{REC}, a quadratic model may not fit the data well. A cubic model was then considered. ANOVA was conducted again to generate a reduced model (Equation 3-9). The interaction between temperature and time and the interaction between temperature and concentration were also significant (Figure 3.3). The lack-of-fit was insignificant and the R-

squared value was 0.9975. According to the cubic model, the highest glucose yield was expected to be 82.07% at the optimal condition of 157.7°C, 41.6min and 1.27% acid concentration. Further experiments at this condition were conducted and the expected value was obtained (82.2%), which means that RSM was used successfully in processing optimization.

$$Y_p = -193.26 - 1424.9 \times C + 0.06042 \times A \times B + 19.58 \times A \times C + 7.855 \times 10^{-3} \times A^2 - 0.02683 \times B^2 - 17.14 \times C^2 - 2.930 \times 10^{-4} \times A^2 \times B - 0.06494 \times A^2 \times C$$ **[Equation 3-9]**

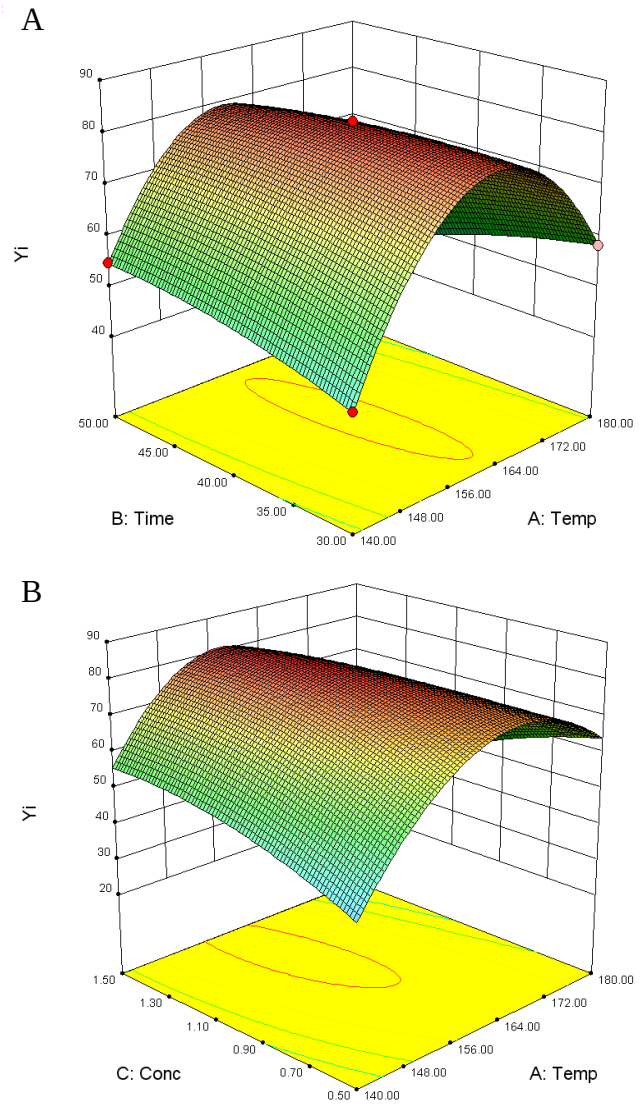

Figure 3.3 3-D response surface of total glucose yield in relation to (A) temperature and time, and (B) temperature and concentration.

In addition, for maximizing utilization of those available resources (including glucose and water) optimization of glucose yield is suggested to include both the solid and liquid parts after pretreatment (Equation 3-10). The undegraded glucose in solution was supposed to be added to SSF system for ethanol production. Then a neutralization of the filtrate after pretreatment could be suggested. However, the neutralized filtrate contains different compounds which could have complicated effects on yeast fermentation. The coefficient (k) that takes into account the negative effect was introduced, although it is not easy to obtain because of complicated interactions in SSF system. If the molecules degraded from glucose (such as HMF) have negative effects on yeast fermentation, the maxima of Y_p' and Y_p could be obtained at the same certain pretreatment condition in which glucose degradation is not significant (less than 0.5% of total glucan/cellulose, as found in the liquid with optimized pretreatment). In this case, the coefficient k tends to be equal to 1; then, Y_p could be used in this optimization for simplifying the calculation. In addition, depending on the substrate used in fermentation process, xylose also could be considered for optimization with this method, although it is not the focus of the present study.

$$Y_p^{'} = k\left(Y_p + Y_G\right) \quad \textbf{[Equation 3-10]}$$

where Y_G represents the glucose amount degraded from cellulose in liquid after pretreatment; Y_p' represents the total glucose amount that could be efficiently converted to ethanol by yeast, and the coefficient k represents the negative effects (inhibitors) to yeast-ethanol fermentation.

3.4.2 Effect of temperature and inoculation on SSF

Ethanol yields were previously compared by performing a separate fermentation in which the washing juice and solids were used for fermentation (or SSF) separately and a co-fermentation in which the washing juice and solids were mixed together. The results showed that there were no significant difference in the total ethanol yield between the separated fermentation and co-fermentation (data not shown). Then different inoculation amounts and SSF temperatures were investigated (Figure 3.4). In CT-SSF at 38°C, initial ethanol production was found at 2 h, and the initial conversion rate in the first 6 h increased as the inoculation amount increased. The highest ethanol yield (894 mg) was found with an inoculum of 0.05 g (dry yeast cells)/L (Fig. 4a). Although a longer lag phase was found with this inoculation, more than 95% of final ethanol yield was obtained in 27 h, indicating that the small amount of inoculum (0.05 g/L) is sufficient

for fermentation of current substrate loading at a low cost. The ethanol yields with inoculation amounts of 0.1 g/L and 0.2 g/L were relatively lower than that with inoculation amount of 0.05 g/L, which was also found in VT-SSF (Figure 3.4b). The reason could be that the initial sugar concentration was relatively low (about 15 g/L) compared with high-loading starch-based fermentation. No soluble sugar was detected after 24 h, indicating the consumption rate of glucose was higher than the hydrolysis rate. In this case, the larger yeast inoculum could be consuming more sugar initially for non-fermentative pathways. Future study of variation in viable yeast cells during SSF is suggested to understand kinetics of cell growth. Since there was no significant difference occurred in ethanol yield after 48 h with 0.05 g/L inoculation, the SSF could be finished in less than two days, thus reducing processing cost.

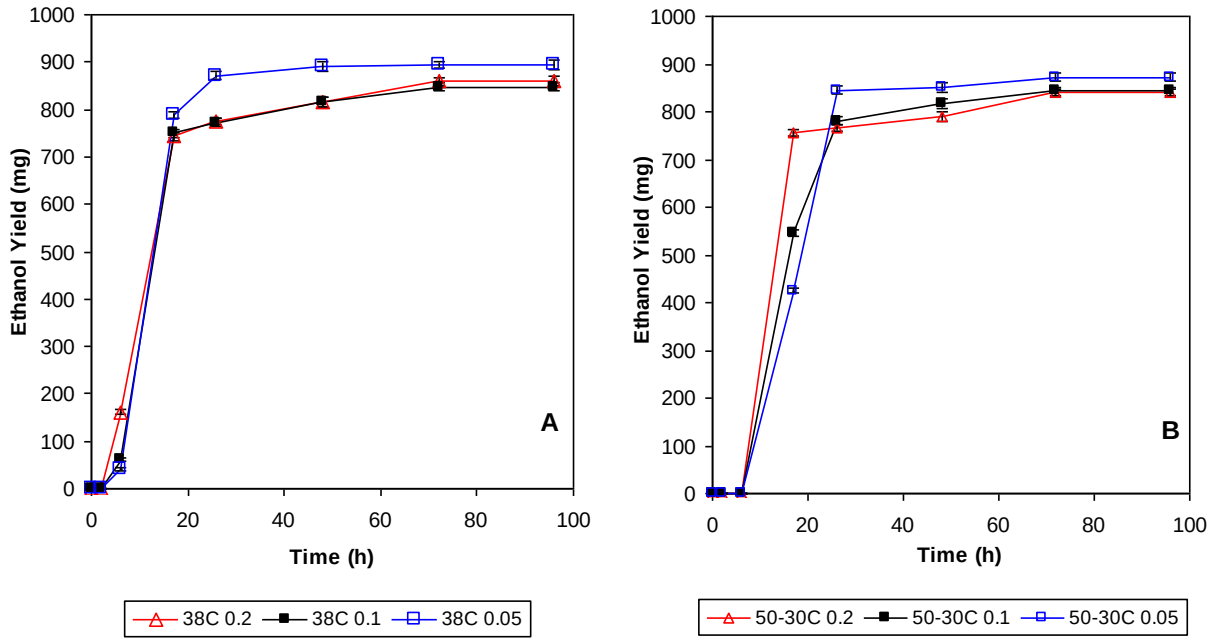

Figure 3.4 Effect of inoculation on constant-temperature (38°C) simultaneous saccharification and fermentation (SSF) (A), and variable-temperature SSF (50°C for 6h enzymatic hydrolysis and 30°C for SSF) (B).

For VT-SSF, the effect of inoculation amount on ethanol fermentation was similar to that of CT-SSF. The optimal temperature for yeast-ethanol fermentation was reported to be 30 °C (Lin and Tanaka 2006). In this study, however, the final ethanol yield of VT-SSF, in which ethanol fermentation was conducted at 30°C, was lower than that of CT-SSF (38 °C) with the

same inoculum. Considering the fact that the enzymatic hydrolysis could not finish in the first 6 h at 50°C, we suggest that the reason for low ethanol yield could be the low activity of cellulases at 30°C during the subsequent hydrolysis. Composition test of the residues after SSF was conducted to verify the hypothesis. The results showed that the cellulose amount in the residue after VT-SSF was 5.8% higher than that in the residue of CT-SSF, indicating that the EEH of VT-SSF was lower than that of CT-SSF, which ultimately resulted in the lower ethanol yield.

3.4.3 Effect of buffer (acetic acid) on SSF

Acetic acid has been reported to inhibit yeast fermentation because acetate is considered soluble in the lipids of yeast cell membranes, which results in membrane disruption and affects the membrane transport of phosphate (Conway and Downey 1950). However, by comparing the ethanol yield of SSF with different buffer concentrations, we found that the ethanol yield of 900 mg occurred at 100 mM buffer concentration (about 34 mM acetic acid), and the lowest ethanol yield occurred with no buffer (Figure 3.5). The increase in ethanol yield could be explained by the increase in requirement of adenosine triphosphate (ATP) (Maiorella et al. 1983). When acetic acid exists at a low concentration, the negative effect of membrane disruption on yeast cells is not significant, and yeast cells are supposed to pump the protons out of the cells to neutralize intracellular pH, and the ATP needed to accomplish this procedure could be obtained from ethanol formation in anaerobic environment. When a higher concentration of acetic acid (200 mM buffer, equal to 68 mM acetic acid) is applied, however, the membrane of yeast cell is disrupted to a higher degree and membrane transport of phosphate is significantly affected, which ultimately results in a decreased ethanol yield. For the SSF without buffer, the final pH was found to be 3.55, which is significantly lower than the pH range (4.8 to 5.0) needed to maintain enzyme (cellulase) activity. Thus, the EEH may decrease with low enzyme activity. This could be one of the reasons for the decrease in ethanol yield. To verify this assumption, we conducted a composition test after fermentation. The undigested cellulose after SSF without buffer was 30.3% more than that after SSF with 50 mM buffer, which confirmed that the buffer system is helpful in improving ethanol yield. Since no significant difference occurred in the ethanol yield between 50 mM and 100 mM, we suggested using 50 mM to reduce cost.

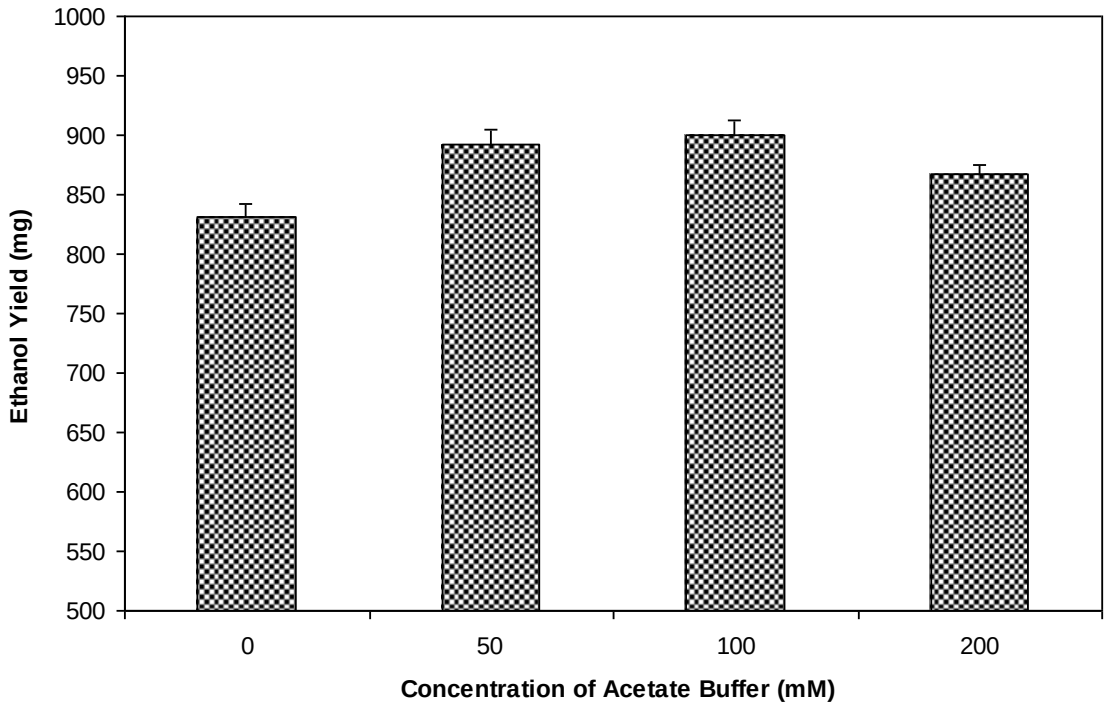

Figure 3.5 Effect of acetate buffer concentration on ethanol yield.

3.4.4 Cellulose balance

A detailed cellulose (glucose) balance, as well as mass balance, for the whole conversion process at the optimal conditions is shown in Figure 3.1. About 88.7% of cellulose could be recovered in the solid part for the following SSF after the optimal pretreatment process. Under the conditions of 38°C, 50 mM acetate buffer, and 0.05 g/L yeast inoculation, 77.2% of the total sugar source (including cellulose and soluble sugar) could be converted to ethanol with SSF. The total ethanol yield was 894 mg after 72 h of co-fermentation from 4.23 g PS sorghum (about 0.21 g ethanol per gram dry mass).

3.5 Conclusions

The sulfuric acid pretreatment and enzymatic hydrolysis of PS sorghum were optimized together using RSM, and three models were obtained successfully for analysis. The maximum glucose yield from the solid part is 82.2%. Cellulose recovery from the solid part decreased and EEH increased as the pretreatment temperature, resident time, and acidic concentration

increased. The optimization on SSF suggested that the conditions of 0.05g/L inoculation and 38°C CT-SSF were effective for ethanol production (894 mg/50mL, 2.3 %(v/v)). Acetate acid was found to affect ethanol fermentation, and the optimal buffer concentration is 50mM. Under the optimal process conditions, 77.2% of total sugar source could be converted to ethanol, which is equal to a final yield of 0.21g ethanol/g dry mass. Further study of obtaining concentrated ethanol in final broth is suggested to reduce recovery cost.

Chapter 4 - Structural features and changes of lignocellulosic biomass during thermochemical pretreatments: A synchrotron X-ray scattering study on photoperiod-sensitive sorghum[3]

4.1 Abstract

Fundamental understanding of the structural changes during pretreatment of lignocellulosic biomass could lead to improved processes and cost reductions for bioethanol production. Synchrotron wide-angle X-ray diffraction (WAXD) and small-angle X-ray scattering (SAXS) were used to study the structures of different parts of photoperiod-sensitive sorghum and structural changes during various pretreatments. Wide-angle X-ray diffraction study showed that the PS sorghum rind had oriented crystal peaks and the highest degree of crystallinity, whereas the crystalline structures of the inner pith and leaf were less ordered. Orientation distribution of cellulose changed during pretreatments. Crystalline cellulose was degraded partially by acid pretreatment and a smooth pore-boundary surface structure of cellulose was noted by SAXS. Alkali pretreatment transformed part of the cellulose to a more stable form and increased the crystal size of cellulose. The study provides information on a large length scale to understand how structure changes with different pretreatments.

4.2 Introduction

Lignocellulosic biomass has become an important source for production of bioethanol and other products (Mielenz 2001). Photoperiod-sensitive (PS) sorghum, with the advantages of high biomass yield and drought tolerance, can be grown in semiarid areas that are too dry for corn growth (Alagarswamy et al. 1998; Clerget et al. 2008; Rosenow et al. 1983). The low lignin content in PS sorghum makes it competitive for biofuel production (Xu et al. 2011a).

Pretreatment, including physical size reduction and chemical reaction, is important for cellulosic ethanol production because, unlike starch-ethanol production, cellulose in biomass is usually embedded in a network structure (Rubin 2008). Lignin, one of the amorphous

[3] This chapter has been published as a peer-reviewed research paper in Carbohydrate Polymers. 2012. In press. (http://www.sciencedirect.com/science/article/pii/S0144861712000616)

components, acts as a cellulase absorber during enzymatic hydrolysis (Berlin et al. 2005; Hidaka et al. 1984), which significantly increases processing cost and makes biomass conversion less effective. A successful pretreatment would maximize all available biomass components for economical processing. Different pretreatment strategies have been proposed for biomass processing, some of which have proven effective (Mosier et al. 2005b); however, profitable commercialization of cellulose-ethanol production is still lacking. Knowing the detailed structural features of lignocellulosic biomass and the structural changes during pretreatment would help develop effective ways to reduce pretreatment costs.

Until now, the effects of pretreatment on changes at the molecular level have not been fully understood. Wide-angle X-ray diffraction (WAXD) has been used for a long time in studying the crystalline structure of cellulose (Nishiyama et al. 2002) and has been used frequently for the study of crystalline structure in biomass processing (Oh et al. 2005). For samples with crystal orientation, such as natural cellulose in biomass, crystals generate certain aligned arcs in a 2D WAXD pattern, which provides much more information about 3D structure order (Burger et al. 2010). Previous X-ray studies on biomass focused primarily on powder diffraction, and no detailed study is available on orientation discrepancy as well as orientation changes during biomass processing. Small-angle scattering techniques, including small-angle neutron scattering (SANS) and small-angle X-ray scattering (SAXS), are able to probe structures over a size ranging from approximately 1 nm to several hundred nanometers, larger than those found with WAXD, and have been applied to the study of synthetic and natural polymers (Blazek and Gilbert 2011; Chu and Hsiao 2001). However, only limited SAXS studies have been reported on biomass structure (Lichtenegger et al. 1999). Recently, SANS has been used to study cellulose extract from switchgrass (Pingali et al. 2010a) and cell wall nanostructure in dilute acid pretreated biomass (Pingali et al. 2010b). The diameter of cellulose fibrils was reported to be 2.5 nm in sprucewood (*Picea abies*) through SAXS study (Jakob et al. 1994). In addition, SAXS has been used to study individual components including cellulose and lignin (Astley and Donald 2001; Canetti et al. 2006; Nishiyama et al. 2002; Vickers et al. 2001). Therefore, SAXS could be a useful tool to study the effects of different pretreatments on biomass structure. Synchrotron radiation, with the benefits of a high ratio of signal to noise and high intensity, has been employed in a number of studies (Yu et al. 2003). The small beam divergence of incident X-ray and the high-energy source of synchrotron X-ray enable the performance of advanced

experiments. The synchrotron X-ray allows completing data collection in less than one minute, making possible real-time monitoring of structural changes.

In this study, we used a combination of WAXD and SAXS to reveal the structure of lignocellulosic biomass, including multiple components in both crystalline and amorphous state. Instead of ground powder, we used biomass chips, making it possible to reveal crystal orientation distribution changes and their effects on subsequent biomass processing. For the first time, the structure of different parts of PS sorghum and structural changes during pretreatments were studied by both WAXD and SAXS. The objectives of this study were to understand the structural differences of the parts of PS sorghum, and to study how their structures change during pretreatments at a molecular level using WAXD and SAXS.

4.3 Materials and methods

4.3.1 Materials

The PS sorghum was harvested at physiological maturity from Riley County, Kansas. Different parts of the biomass, including rind, pith, and leaf, were obtained from three strains for comparison and prepared by knife-cutting and air-drying in an oven at 50 °C for 12 h. A detailed explanation of the three biomass parts is depicted in Fig. 1. The samples of PS rind and pith were cut from PS stalk between internodes. All chemicals used in this research were of analytical grade and purchased from Sigma-Aldrich, Inc. (St. Louis, MO, USA).

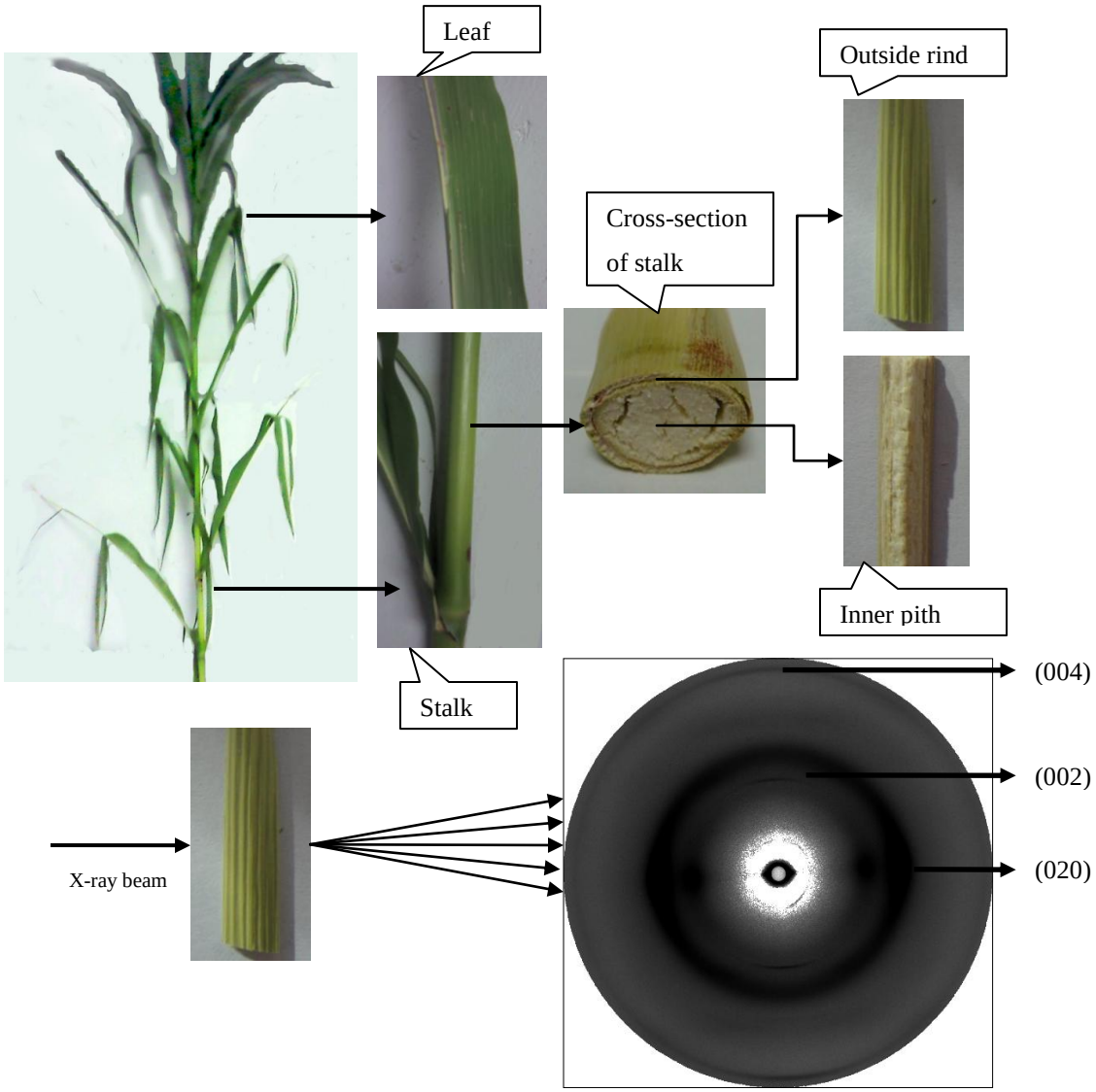

Figure 4.1 Illustration of photoperiod-sensitive sorghum in different parts and a typical 2D wide-angle X-ray diffraction pattern of chip.

4.3.2 Pretreatments

Pretreatment of biomass was conducted under different conditions (Silverstein et al. 2007b). A small piece of chip, with a surface dimension of 0.5 × 2 cm, was loaded into 10 ml chemical solution for pretreatment. For acid pretreatment, a chip sample was loaded into a pressure tube (No. 8648, Ace Glass Inc., Vineland, NJ, USA) containing 2% (w/w) sulfuric acid solution, the temperature was increased to 120°C, and the solution was held at this temperature

for 1 h. For alkali pretreatment, a chip sample was loaded into a pressure tube containing 1% (w/w) of sodium hydroxide and the temperature was maintained at 90°C for 2 h. For ammonia pretreatment, a chip sample was loaded into a pressure tube containing 10% (v/v) ammonia solution and the temperature was then maintained at 90°C for 2 h. All the pretreatment experiments were done in triplicate. After pretreatment, the solid samples were air-dried (~8% moisture content) for X-ray testing, and the solutions were subjected to reducing sugar analysis with high performance liquid chromatography, as previously reported (Xu et al. 2011a). In addition, the biomass chips were determined for mass loss after pretreatments.

4.3.3 Synchrotron WAXD and SAXS

Wide-angle X-ray diffraction and SAXS experiments were carried out at the advanced polymers beamline (X27C), National Synchrotron Light Source, Brookhaven National Laboratory, in Upton, NY. Details of the experimental setup at the X27C beamline have been reported elsewhere (Chu and Hsiao 2001). The wavelength used was 0.13714 nm. The sample-to-detector distance was 129.3 mm for WAXD and 1789.3 mm for SAXS, respectively. A 2D MAR-CCD X-ray detector (MAR USA, Inc.) was used for data collection. For X-ray study of chips, the direction of the X-ray is perpendicular to fiber direction. Three locations along fiber direction in each chip were used for measurement.

4.3.4 Data processing

Two dimensional WAXD patterns were first corrected with air background, then performed with Fraser correction using Polar software (Precision Works, NY) (Ran et al. 2002). The orientation of cellulose was analyzed from the 2D corrected pattern, and crystallinity and crystal size were estimated from the integrated 1D diffraction intensity profile. Crystallinity (mass crystallinity if not specified, percentage of crystalline cellulose in biomass) was estimated from an integrated diffraction intensity profile as the ratio of the total crystal peak diffraction intensity to the total diffraction intensity. A peak-fitting process was employed with Igor Pro 6.20 (WaveMetrics Inc. Lake Oswego, OR). The monoclinic crystal system was assumed to be the crystal unit of cellulose I_β (Heiner and Teleman 1997). Crystal size along and perpendicular (an axis of unit cell) to the fiber direction (c axis) were estimated from planes (004) and (020), respectively (Equation 4-1). Since the Bragg reflection may be broadened by both crystallites

with finite size and possible imperfections in crystal lattice, the equation here could be used only as a lower bound estimation of crystal size.

$$L_{w(hkl)} = \frac{K\lambda}{FWHM_{2\theta}\cos\theta} \quad \textbf{[Equation 4-1]}$$

where θ is the Bragg angle corresponding to the plane, K is the constant of 0.9 for cellulose (Alexander 1954), λ is the wavelength, and $FWHM_{2\theta}$ is the full width at half maximum of the reflection in the radial direction.

For crystal orientation analysis, it was assumed that the cellulose in biomass is cylindrically symmetrical similar to a fiber-like system. Thus, the orientation parameter could be calculated with plane (020) as described elsewhere (Burger et al. 2010). The Hermans' orientation parameter $\overline{P}_2$ varies from 0 for completely isotropic systems to 1 for perfectly oriented systems.

Two-dimensional SAXS data was first corrected with air background, then integrated into 1D intensity data. The 1D data was analyzed using Igor Pro 6.20 with the Irena package. The unified equation was used for analysis of SAXS data (Beaucage 1995). The equation defines multiple levels, and each level may contain Guinier region describing an average structural size and power-law region describing the mass or surface fractal. The unified model is given by:

$$I(q) = G_i \exp\left(-q^2 R_{gi}^2/3\right) + B_i \exp\left(-q^2 R_{g(i-1)}^2/3\right) \times \left\{\left[erf\left(qR_{gi}/6^{1/2}\right)\right]^3/q\right\}^{Pi} \quad \textbf{[Equation 4-2]}$$

where i represents the structural levels; G_i is the exponential prefactor; R_{gi} is the radius of gyration; B_i is a constant prefactor specific to the type of power-law scattering, P_i; and the magnitude of the scattering vector is defined as $q = 4\pi \sin\theta/\lambda$ (θ is half of the scattering angle).

4.4 Results and discussion

4.4.1 Structure features in different parts

4.4.1.1 WAXD study

A typical 2D WAXD pattern of lignocellulosic biomass is shown with indexed peaks (Figure 4.1). We compared the samples from three strains of PS sorghum and found that the crystalline structure of the different strains were identical. Three parts of PS sorghum (rind, pith, and leaf) were chosen as objects in this research. The crystal of the PS sorghum rind contained a

significant oriented portion (020 plane) that was not observed in the other patterns (Figure 4.2) because they were isotropic. Note that the reflections here were indexed (Figure 4.1) according to the monoclinic two-chain unit cell (Gardner and Blackwell 1974). The oriented pattern showed the features of native cellulose (I) in the plant as previously reported (Jakob et al. 1995; Konnerth et al. 2009; Nishiyama et al. 2002). The Hermans' orientation factor was then calculated as shown in Table 4.1. Generally, the orientation factor for a perfectly oriented system is 1. In this case, the factor of the PS sorghum rind is 0.26, indicating that the natural cellulose in the rind has oriented structure, whereas the cellulose structure in sorghum pith and leaf was isotropic with factors close to zero. The oriented pattern was only observed from the PS sorghum rind, suggesting that the structural order of cellulose in different parts of PS sorghum is different. Crystal orientation was reported to be related to the mechanical properties of polymer (Britton et al. 2010; Gurarie et al. 2002), but it is not yet clear how the mechanical properties of certain biomass is correlated to the orientation characteristics of cellulose. The difference in cellulose assembly between the different plant parts may influence the downstream processing of biomass conversion such as enzymatic hydrolysis. Study of the effects of the preferred orientation on processing is suggested for improving processing efficiency and for development of plant breeding strategies. Compared with the strong crystalline pattern of PS sorghum pith, the diffraction circle of the leaf is diffused, indicating an increased amount of amorphous components in the leaf, as confirmed by the crystallinity study below.

Table 4.1 Crystallinity, crystal size, and orientation factor of photoperiod-sensitive sorghum in different parts estimated from the wide-angle X-ray diffraction.

	Crystallinity (%)	Crystal size (020) (nm)	Hermans' orientation factor $\overline{P}_2$
Rind	29	2.49	0.26
Pith	24	2.45	0.08
Leaf	10	2.62	0.06

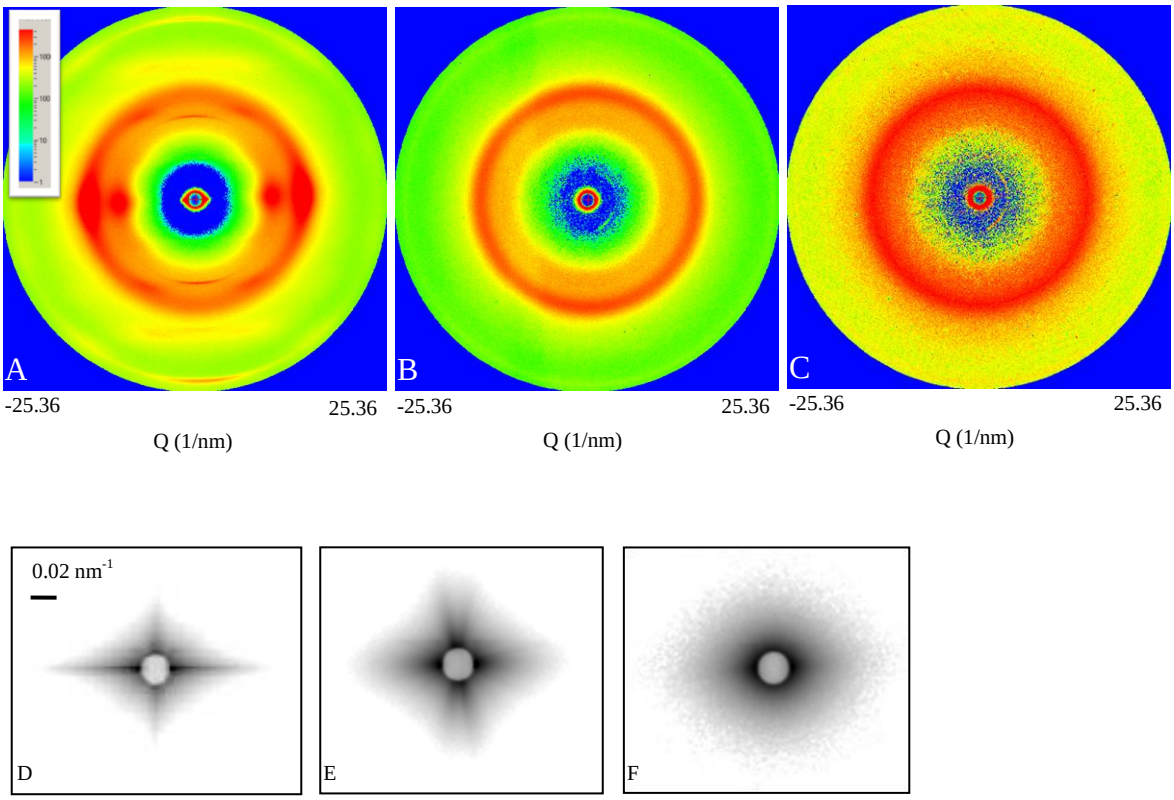

Figure 4.2 Wide-angle X-ray diffraction (WAXD) and small-angle X-ray scattering (SAXS) patterns of photoperiod-sensitive sorghum in different parts (WAXD, A: outside rind; B: inner pith; C: leaf; SAXS, D: outside rind; E: inner pith; F: leaf).

One-dimensional profiles were then obtained by integrating the corrected 2D pattern. Notably, for the oriented pattern, the integration of the 2D pattern without Fraser correction would result in significant deviation (Ran et al. 2002). Different crystal peaks were deconvoluted from the diffraction plot with a peak-fitting process. Crystallinity and crystal size were then calculated (Table 4.1). The PS sorghum rind had the highest crystallinity (29%) among those samples, whereas the leaf had a low crystallinity (10%). Crystallinity is considered an important index related to mechanical properties (Gassan and Bledzki 1999), and a high crystallinity could be one of the reasons for increasing the cost of size reduction. Different parts of PS sorghum exhibited no significant difference in crystal size (plane 020) (Table 4.1). Similar results were also reported about the crystal size (plane 020) of lemon and maize cellulose (Rondeau-Mouro et al. 2003). Since other factors may broaden the peak that was used for crystal size estimation, such as internal lattice defects, the estimates here are minimal.

4.4.1.2 SAXS study

SAXS study of biomass parts is reported here for the first time. The 2D SAXS patterns of different parts of PS sorghum were significantly different (Figure 4.2). Anisotropic patterns were found with both rind and pith parts, indicating oriented structure of biomass on this length scale (Jungnikl et al. 2008). For PS sorghum rind, both equatorial streak and meridional streak were shown on the SAXS 2D pattern (Figure 4.2D). The elongated shape of the equatorial streak indicated that microvoids were needle-shaped and aligned parallel to the fiber direction (Chen et al. 2007). The meridional scattering suggested that periodic lamellar structure existed between the crystalline and amorphous regions (Chen et al. 2007). It is possible that there are two directions of microvoids in pith that are vertical to each other. For PS sorghum pith, the meridional streak, unlike the equatorial streak, was found to be splitting. The similar split pattern in equatorial direction was also reported in SAXS pattern of latewood as a result of the existence of microfibril angle (Jakob et al. 1994; Lichtenegger et al. 1999), suggesting that tilted microvoids are perpendicular to the c axis (fiber direction). The evidence here, however, is not sufficient to support the particular structure of PS pith. Complementary structure technologies are needed for further investigation. The periodic interval along the microfibrils, which could be estimated from the position of the maximum scattering in the meridional direction (Chen et al. 2006), was about 178 nm for the PS sorghum rind. This value was close to a microfibrils periodic interval of 150 nm for ramie cellulose (Nishiyama et al. 2003). In this study, the PS sorghum rind did not give any peak corresponding to 6-7 nm repeat reported on flax (Astley and Donald 2001). For PS sorghum leaf, no significant streak in either direction was observed. The diffused SAXS leaf pattern, together with the WAXD pattern, suggested that the structure of the leaf was less ordered.

One-dimensional SAXS profile was then obtained by integrating 2D patterns for analysis, and the P values in the power-law region of the different parts were calculated to be in the range of 3.5-4.0, indicating that the materials are surface fractals (Koberstein et al. 1980; Schmidt 1991).

4.4.2 Effects of pretreatments on PS rind

4.4.2.1 WAXD study

The effects of different pretreatments on the structure of PS sorghum rind were studied to reveal how chemicals changed the biomass structure at a molecular level, such as cellulose structure in orientation distribution and crystalline characteristics. With the acid pretreatment, the 2D pattern changed (Fig. 3) and the orientation factor (P_2) decreased (Table 4.2), indicating that the spatially ordered cellulose was distorted. However, the orientation factor increased with both the alkali and ammonia pretreatment. With the alkali pretreatment, new crystal peaks were found at 2θ angle of 26.7° and 28.7° in the 1D plot (corresponding to the circles in the 2D pattern of Figure 4.3C), which are the diffraction of chemicals (e.g., Na_2CO_3) during the alkali pretreatment (Gancy 1963). A new oriented pattern (plane 103) was found, that was not shown in the WAXD pattern of cellulose I (Figure 4.3A&C) and was reported in the WAXD pattern of cellulose II (Chen et al. 2007). The new oriented peak is one reason why the orientation factor increased; however, the alkali treatment conditions used in this study were too mild to completely convert cellulose I in the PS sorghum rind to cellulose II, which is a more stable form with antiparallel chain structure in NaOH solution (Aravindanath et al. 1986; Kolpak and Blackwell 1976). For biomass system, the removal of lignin by the alkali pretreatment could result in an increase in the accessible area of cellulose and a decrease in the amount of cellulase absorbed on lignin, which is favored for improving the efficiency of enzymatic hydrolysis. The partial transition of cellulose to a stable form, however, could increase the resistance of cellulose to cellulase reaction. Notably, the transition of cellulose usually takes place with the change of cellulose crystallinity (percentage of crystalline cellulose in cellulose), which is another factor affecting enzymatic hydrolysis. Thus, the extent of enzymatic hydrolysis is affected by multiple factors.

Table 4.2 Crystallinity, crystal size, and orientation factor of photoperiod-sensitive sorghum with different pretreatments.

	Crystallinity (%)	Crystal size (nm)		Hermans' orientation factor $\overline{P}_2$
		(020)	(004)	
Untreated	29	2.49	2.75	0.26
Acid treated	32	2.52	2.74	0.21
Alkali treated	32	2.86	3.13	0.32
Ammonia treated	39	2.47	2.64	0.33

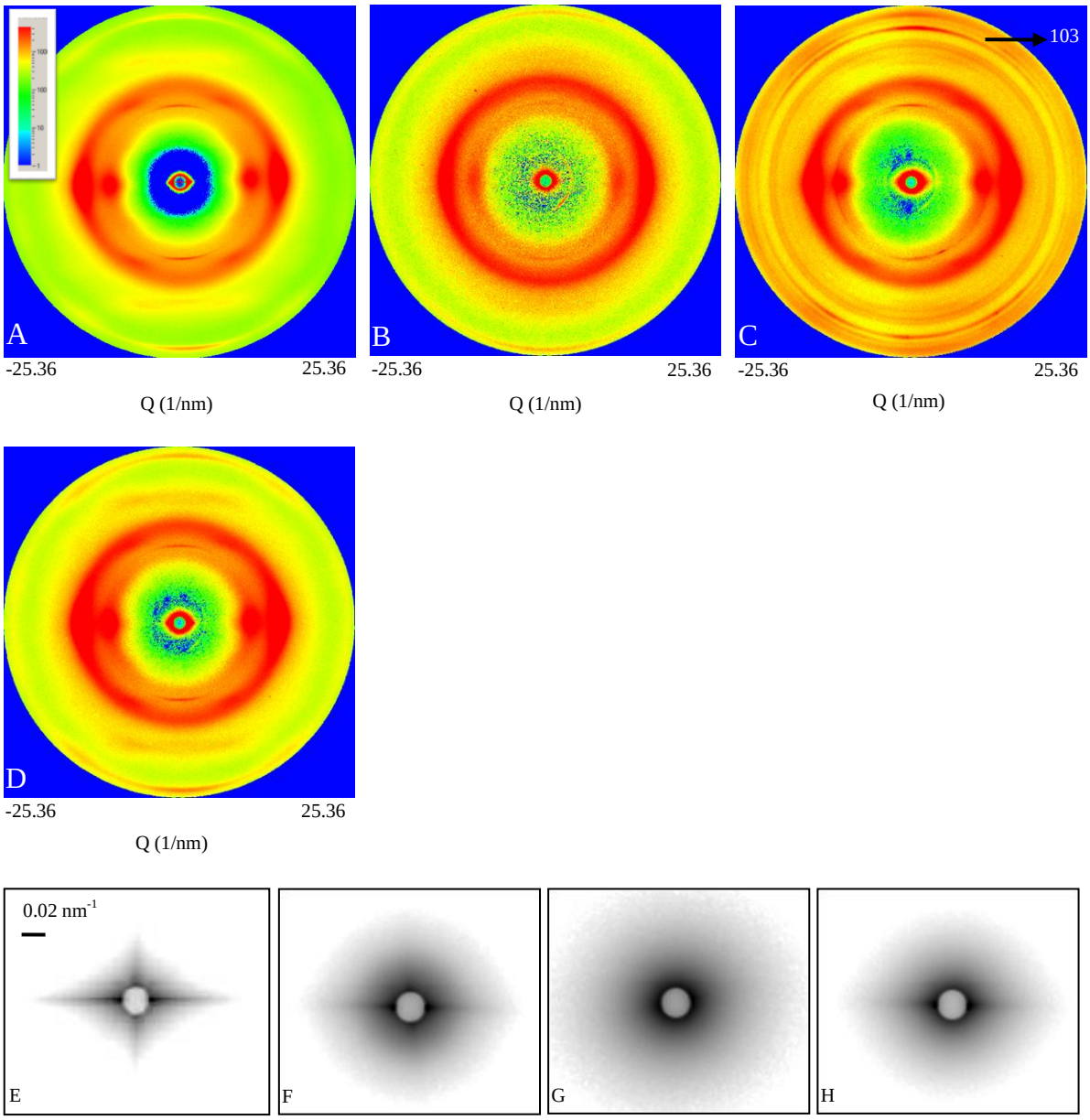

Figure 4.3 Wide-angle X-ray diffraction (WAXD) and small-angle X-ray scattering (SAXS) patterns of photoperiod-sensitive sorghum rind with different pretreatments (WAXD, A: untreated; B: acid treated; C: alkali treated; D: ammonia treated; SAXS, E: untreated; F: acid treated; G: alkali treated; H: ammonia treated).

Crystallinity increased after all the pretreatments. Since a significant mass loss (about 30%) was found after the acid pretreatment and both glucose and xylose were detected in the solution (data not shown), the increase in crystallinity could be a result of the removal of amorphous parts, including hemicellulose and amorphous cellulose. Considering that the

crystallinity increased only 4% and the mass loss was about 30%, we believe that part of the crystalline cellulose was hydrolyzed by acid and crystalline structure might have changed, which could be related to the decrease in orientation factor. More detail will be discussed in section 4.4.2.2. Lignin extraction by NaOH is one of the reasons for increased crystallinity with the alkali pretreatment. In addition, recrystallization was reported to take place during the mercerization (Hermans et al. 1950; Kroon-Batenburg et al. 1996). For the ammonia pretreatment, depolymerization of lignin, which resulted in lignin removal from biomass to solution (Balan et al. 2009), could be one cause of an increase in crystallinity (Mosier et al. 2005b).

The 2D WAXD patterns showed that the alkali pretreatment changed the crystalline structure significantly. Compared with the untreated sample, the crystal sizes of cellulose in both planes (020) and (004) increased significantly (Table 4.2). This could be explained by the aggregation of cellulose in NaOH solution. An increased temperature (90 °C, in this case) favored cellulose aggregation (Roy et al. 2003). The effect of crystal size on enzymatic hydrolysis is not yet known, but the aggregation of cellulose could decrease the accessible surface area of cellulose. Therefore, as discussed in cellulose transition, the structural change of cellulose itself by the alkali pretreatment might not be helpful for enzymatic hydrolysis.

4.4.2.2 SAXS study

After the ammonia pretreatment, the elongated shape in the equatorial direction was reduced (Figure 4.3), indicating that microvoids were reduced during the pretreatments. The elongated shape almost disappeared after the alkali pretreatment, indicating a decrease in orientation and length of microvoids (Crawshaw et al. 2002). Since sodium hydroxide could effectively dissolve lignin and partially remove hemicellulose (Silverstein et al. 2007b), the shortening or disappearance of microvoids could be a result of significant structure disruption with the alkali pretreatment. In addition, the drying process may cause irreversible cellulose pore closure (McMillan 1994), which might be another reason for the shape change.

After the 1D intensity profile was obtained by integrating the 2D pattern (see Supporting Information), curve features were analyzed using a model fitting procedure. A unified model, which contains a Guinier region and a power-law region, was successfully employed to fit the intensity data with different levels (Figure 4.4). The related parameters were compared in Table

4.3. In level 1, a length scale of about 100-600 Å, the R_g decreased significantly after the pretreatments. The particles in this length scale showed the characteristic of a surface fractal.

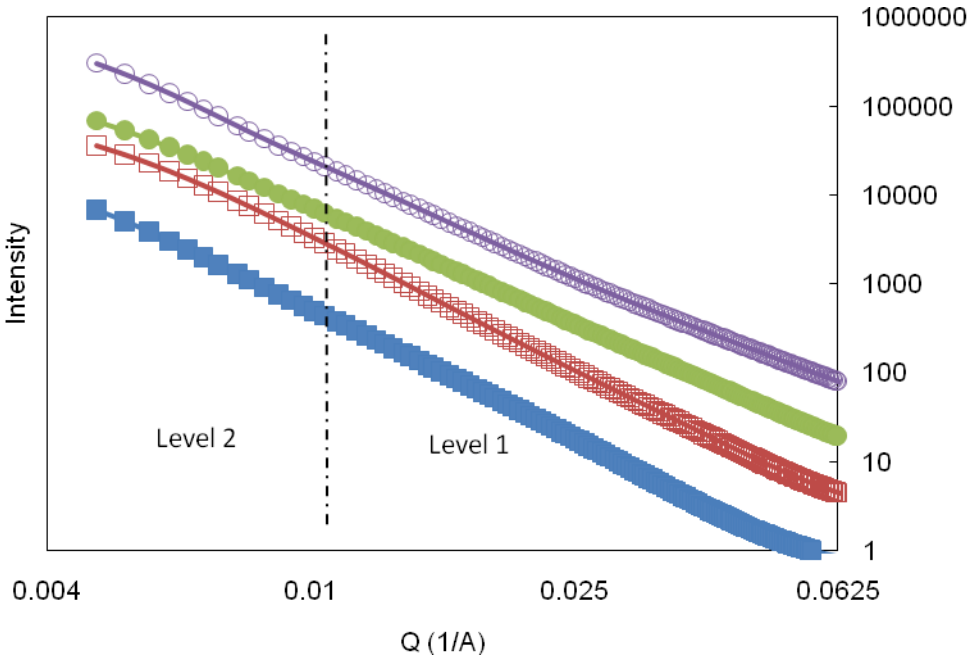

Figure 4.4 The unified fit of small-angle X-ray scattering profile of photoperiod-sensitive sorghum with different pretreatments ((■) untreated; (□) acid treated; (●) alkali treated; (○) ammonia treated). The curves were shifted vertically for better visualization.

In level 2, a length scale ranging from 600-1400 Å, both treated and untreated samples showed downward curves that could be used to calculate the R_g of particles (Table 4.3). The level at length scale from 1000 Å was considered to correspond to cellulose structure (Pingali et al. 2010b). In this case, the results showed that the radius of cellulose aggregates decreased from 481.6 Å with various pretreatments. The R_g of the acid treated sample was significantly reduced to 418.7 Å. It is well known that the glycosidic linkage of cellulose is susceptible to acid-catalyzed hydrolysis (Chang et al. 1973), and cellulose is easily degraded during the acid pretreatment at a high temperature (Mosier et al. 2005a). The results from WAXD also suggested that both crystalline and amorphous cellulose were degraded during acid pretreatment. Thus, the significantly reduced R_g could be a result of cellulose degradation. After the acid pretreatment, the cellulose structure displayed the characteristic of surface fractal with a surface

fractal dimension (d_s) of 2.02, reflecting a smooth pore-boundary surface (Bale and Schmidt 1984; Pingali et al. 2010b).

Table 4.3 Small-angle X-ray scattering results with unified model.

Pretreatment[a] [b]	Level 1		Level 2		
	R_g (Å)	P	R_g (Å)	P	d_s
Untreated	100.8 ± 4.8	2.93	481.6 ± 2.0	3.57	2.43
Acid treated	62.4 ± 0.8	3.41	418.2 ± 0.9	3.98	2.02
Alkali treated	46.5 ± 0.7	3.17	436.9 ± 1.2	3.30	2.70
Ammonia treated	43.4 ± 0.9	3.17	460.2 ± 0.9	3.37	2.63

[a] R_g is radius of gyration. P is power-law exponent. d_s is surface fractal dimension.
[b] Errors reported were propagated from the counting error in the raw data.

The structural changes of cellulose with acid pretreatment are complicated and dependent on pretreatment conditions and probably on the type of biomass. In this study, the crystalline structure of cellulose was distorted as the orientation factor decreased (Table 4.2), and part of the crystalline cellulose was degraded. It is not conclusive yet that the structural changes of cellulose are favorable cellulase digestion. A previous study using biomass powder suggested a decrease in cellulose crystallinity after acid pretreatment (Xu et al. 2011a), but a recent study of pure cellulose showed different results and suggested that sulfuric acid increased cellulose crystallinity because amorphous cellulose was hydrolyzed preferentially by acid (Zhao et al. 2006). The discrepancy could be due to the differences in processing conditions and in the complicated 3D structure of biomass. Bonds in the amorphous regions of cellulose are initially susceptible to acid hydrolysis but the fragments released during hydrolysis could associate into crystalline form (Bertran and Dale 1985; Wadehra and Manley 1965). Thus, cellulose crystallinity, which is related to the initial rate and the overall conversion efficiency of enzymatic hydrolysis (Bertran and Dale 1985; Fan et al. 1980), changes depending on biomass structure and pretreatment conditions.

Notably, for the changes of the network structure of biomass with the acid pretreatment, significant removal of hemicellulose, as well as the structural disruption of lignin, would have positive effects on the efficiency of enzymatic hydrolysis. For example, lignin disruption reduced lignin-cellulase absorption (Mansfield et al. 1999b). Therefore, acid pretreatment is effective for increasing the conversion efficiency of enzymatic hydrolysis by disrupting biomass structure, but

if the crystallinity of cellulose increases after acid hydrolysis, it is not conclusive that acid pretreatment is effective for making the cellulose itself in the solid form of biomass more susceptible to enzymatic hydrolysis.

Also notable is the effect of the drying process on structure, which is not negligible, although both dry cellulose and water-saturated cellulose were found to contain hydrophobic microregions (Grigoriew et al. 2001). SAXS study on fiber also suggested that microvoids changed significantly during drying and rewetting (Vickers et al. 2001). The removal of the amorphous part, especially delignification, will significantly decrease the density of mass structure and possibly result in structure collapse with drying (Teleman et al. 2001). Thus, in situ study of structural change during pretreatment is suggested.

4.5 Conclusions

For the first time, the structure of different parts of PS sorghum and structural changes during pretreatments were studied by both WAXD and SAXS. Using a combination of WAXD and SAXS revealed the structure of lignocellulosic biomass, including multiple components in both crystalline and amorphous states. Using biomass chips made it possible to reveal crystal orientation distribution changes and their effects on biomass processing. Hence, strategic design of biofuel production could be guided by the structural information at a molecular level.

Fundamentally understanding the structural discrepancies among different parts of biomass is important for utilizing biomass efficiently to reduce processing cost. WAXD study shows that the structure of cellulose in the outside rind has crystal orientation with a parameter of 0.26, whereas the structure of cellulose in other parts is isotropic. Future study should be conducted on the effects of crystal orientation on biomass processing: such efforts could be helpful for biomass breeding, screening, and process design. WAXD results also show that the PS sorghum rind has the highest crystallinity, and the isotropic structure of the leaf is less ordered. Meanwhile, SAXS study suggested that all biomass samples are surface fractals. Needle-shaped microvoids were found in the rind.

Design of pretreatment process has never obtained so much attention. Although many pretreatment studies are reported, the intrinsic mechanism of biomass structural change during pretreatment is not clear yet. With the acid pretreatment, cellulose structure was changed as indicated by a decrease of orientation factor and partial degradation of crystalline cellulose. A

smooth pore-boundary structure of cellulose was suggested by the SAXS results. With the alkali pretreatment, cellulose structure was modified with an increased orientation factor and an increased crystal size, and metastable cellulose I was transformed partially to stable cellulose II.

Chapter 5 - Towards understanding structural changes of biomass during sulfuric acid pretreatment

5.1 Abstract

Wide-angle X-ray diffraction (WAXD) and small-angle X-ray scattering (SAXS) were employed to investigate the structural changes of photoperiod-sensitive sorghum biomass in both crystalline and amorphous domains after sulfuric acid pretreatment. WAXD results suggested that the crystalline cellulose melted at 120 °C without significant degradation. Both the cellulose crystallinity and the crystal size at the dimension lateral to fiber direction increased as the temperature increased from 120 to 160 °C, which might lower cellulose digestibility. WAXD results also suggested a simultaneous hydrolysis and crystallization of cellulose by acid at 160 °C. The efficiency of enzymatic hydrolysis (EEH) increased because the protective structure was damaged and most hemicellulose was removed, resulting in an increase in surface area for enzyme reaction, as suggested by SAXS results. SAXS results also suggested that the radius of gyration of the polymer structure decreased and the lamellar structure was destroyed after the acid pretreatment. The effects of structural changes on the EEH and cellulose recovery were further examined. Both the EEH and cellulose degradation increased as the pretreatment temperature increased from 120 to 160 °C. The total glucose yield increased to 79.7% as the pretreatment temperature increased to 160 °C.

5.2 Introduction

Lignocellulosic biomass for biofuel production has attracted much attention because of its abundance and renewability (Tilman et al. 2006). Photoperiod-sensitive (PS) sorghum, due to its advantages of drought tolerance, relatively low lignin content, and high soluble sugar content, is a promising biomass source for bioethanol production (Xu et al. 2011a). Pretreatment is a crucial step in biomass-ethanol conversion; its goals are to break the lignin seal, disrupt the crystalline structure of cellulose, and increase the surface area of cellulose to make the polysaccharides more susceptible to enzyme hydrolysis (Mosier et al. 2005b). Numerous pretreatment methods have been employed for biomass processing, such as steam explosion, dilute acid, alkali, ammonia fiber explosion, and supercritical CO_2 (Alizadeh et al. 2005; Fernandez-Bolanos et al. 2001; Kim and Hong 2001). Among these methods, diluted sulfuric

acid pretreatment has been used frequently in biomass-ethanol processing (Saha et al. 2005b). An important advantage of acid pretreatment is that it can remove most hemicellulose from biomass and increase the accessible surface area of cellulose for enzymatic hydrolysis (Zeng et al. 2007). The removed hemicellulose could be degraded to monosaccharides, which could be used for ethanol production or be further degraded to furfural (Garrote et al. 2001).

A review of the literature reveals that the structural changes of biomass during pretreatment are complex and not completely understood. There are arguments about the changes of crystalline structure of biomass during pretreatment. The question whether the crystallinity of biomass substrate affects enzymatic hydrolysis is in debate (Mansfield et al. 1999b). Biomass crystallinity, which represents the mass percentage of crystalline component in whole mass rather than in cellulose, has been used frequently as a parameter of structural changes (Park et al. 2010). However, biomass crystallinity could be affected by the compositional changes of non-cellulose amorphous components (e.g., hemicellulose) and even extractives; thus, it provides limited information about crystalline structure.

Both the compositional and structural changes of non-cellulose components (e.g., hemicellulose) by acid pretreatment could affect the digestibility of cellulose in biomass, but it is critical to understand the structural changes of cellulose after pretreatment. Wide-angle X-ray diffraction (WAXD) is effective for studying the crystalline structure of polymers (Park et al. 2010), and small-angle X-ray scattering (SAXS) is able to probe structure from approximately 1 nm to hundreds of nanometers (Chu and Hsiao 2001). Recent studies using small-angle neutron scattering have revealed biomass structural changes during various pretreatments (Li et al. 2011; Pingali et al. 2010b), but questions about the detailed changes of cellulose remained unanswered. Our previous study using both WAXD and SAXS has provided the structural information of different botanic parts of biomass and has shown that biomass goes through structure change in both crystalline and amorphous domains during acid and alkali pretreatments (Xu et al. 2012). Although the results are very promising, a study with variable pretreatment conditions is suggested to provide detailed information on the structure changes of biomass, allowing us to understand the mechanism of pretreatment. In addition, it is necessary to reveal the relationship between structural changes and hydrolysis efficiency.

To the best of our knowledge, the structural changes of biomass during acid pretreatment, especially the detailed changes of crystalline cellulose, have not been fully understood. In this

study, both WAXD and SAXS with synchrotron radiation helped us understand the structural changes of biomass in a large length scale and their effects on enzymatic hydrolysis. Both the biomass rind and powder were used for the investigation of structural change. A study using biomass rind is helpful for understanding the nanostructure related to orientation; a study using biomass powder is more beneficial for understanding the direct effects of pretreatment on subsequent processing such as enzymatic hydrolysis. Furthermore, a better understanding of biomass structural change will enable development of a cost-efficient strategy for biomass processing.

5.3 Meterials and methods

5.3.1 Materials

The PS sorghum was harvested at physiological maturity from Riley County, Kansas, in 2008. Biomass rinds were obtained from 3 strains for comparison and prepared by knife-cutting and air-drying in an oven at 50 °C for 12 h. Powder samples (<1 mm particle size) were prepared using a cutting mill (SM 2000, Retsch Inc., Newtown, PA). All chemicals used in this research were of analytical grade and purchased from Sigma-Aldrich, Inc. (St. Louis, MO, USA).

5.3.2 Pretreatment

Both the PS sorghum powder and the rind were used for acid pretreatment. For biomass powder pretreatment, a prewashed sample in which the soluble extractive had been washed out as described (Xu et al. 2011a) was used as an untreated sample. For biomass rind pretreatment, a piece of PS sorghum rind (0.5 × 2 cm) was submerged in sulfuric acid solution. A reactor (Swagelok, Kansas City Valve & Fitting Co., Shawnee Mission, KS) made from 316L stainless steel with a measured internal volume of 75 mL (outside diameter of 38.1mm, length of 125 mm, and wall thickness of 2.4mm) was used for this study. A working volume of 50mL was used to allow space for expanding liquid water at a high temperature during pretreatment. The loading of the prewashed PS sorghum was 6.1% (w/v, 3.07 g dry mass in 50ml 1.27 % acid solution). A sandbath (Techne, Inc., Princeton, NJ) with a temperature controller was used. After the sand attained a certain temperature, the reactor was submerged in heated sand for 40 min. Then the reactor was immediately transferred and cooled by room-temperature water to decrease the internal temperature to below 50°C in 2 min. The slurry removed from the reactor was washed,

and the solid fraction was separated by filtration. Part of the solid mass from filtration was used for enzymatic hydrolysis, part of the air-dried sample was used for WAXD and SAXS measurement, and the remaining part and the liquid were used for composition analysis. Cellulose recovery yield (Y_{REC}) was defined as shown below.

$$Y_{REC} = \frac{M_{pret} \times C_{pret}}{M_{OR} \times C_{OR}} \times 100\% \quad \textbf{[Equation 5-1]}$$

where M_{pret} is the dry mass weight after pretreatment, M_{OR} is the original dry mass weight, C_{pret} is the cellulose percentage of the solid part after pretreatment, and C_{OR} is the percentage of the cellulose in original dry mass.

5.3.3 Enzymatic hydrolysis

Enzymatic hydrolysis was conducted with the pretreated powder at 2% solids concentration (grams dry weight per 100 mL) in 50 mM sodium acetate buffer (pH 5.00) with the addition of 40 μg/mL of tetracycline and 30 μg/mL of cycloheximide. Accellerase 1500, an enzyme complex including cellulase and β-glucosidase (Endoglucanase activity: 2200-2900 CMC U/g; one CMC U unit of activity liberates 1 μmol of reducing sugars [expressed as glucose equivalents] in 1 min under specific assay conditions of 50°C and pH 4.8), was generously provided by Genencor (Rochester, NY) and was used at the recommended dosages, 0.5 mL per gram cellulose. Total monosaccharide was analyzed at the end of hydrolysis (72 h) on supernatants using high-performance liquid chromatography (HPLC) as described (Xu et al. 2011a). The efficiency of enzymatic hydrolysis (EEH) was defined as shown in the following calculation:

$$EEH = \frac{G_{EH} \times 0.9}{M_{EH} \times C_{pret}} \times 100\% \quad \textbf{[Equation 5-2]}$$

where M_{EH} is the weight of dry mass used in enzymatic hydrolysis, G_{EH} is the glucose content after hydrolysis, C_{pret} is the cellulose percentage of the solid part after pretreatment, and 0.9 is the mass coefficient of glucose to cellulose (g/g). Total glucose yield (Y_p) was defined as the product of cellulose percentage in the solid part after pretreatment and EEH.

$$Y_P = \frac{EEH \times Y_{REC}}{100\%} \quad \textbf{[Equation 5-3]}$$

5.3.4 Synchrotron WAXD and SAXS

The WAXD and SAXS experiments were carried out at the Advanced Polymers Beamline (X27C), National Synchrotron Light Source, Brookhaven National Laboratory, in Upton, NY. Details of the experimental setup at the X27C beamline have been reported elsewhere (Chu and Hsiao 2001). The wavelength used was 0.13714 nm. The sample-to-detector distance was 117.6 mm for WAXD and 1782.9 mm for SAXS. A 2D MAR-CCD X-ray detector (MAR USA, Inc., Norwood, NJ) was used for data collection. For X-ray study of PS rind, the direction of the X-ray beam was perpendicular to chip direction.

Two-dimensional WAXD patterns were first corrected with air background, then performed with Fraser correction using Polar software (Precision Works, NY) (Ran et al. 2002). For the analysis of anisotropic features (e.g., (020) reflection) in a 2D pattern, the integrating range was from 70° to 110° instead of the range used for isotropic pattern, 0° to 360°. Relative mass crystallinity (RCr, the percentage of crystalline cellulose in biomass) was estimated from an integrated diffraction intensity profile as the ratio of the total crystal peak diffraction intensity to the total diffraction intensity. A peak-fitting process was conducted with Igor Pro 6.20 (WaveMetrics Inc. Lake Oswego, OR). Cellulose crystallinity (CCr, the percentage of crystalline part in cellulose) was calculated using the following equation:

$$CCr = \frac{RCr}{C_{cell}} \times 100\% \qquad \textbf{[Equation 5-4]}$$

where C_{cell} (%) is the cellulose content of an examined sample.

Crystal size of the anisotropic part was estimated from (020) reflection. Because the Bragg reflection may be broadened by both crystallites with finite size and possible imperfections in the crystal lattice, the equation here was used only as a lower-bound estimate of crystal size.

$$L_{w(hkl)} = \frac{K\lambda}{FWHM_{2\theta}\cos\theta} \qquad \textbf{[Equation 5-5]}$$

where θ is the Bragg angle corresponding to the plane, K is constant of 0.9 for cellulose (Alexander 1954), λ is wavelength (nm), and $FWHM_{2\theta}$ is the full width at half maximum of the reflection in the radial direction.

Two-dimensional SAXS data were corrected with air background before further analysis. The equatorial streak in the 2D pattern was analyzed for parameters related to the needle shaped

microvoids aligned along the fiber direction following the equations below (Perret and Ruland 1969; Ruland 1969).

$$s^2 B_{obs}^2 = 1/L^2 + s^2 B_\phi^2 \quad \textbf{[Equation 5-6]}$$

$$sB_{obs} = 1/L + sB_\phi \quad \textbf{[Equation 5-7]}$$

Where B_{obs} is the integral breadth at a given value of s, $s = 2(\sin\theta)/\lambda$, L is a uniform finite length of microvoids, and B_φ is the spread of the misorientation. The equations [5-6] and [5-7] are used if the azimuthal peak profiles are assumed to be Gaussian and Lorentzian, respectively. In this case, the Lorentzian function fit the peaks better and was employed.

The integrated 1D data were analyzed using Igor Pro 6.20 with the Irena package. The unified equation was used for analysis of SAXS data (Beaucage 1995). The equation defines multiple levels, and each level may contain a Guinier region describing average structural size and a power-law region describing the mass or surface fractal. The unified model is given by:

$$I(q) = G_i \exp\left(-q^2 R_{gi}^2/3\right) + B_i \exp\left(-q^2 R_{g(i-1)}^2/3\right) \times \left\{\left[erf\left(qR_{gi}/6^{1/2}\right)\right]^3/q\right\}^{Pi} \quad \textbf{[Equation 5-8]}$$

where i represents the structural levels, G_i is the exponential prefactor, R_{gi} is the radius of gyration, B_i is a constant prefactor specific to the type of power-law scattering, P_i, and the magnitude of the scattering vector is defined as $q = 4\pi \sin\theta/\lambda$ (θ is half of the scattering angle).

5.4 Results and discussion

5.4.1 Structure change of PS sorghum after acid pretreatment

5.4.1.1 Composition changes

Our previous study of the effects of pretreatment conditions on enzymatic hydrolysis showed temperature to be one of the most significant factors (Xu et al. 2011b). Thus, this study was designed to understand how the biomass structure changes at different temperatures. The compositional changes of the biomass after pretreatment were listed in Table 5.1. Biomass structure was disrupted during sulfuric acid pretreatment as previous reported (Xu et al. 2011a), resulting in significant compositional change. Xylan content was dramatically reduced because sulfuric acid effectively hydrolyzed hemicellulose. The increases in the percentage of β(1-4) glucan and lignin were results of mass loss (e.g., xylan removal) after the acid pretreatment.

Table 5.1 Compositional changes of photoperiod-sensitive sorghum with acid pretreatment.

Conditions	Lignin*	Xylan	Glucan
untreated	16.6(0.9)	27.0(0.3)	44.3(0.8)
120 °C	21.9(1.5)	14.7(0.4)	57.3(0.4)
140 °C	24.8(1.8)	5.5(0.05)	64.9(0.9)
160 °C	27.4(1.6)	2.2(0.05)	64.2(0.7)

*Values (%, dry based) in parenthesis represent standard deviation.

5.4.1.2 WAXD study

After the sulfuric acid pretreatment, the crystalline structure of remaining biomass changed. Our previous study on PS sorghum rind suggested that a decrease in orientation factor was because the oriented crystalline structure was distorted by acid (Xu et al. 2012). In this study, the anisotropic flection was further investigated (Table 5.2). The crystallinity of the anisotropic fraction increased with the increasing pretreatment temperature as a result of the removal of the amorphous components after the pretreatment. The change in crystal size estimated from the anisotropic fraction showed the similar trend of increase. The acid pretreatment at a relatively low temperature (120 °C) did not change the crystal size. A similar result was reported in our previous study at the same temperature (Xu et al. 2012). Further increasing the temperature resulted in an increase in crystal size. Crystallization of amorphous cellulose could be one reason for the increase in crystal size as found in the production of microcrystalline cellulose (Tang et al. 1996). A recent report also suggested the existence of templates of crystalline components at the dimension lateral to fiber direction (Ibbett et al. 2008); therefore, crystallization could begin at this dimension, resulting in the increase of crystal size in reflection (020). The increase in crystal size was possibly related to a decrease in surface area, which could reduce chemical absorptions of cellulose fiber (Reddy and Yang 2005) and might not be helpful for increasing the reaction rate of enzymatic hydrolysis.

Table 5.2 Crystallinity and crystal size of anisotropic part in photoperiod-sensitive sorghum rind analyzed by wide-angle X-ray diffraction.

Conditions	Mass Crystallinity of anisotropic part (%)	Crystal size of anisotropic part (020) reflection (nm)
Untreated	40.7(0.4)	3.37(0.09)
120 °C	46.4(0.6)	3.37(0.12)
140 °C	49.3(0.7)	3.62(0.02)
160 °C	53.5(0.6)	3.93(0.14)

In addition to the study of fiber diffraction, WAXD was used to investigate biomass powder. Relative mass crystallinity was calculated with a peak-fitting procedure, as shown in Table 5.3. Because mass crystallinity provided limited information about crystalline cellulose, CCr was calculated. Compared with the untreated sample, the CCr of pretreated samples decreased, suggesting that part of the crystalline cellulose was destroyed. Previous studies of acid treatment on cellulose reported that amorphous cellulose was preferentially hydrolyzed by acid (Bondeson et al. 2006; Zhao et al. 2006). In this study, at 120 °C, acid preferentially hydrolyzes hemicellulose rather than amorphous cellulose (Table 5.1), possibly because the network structure of hemicellulose and lignin may protect amorphous cellulose from degradation (over 99% recovery of cellulose) under this condition. In addition, the removal of hemicellulose by acid may help allow part of the crystalline cellulose to be melted at 120 °C, which could be related to a decrease in orientation factor as reported (Xu et al. 2012). The CCr increased as the temperature increased from 120 to 160 °C. This result has two possible explanations: acid preferentially hydrolyzed amorphous cellulose after removing most hemicellulose and eventually degraded much more amorphous cellulose than crystalline cellulose, and/or amorphous cellulose was crystallized simultaneously during acid hydrolysis (Battista 1950; Bertran and Dale 1985).

Cellulose recovery decreased as the temperature increased, indicating that cellulose degradation was enhanced as the severity of treatment conditions (e.g., temperature) increased. This was supported by our previous study using different acid concentration (Xu et al. 2011a). The recovery of crystalline cellulose was calculated to illuminate the effects of the acid treatment on the crystalline component in the insoluble fraction (Table 5.3). With acid pretreatment at either 120 °C or 140 °C, the recovery of crystalline cellulose did not change significantly, but the recovery increased to 74.6% when the temperature was 160 °C. Since the cellulose recovery

decreased from 96.8% to 87.4%, we confirmed the simultaneous hydrolysis and crystallization during acid pretreatment at 160 °C.

Table 5.3 Changes of cellulose content and crystallinity of photoperiod-sensitive sorghum analyzed using wide-angle X-ray diffraction.

Conditions	Cellulose recovery (%)	Mass crystallinity* (%)	Cellulose crystallinity (%)	Recovery of crystalline cellulose (%)
Untreated	100.0	32.4(0.9)	78.5	100.0
120 °C	99.1(0.1)	28.6(0.5)	51.2	64.6
140 °C	96.8(0.3)	33.3(0.9)	53.6	66.1
160 °C	87.4(0.3)	41.3(0.8)	67.0	74.6

*Calculated from air-dried PS sorghum powder. Values in basket represent standard deviation.

5.4.1.3 SAXS study

The effect of acid treatment on fiber structure was also investigated by SAXS. Two dimensional anisotropic patterns of PS sorghum rind (Figure 5.1) suggested a high degree of orientation of the cellulose fibrils (Jungnikl et al. 2008). The untreated rind has both equatorial and meridional streaks (Figure 5.1a), representing needle-shaped microvoids and periodic lamellar structure between the crystalline and amorphous regions, respectively (Chen et al. 2007). As the pretreatment temperature increased, the meridional streaks decreased, as found in the previous study (Xu et al. 2012). After the temperature was increased to 140 °C, the meridional streak eventually disappeared, indicating that the lamellar structure was destroyed (Chen et al. 2007).

The lengths and diameters of the needle-shaped microvoids could be estimated using Ruland's method (Ruland 1969). The length of microvoids could be changed due to various processing methods, and a recent report showed that the length of microvoids in regenerated cellulose fibers ranges from 333 to 1320 nm (Jiang et al. 2011). In this study, the estimated lengths of the microvoids increased as the temperature increased (Table 5.4), possibly because of the acid disruption of fiber structure. The length of the equatorial streak, which was considered a reciprocal of the diameter (D) of the microvoids in cellulose fibers (Ran et al. 2001), did not change significantly after acid treatment, indicating that the average diameter did not change. Considering that the length increased, we suggest that the total volume of the microvoids

increased. In addition, the misorientation (B_φ) did not change at the relatively low temperatures but increased at a high temperature (160 °C) (Table 5.4), suggesting that the ordered structure could be disrupted under escalated pretreatment condition (Ran et al. 2001).

Table 5.4 Parameters of structural changes using small-angle X-ray scattering.

Conditions[a]	R_g (Å)	L (nm)	B_φ (rad)
Prewashed powder	350	790	0.15
120 °C acid	351	974	0.14
140 °C acid	330	1166	0.14
160 °C acid	277	1319	0.21

[a]R_g is radius of gyration; L is a uniform finite length of microvoids; and B_φ is the spread of the misorientation

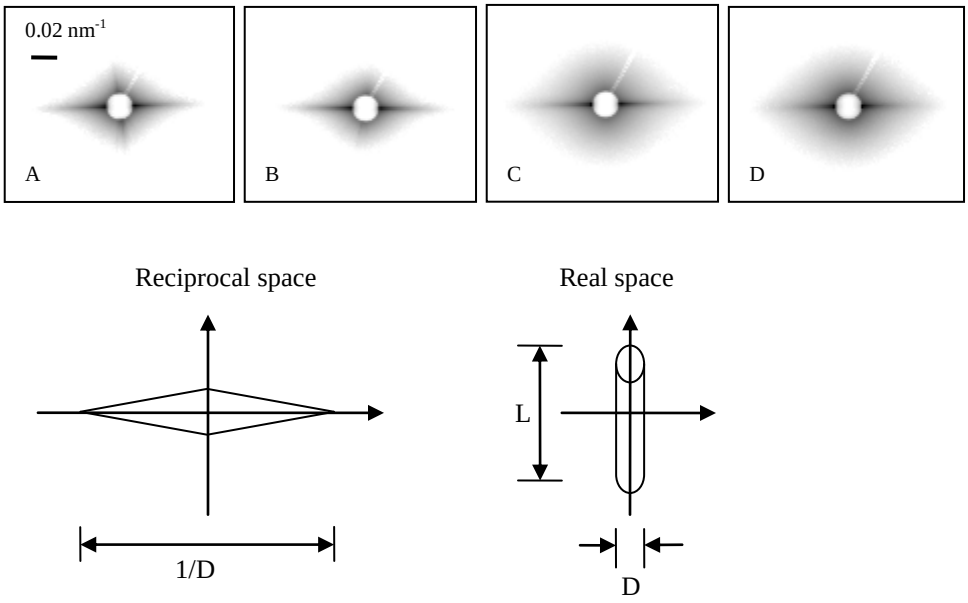

Figure 5.1 Small-angle X-ray scattering of the photoperiod-sensitive sorghum rinds (A: untreated; B: acid treated at 120 °C; C: acid treated at 140 °C; D: acid treated at 160 °C) and a schematic diagram of microvoids. (D represents the average diameter of the needle-shaped microvoids.)

.

A unified model was then employed to investigate the 1D SAXS curves from biomass powder (Figure 5.2), and the related structural parameters were obtained (Table 5.4). In our previous study of PS sorghum rind, the R_g decreased after acid treatment (Xu et al. 2012). A similar trend was found in this study using powder at a length scale of 600 to 1000 Å (Table 5.4). At 120 °C, the R_g did not change significantly, suggesting that the size of cellulose aggregates

did not change. The results of cellulose composition and WAXD also suggested that part of cellulose melted but not degraded. The R_g decreased as the temperature further increased to over 140 °C, reflecting that part of cellulose was hydrolyzed by acid.

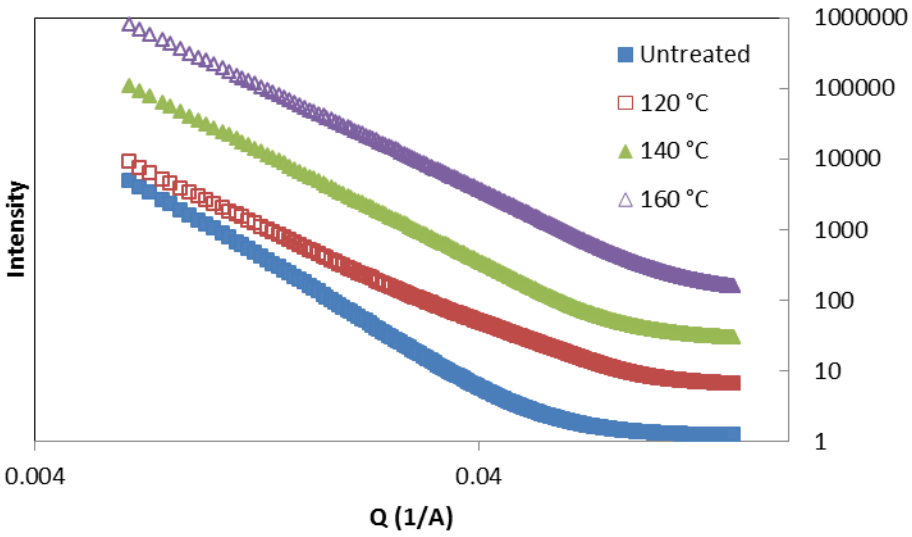

Figure 5.2 The unified fit of small-angle X-ray scattering profile of photoperiod-sensitive sorghum with acid pretreatments. The curves were shifted vertically for better visualization.

5.4.2 The effect on enzymatic hydrolysis

The EEH and glucose yield of the pretreated PS sorghum powder increased significantly compared with that of untreated biomass (Figure 5.3). As suggested by the composition analysis, the increase of the EEH was due to the sealed structure of amorphous components, such as hemicellulose, was disrupted and the cellulose in PS sorghum was exposed for the enzyme reaction. The increased volume of microvoids noted by SAXS also indicated an increase in accessible surface area for the enzyme reaction. Another reason was that the decreased CCr after the pretreatment is helpful for increasing the reaction rate of enzymatic hydrolysis (Fan et al. 1980). As the pretreatment temperature increased, both the EEH and the CCr increased, whereas the cellulose recovery decreased. Previous study (Fan et al. 1980) on highly pure cellulose (99.5%) showed that hydrolysis yield increased as the crystallinity of cellulose substrate decreased. In this study, the acid pretreatment not only changed cellulose structure but also affected other components in the PS sorghum. Cellulose is embeded in the matrix of

hemicellulose and lignin. The removal of hemicellulose with enhanced conditions of pretreatment exposed cellulose to enzymatic hydrolysis, but crystalline structure of cellulose remained to be resistant to enzymatic hydrolysis. At 160 °C, The total glucose yield increased and was maximized at 79.7% with an EEH of 91.2% and a cellulose recovery of 87.4%. As found in our previous study, the EEH could be enhanced up to 100% at a higher temperature (e.g., 180 °C), but the significant cellulose degradation made the total glucose yield less than 60 % (Xu et al. 2011b). Therefore, a pretreatment for maximizing glucose yield needs to balance between EEH and cellulose recovery.

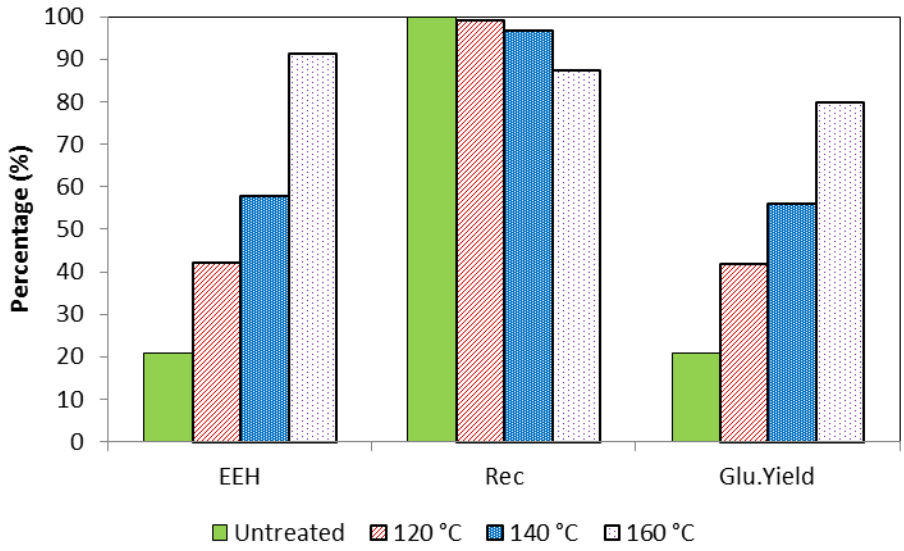

Figure 5.3 The effects of the pretreatment on efficiency of enzymatic hydrolysis (EEH), cellulose recovery (Rec), and glucose yield (Glu. Yield).

5.4.3 Understanding sulfuric acid pretreatment on biomass

For the whole biomass, the acid pretreatment disrupted the network structure among carbohydrate polymers and broke the hydrogen bonds between hemicellulose and cellulose, which eventually increased the enzymatic-accessible area of cellulose (Mosier et al. 2005b). The SAXS results suggested an increased volume of microvoids after the acid pretreatment, which could be related to the conclusion in a previous study that the presence of hollow area after acid pretreatment is due to “peeling-away” of the components in plant cell wall (Zeng et al. 2007). Therefore, the increase of the surface area of cellulose explained the enhanced yield of

enzymatic hydrolysis. The acid pretreatment at 120 °C partially removed hemicellulose and caused melting of part of crystalline cellulose rather than significantly changed cellulose content, possibly because the remaining lignin and hemicellulose, at the relatively mild condition, maintained a protective structure, preventing the acid hydrolysis of cellulose (Chen and Dixon 2007). The acid reaction at an escalated condition (e.g., the increased temperature in this study or the increased acid concentration in the previous study) dramatically disrupted the biomass structure by removing most of hemicellulose and hydrolyzed the glucosidic linkages of glucan trains, eventually resulting in the significant degradation of cellulose.

For the component of cellulose, the WAXD results suggested the melting of part of crystalline cellulose at 120 °C, possibly because acid broke up the interchain hydrogen-bonds and damaged part of the ordered crystalline structure of the cellulose. The fact that over 99% of cellulose was recovered at 120 °C is consistent with the result that the R_g did not change significantly (Table 5.4). When the temperature was over 140 °C, the lamellar structure was destroyed, and the amount of both crystalline and amorphous cellulose decreased, as confirmed by the decreased R_g. The acid pretreatment at 160 °C eventually resulted in significant cellulose loss and an increased misorientation factor, indicating the disruption of biomass by acid. Crystallization of amorphous cellulose was confirmed by the increased recovery of crystalline cellulose and the increased crystal size in the dimension lateral to fiber direction. Simultaneous degradation and crystallization of amorphous cellulose was suggested. The significant decrease of CCr after the acid pretreatment made cellulose more susceptible to enzyme reaction (Chang and Holtzapple 2000; Fan et al. 1980). However, the increase in the crystal size may not be helpful for enzyme reaction.

Lignin serves as a protective seal for cellulose (Mosier et al. 2005b) and was considered as a cellulase inhibitor because of its irreversible absorption onto the enzyme (Berlin et al. 2005). The PS sorghum used in this study contained a relatively low lignin content compared with corn stover (17 - 21%), which is an advantage for enzymatic hydrolysis. After the acid pretreatment, most lignin was preserved because sulfuric acid pretreatment is not effective for removing lignin. A previous study suggested that the structure of lignin could be rearranged during acid treatment, and the deposition of formed droplet would have a negative effect on enzymatic hydrolysis (Selig et al. 2007). In this study, the hydrolysis yield after pretreatment increased significantly.

Because lignin composition and structure varies in different biomass, further research is needed to study the effect of the structural change of lignin on biomass processing.

5.5 Conclusions

Sulfuric acid pretreatment changed the composition and structure of the PS sorghum, made cellulose more exposed and susceptible for enzymatic hydrolysis. Acid preferentially hydrolyzes hemicellulose rather than amorphous cellulose at 120 °C. Both the CCr and the crystal size of cellulose increased as the temperature increased from 120 to 160 °C, indicating that a higher temperature could make cellulose less susceptible. A simultaneous hydrolysis and crystallization was suggested during acid pretreatment at 160 °C. The SAXS results suggested an increased total volume of the microvoids, indicating an increased accessible surface area for enzymatic hydrolysis. The radius of gyration of the polymer structure decreased and the lamellar structure was destroyed after the acid pretreatment. It would be interesting to develop a pretreatment that removes protective barriers (e.g., lignin) and melts crystalline cellulose.

Chapter 6 - Conclusion and future work

Cellulosic ethanol has attracted much attention because lignocellulosic biomass is renewable and low cost. Photoperiod-sensitive sorghum, with high soluble sugar content, high mass yield and drought tolerance in dryland environments, has great potential for ethanol production. Both the cellulose and soluble sugar in PS sorghum have been utilized in an integrated process. The effect of diluted sulfuric acid pretreatment on enzymatic hydrolysis was investigated. Hydrolysis efficiency increased from 78.9 to 94.4% as the acid concentration increased from 0.5 to 1.5%. However, the highest total glucose yield (80.3%) occurred at the 1.0% acid condition because of the significant cellulose degradation at the 1.5% concentration. Response surface methodology was further employed to study the relationship between pretreatment variables (including temperature, sulfuric acid concentration, and reaction time) and cellulose recovery, as well as the EEH in the solid part. Recovery yield decreased and EEH increased as the pretreatment temperature, acidic concentration, and reaction time increased. A model was successfully developed with RSM to predict total glucose yield with a maximum value of 82.2%. Conditions of co-fermentation were also optimized, and the optimal ethanol yield was obtained with constant-temperature simultaneous saccharification and fermentation at 38 °C. Acetate buffer at a concentration of 50 mM was found helpful for increasing the EEH, as well as the ethanol yield. The maximum ethanol yield was 0.21 g ethanol per dry mass at the conditions of 38°C, 0.05 g yeast/L, and 50 mM acetate buffer. A complete cellulose balance was provided for the whole process.

Fundamental understanding of the structural changes during pretreatment of lignocellulosic biomass could lead to improved processes and cost reductions for bioethanol production. Scanning electron microscopy was employed to understand how the morphological structure of PS sorghum changed after pretreatment. Synchrotron WAXD and SAXS were used to study the structures of different parts of photoperiod-sensitive sorghum and structural changes during various pretreatments. Wide-angle X-ray diffraction study showed that the PS sorghum rind had oriented crystal peaks and the highest degree of crystallinity, whereas the crystalline structures of the inner pith and leaf were less ordered. Orientation distribution of cellulose changed during pretreatments. Crystalline cellulose was degraded partially by acid pretreatment

and a smooth pore-boundary surface structure of cellulose was noted by SAXS. Alkali pretreatment transformed part of the cellulose to a more stable form (cellulose II) and increased the crystal size of cellulose.

The structural changes of PS sorghum biomass during acid pretreament and their effects on the subsequent enzymatic hydrolysis have been revealed with WAXD and SAXS. Wide-angle X-ray diffraction results suggested that part of crystalline cellulose melted at 120 °C before its significant degradation. Both the cellulose crystallinity and the crystal size at the dimension lateral to fiber direction increased as the temperature increased from 120 to 160 °C, indicating that a higher temperature could make cellulose less susceptible. Wide-angle X-ray diffraction results also suggested a simultaneous hydrolysis and crystallization of cellulose by acid. The EEH increased because the protective structure was damaged and most hemicellulose was removed, resulting in the increase in surface area as suggested by the SAXS result of the increased length of microvoids. Small-angle X-ray scattering results also suggested that the radius of gyration of the polymer structure decreased and the lamellar structure was destroyed after the acid pretreatment. The effects of structural changes on the EEH and cellulose recovery were further examined. Both the EEH and cellulose degradation increased as the pretreatment temperature increased from 120 to 160 °C. The total glucose yield increased up to 79.7% as the pretreatment temperature increased to 160 °C.

For future work, several issues deserve attention. After diluted sulfuric acid pretreatment, the liquid fraction, which contains about 3% (in dry mass) glucose and most xylose, has not been well utilized in current process (Figure 3.1). One reason is that the microbe which is able to convert both hexose and pentose is still in developing, and the conversion efficiency is relatively low compared with the traditional yeast-glucose fermentation (Lau et al. 2010). An alternative option is to conduct fermentation of xylose in a separated route instead of the co-fermentation. In addition, an efficient utilization of the fermentation residue is important to reduce processing cost and avoid possible environmental issues. Lignin, the major component in the residue, is an excellent source for some industrial application. For example, lignin has been developed as gel with unique swelling property (Nishida et al. 2003).

For the study of biomass structure, full-scale study of X-ray diffraction and scattering, including WAXD and SAXS, is supposed to be well employed in study of biomass structural changes. The naturally oriented cellulose structure and its effect on biomass processing should

gain attention. With the new generation of photon technology, X-ray is definitely a reliable source for the study of real-time structural change. In addition, other advance techniques, such as atomic force microscopy and solid-state nuclear magnetic resonance, are supposed to be employed together for revealing biomass structure at a molecular level. Finally, the current work was focusing on the principle of reaction and the fundamental characteristics of biomass structure, which could be scaled up for examining the possibility of industrial application.

References

Alagarswamy G., Reddy D., Swaminathan G. (1998). Durations of the photoperiod-sensitive and-insensitive phases of time to panicle initiation in sorghum. Field Crops Research 55(1-2):1-10.

Alexander L. (1954). The synthesis of X-ray Spectrometer line profiles with application to crystallite size measurements. J. Appl. Phys. 25:155.

Alizadeh H., Teymouri F., Gilbert T., Dale B. (2005). Pretreatment of switchgrass by ammonia fiber explosion (AFEX). Appl. Biochem. Biotechnol. 124(1):1133-1141.

Andersson S., Wikberg H., Pesonen E., Maunu S., Serimaa R. (2004). Studies of crystallinity of Scots pine and Norway spruce cellulose. Trees-Structure and Function 18(3):346-353.

Aravindanath S., Iyer P., Sreenivasan S. (1986). Communications to the editor. Further evidence for the presence of cellulose I and II in the same cross section of partially mercerized cotton fibers. Textile Research Journal 56(3):211-212.

Astley O., Donald A. (2001). A small-angle X-ray scattering study of the effect of hydration on the microstructure of flax fibers. Biomacromolecules 2(3):672-680.

Atalla R. 1979. Conformational effects in the hydrolysis of cellulose. In: Ross D. Brown J, Lubo Jurasek, editor. Hydrolysis of Cellulose: Mechanisms of Enzymatic and Acid Catalysis. Washington: American Chemical Society. p 55.

Bak J., Ko J., Choi I., Park Y., Seo J., Kim K. (2009). Fungal pretreatment of lignocellulose by Phanerochaete chrysosporium to produce ethanol from rice straw. Biotechnol. Bioeng. 104(3):471-482.

Balan V., da Costa Sousa L., Chundawat S., Marshall D., Sharma L., Chambliss C., Dale B. (2009). Enzymatic digestibility and pretreatment degradation products of AFEX-treated hardwoods (Populus nigra). Biotechnol. Progr. 25(2):365-375.

Bale H., Schmidt P. (1984). Small-angle X-ray-scattering investigation of submicroscopic porosity with fractal properties. Phys. Rev. Lett. 53(6):596-599.

Bansal P., Vowell B. J., Hall M., Realff M. J., Lee J. H., Bommarius A. S. (2012). Elucidation of Cellulose Accessibility, Hydrolysability and Reactivity as the Major Limitations in the Enzymatic Hydrolysis of Cellulose. Bioresour. Technol. 107(5):243-250.

Barnett J. (1981). Xylem cell development. Castle House Publ. Ltd., Tunbridge Wells.

Battista O. A. (1950). Hydrolysis and crystallization of cellulose. Industrial & Engineering Chemistry 42(3):502-507.

Beaucage G. (1995). Approximations leading to a unified exponential/power-law approach to small-angle scattering. J. Appl. Crystallogr. 28(6):717-728.

Berlin A., Gilkes N., Kurabi A., Bura R., Tu M., Kilburn D., Saddler J. (2005). Weak lignin-binding enzymes. Appl. Biochem. Biotechnol. 121(1):163-170.

Bertran M., Dale B. (1985). Enzymatic hydrolysis and recrystallization behavior of initially amorphous cellulose. Biotechnol. Bioeng. 27(2):177-181.

Bienkowski P., Ladisch M., Narayan R., Tsao G., Eckert R. (1987). Correlation of Glucose (Dextrose) Degradation at 90 to 190 C in 0.4 to 20% Acid. Chem. Eng. Commun. 51(1):179-192.

Bish D., Howard S. (1988). Quantitative phase analysis using the Rietveld method. J. Appl. Crystallogr. 21(2):86-91.

Blazek J., Gilbert E. P. (2011). Application of small-angle X-ray and neutron scattering techniques to the characterisation of starch structure: A review Carbohydr. Polym. 85(2):281-293.

Bondeson D., Mathew A., Oksman K. (2006). Optimization of the isolation of nanocrystals from microcrystalline cellulose by acid hydrolysis. Cellulose 13(2):171-180.

Britton T., Liang H., Dunne F., Wilkinson A. (2010). The effect of crystal orientation on the indentation response of commercially pure titanium: Experiments and simulations. Proceedings of the Royal Society A: Mathematical, Physical and Engineering Science 466(2115):695.

Burger C., Hsiao B. S., Chu B. (2010). Preferred orientation in polymer fiber scattering. Polymer Reviews 50(1):91 - 111.

Cael J., Gardner K., Koenig J., Blackwell J. (1975). Infrared and Raman spectroscopy of carbohydrates. Paper V. Normal coordinate analysis of cellulose I. The Journal of Chemical Physics 62:1145.

Canetti M., Bertini F., De Chirico A., Audisio G. (2006). Thermal degradation behaviour of isotactic polypropylene blended with lignin. Polym. Degrad. Stab. 91(3):494-498.

Cao Y., Tan H. (2005). Study on crystal structures of enzyme-hydrolyzed cellulosic materials by X-ray diffraction. Enzyme Microb. Technol. 36(2-3):314-317.

Chang M., Pound T., Manley R. (1973). Gel-permeation chromatographic studies of cellulose degradation. I. Treatment with hydrochloric acid. Journal of Polymer Science: Polymer Physics Edition 11(3):399-411.

Chang V., Holtzapple M. (2000). Fundamental factors affecting biomass enzymatic reactivity. Appl. Biochem. Biotechnol. 84(1):5-37.

Chen F., Dixon R. A. (2007). Lignin modification improves fermentable sugar yields for biofuel production. Nat. Biotechnol. 25(7):759-761.

Chen X., Burger C., Fang D., Ruan D., Zhang L., Hsiao B., Chu B. (2006). X-ray studies of regenerated cellulose fibers wet spun from cotton linter pulp in NaOH/thiourea aqueous solutions. Polymer 47(8):2839-2848.

Chen X., Burger C., Wan F., Zhang J., Rong L., Hsiao B., Chu B., Cai J., Zhang L. (2007). Structure study of cellulose fibers wet-spun from environmentally friendly NaOH/urea aqueous solutions. Biomacromolecules 8(6):1918-1926.

Christakopoulos P., Koullas D., Kekos D., Koukios E., Macris B. (1991). Direct conversion of straw to ethanol by Fusarium oxysporum: effect of cellulose crystallinity. Enzyme Microb. Technol. 13(3):272-274.

Chu B., Hsiao B. (2001). Small-angle x-ray scattering of polymers. Chem. Rev. 101(6):1727-1762.

Chu B., Wang Z. (1988). An extended universal coexistence curve for polymer solutions. Macromolecules 21(7):2283-2286.

Chum H., Johnson D., Black S., Overend R. (1990). Pretreatment-catalyst effects and the combined severity parameter. Appl. Biochem. Biotechnol. 24(1):1-14.

Clerget B., Dingkuhn M., Goze E., Rattunde H., Ney B. (2008). Variability of phyllochron, plastochron and rate of increase in height in photoperiod-sensitive sorghum varieties. Annals of Botany 101(4):579-594.

Conway E., Downey M. (1950). An outer metabolic region of the yeast cell. Biochem. J. 47(3):347.

Crawshaw J., Bras W., Mant G., Cameron R. (2002). Simultaneous SAXS and WAXS investigations of changes in native cellulose fiber microstructure on swelling in aqueous sodium hydroxide. J. Appl. Polym. Sci. 83(6):1209-1218.

Curreli N., Fadda M., Rescigno A., Rinaldi A., Soddu G., Sollai F., Vaccargiu S., Sanjust E., Rinaldi A. (1997). Mild alkaline/oxidative pretreatment of wheat straw. Process Biochem. 32(8):665-670.

Davison B. H., Evans B. R., Finkelstein M., McMillan J. D., Laureano-Perez L., Teymouri F., Alizadeh H., Dale B. E. 2005. Understanding Factors that Limit Enzymatic Hydrolysis of Biomass. Twenty-Sixth Symposium on Biotechnology for Fuels and Chemicals: Humana Press. p 1081-1099.

Donohoe B., Decker S., Tucker M., Himmel M., Vinzant T. (2008). Visualizing lignin coalescence and migration through maize cell walls following thermochemical pretreatment. Biotechnol. Bioeng. 101(5):913-925.

Duguid K., Montross M., Radtke C., Crofcheck C., Wendt L., Shearer S. (2009). Effect of anatomical fractionation on the enzymatic hydrolysis of acid and alkaline pretreated corn stover. Bioresour. Technol. 100(21):5189-5195.

El Mansouri N., Salvadó J. (2007). Analytical methods for determining functional groups in various technical lignins. Industrial crops and products 26(2):116-124.

Esteghlalian A., Hashimoto A., Fenske J., Penner M. (1997). Modeling and optimization of the dilute-sulfuric-acid pretreatment of corn stover, poplar and switchgrass. Bioresour. Technol. 59(2-3):129-136.

Fan L., Lee Y., Beardmore D. (1980). Mechanism of the enzymatic hydrolysis of cellulose: effects of major structural features of cellulose on enzymatic hydrolysis. Biotechnol. Bioeng. 22(1):177-199.

Fargione J., Hill J., Tilman D., Polasky S., Hawthorne P. (2008). Land clearing and the biofuel carbon debt. Science 319(5867):1235.

Fernandez-Bolanos J., Felizon B., Heredia A., Rodrıguez R., Guillen R., Jiménez A. (2001). Steam-explosion of olive stones: hemicellulose solubilization and enhancement of enzymatic hydrolysis of cellulose. Bioresour. Technol. 79(1):53-61.

Focher B., Marzetti A., Sarto V., Beltrame P. L., Carniti P. (1984). Cellulosic materials: Structure and enzymatic hydrolysis relationships. J. Appl. Polym. Sci. 29(11):3329-3338.

Foster B., Dale B., Doran-Peterson J. (2001). Enzymatic hydrolysis of ammonia-treated sugar beet pulp. Appl. Biochem. Biotechnol. 91(1):269-282.

Gancy A. (1963). Thermal Decomposition of Sodium Sesquicarbonate. J. Chem. Eng. Data 8(3):301-306.

Gardner K., Blackwell J. (1974). The structure of native cellulose. Biopolymers 13(10):1975-2001.

Garrote G., Dominguez H., Parajó J. C. (2001). Manufacture of xylose-based fermentation media from corncobs by posthydrolysis of autohydrolysis liquors. Appl. Biochem. Biotechnol. 95(3):195-207.

Gassan J., Bledzki A. (1999). Alkali treatment of jute fibers: Relationship between structure and mechanical properties. J. Appl. Polym. Sci. 71(4):623-629.

Gharpuray M. M., Lee Y.-H., Fan L. T. (1983). Structural modification of lignocellulosics by pretreatments to enhance enzymatic hydrolysis. Biotechnol. Bioeng. 25(1):157-172.

Giddings T., Brower D., Staehelin L. (1980). Visualization of particle complexes in the plasma membrane of Micrasterias denticulata associated with the formation of cellulose fibrils in primary and secondary cell walls. The Journal of cell biology 84(2):327.

Gollapalli L., Dale B., Rivers D. (2002). Predicting digestibility of ammonia fiber explosion (AFEX)-treated rice straw. Appl. Biochem. Biotechnol. 98(1/3):23-36.

Goppel J. (1949). On the degree of crystallinity in natural rubber I. Appl. Sci. Res. 1(1):3-17.

Graham R., Nelson R., Sheehan J., Perlack R., Wright L. (2007). Current and potential US corn stover supplies. Agron. J. 99(1):1.

Grethlein H. E. (1985). The effect of pore size distribution on the rate of enzymatic hydrolysis of cellulosic substrates. Nat Biotech 3(2):155-160.

Grigoriew H., Chmielewski A., Amenitsch H. (2001). Structural temperature transformation of the cellulose-water system using time-resolved SAXS. Polymer 42(1):103-108.

Grous W., Converse A., Grethlein H. (1986). Effect of steam explosion pretreatment on pore size and enzymatic hydrolysis of poplar. Enzyme Microb. Technol. 8(5):274-280.

Gupta B., Revagade N., Hilborn J. (2007). Poly (lactic acid) fiber: An overview. Prog. Polym. Sci. 32(4):455-482.

Gurarie V. N., Otsuka P. H., Jamieson D. N., Williams J. S., Conway M. (2002). The effect of crystal orientation on thermal shock-induced fracture and properties of ion implanted sapphire. Nuclear Instruments and Methods in Physics Research Section B: Beam Interactions with Materials and Atoms 190(1-4):751-755.

Haigler C. H. 1985. The functions and biogenesis of native cellulose. In: Nevell T, Zeronian S, editors. Cellulose chemistry and its applications. Chichester: Ellis Horwood Ltd. p 30-83.

Haw J., Maciel G., Biermann C. (1984). Carbon-13 Nuclear Magnetic Resonance Study of the Rapid Steam Hydrolysis of Read Oak. Holzforschung-International Journal of the Biology, Chemistry, Physics and Technology of Wood 38(6):327-331.

Heiner A., Teleman O. (1997). Interface between monoclinic crystalline cellulose and water: Breakdown of the odd/even duplicity. Langmuir 13(3):511-518.

Hermans P., Vermaas D., Weidinger A. (1950). Recrystallization of regenerated cellulose upon mercerization. Nature 165:238.

Hernandez-Blanco C., Feng D., Hu J., Sanchez-Vallet A., Deslandes L., Llorente F., Berrocal-Lobo M., Keller H., Barlet X., Sanchez-Rodriguez C. (2007). Impairment of cellulose synthases required for Arabidopsis secondary cell wall formation enhances disease resistance. The Plant Cell Online 19(3):890.

Hidaka H., Takizawa T., Fujikawa H., Ohneda T., Fukuzumi T. (1984). A study on the inhibition of cellulolytic activities by lignin. Appl. Biochem. Biotechnol. 9(4):367-367.

Ho N., Chen Z., Brainard A. (1998). Genetically engineered Saccharomyces yeast capable of effective cofermentation of glucose and xylose. Appl. Environ. Microbiol. 64(5):1852.

Hu Z., Wen Z. (2008). Enhancing enzymatic digestibility of switchgrass by microwave-assisted alkali pretreatment. Biochem. Eng. J. 38(3):369-378.

Hult E., Iversen T., Sugiyama J. (2003). Characterization of the supermolecular structure of cellulose in wood pulp fibres. Cellulose 10(2):103-110.

Ibbett R., Domvoglou D., Phillips D. A. S. (2008). The hydrolysis and recrystallisation of lyocell and comparative cellulosic fibres in solutions of mineral acid. Cellulose 15(2):241-254.

Inlow D., McRae J., Ben-Bassat A. (1988). Fermentation of corn starch to ethanol with genetically engineered yeast. Biotechnol. Bioeng. 32(2):227-234.

Ivan Krakovský M. (1997). Elastic and swelling behavior of 2-hydroxyethyl methacrylate, diethylene glycol methacrylate, and methacrylic acid copolymers. J. Appl. Polym. Sci. 64(11):2141-2148.

Jakob H., Fengel D., Tschegg S., Fratzl P. (1995). The elementary cellulose fibril in Picea abies: comparison of transmission electron microscopy, small-angle X-ray scattering, and wide-angle X-ray scattering results. Macromolecules 28(26):8782-8787.

Jakob H., Fratzl P., Tschegg S. (1994). Size and arrangement of elementary cellulose fibrils in wood cells: A small-angle X-ray scattering study of Picea abies. Journal of Structural Biology 113(1):13-22.

Jiang G., Huang W., Li L., Wang X., Pang F., Zhang Y., Wang H. (2011). Structure and properties of regenerated cellulose fibers from different technology processes. Carbohydr. Polym. doi:10.1016/j.carbpol.2011.10.022.

Johansson M., Samuelson O. (1975). End-wise degradation of hydrocellulose during hot alkali treatment. J. Appl. Polym. Sci. 19(11):3007-3013.

Jungnikl K., Paris O., Fratzl P., Burgert I. (2008). The implication of chemical extraction treatments on the cell wall nanostructure of softwood. Cellulose 15(3):407-418.

Karimi K., Kheradmandinia S., Taherzadeh M. (2006). Conversion of rice straw to sugars by dilute-acid hydrolysis. Biomass Bioenergy 30(3):247-253.

Kim K. H., Hong J. (2001). Supercritical CO2 pretreatment of lignocellulose enhances enzymatic cellulose hydrolysis. Bioresour. Technol. 77(2):139-144.

Kim S., Holtzapple M. (2006). Effect of structural features on enzyme digestibility of corn stover. Bioresour. Technol. 97(4):583-591.

Kim T., Kim J., Sunwoo C., Lee Y. (2003). Pretreatment of corn stover by aqueous ammonia. Bioresour. Technol. 90(1):39-47.

Klinke H., Thomsen A., Ahring B. (2004). Inhibition of ethanol-producing yeast and bacteria by degradation products produced during pre-treatment of biomass. Appl. Microbiol. Biotechnol. 66(1):10-26.

Koberstein J., Morra B., Stein R. (1980). The determination of diffuse-boundary thicknesses of polymers by small-angle X-ray scattering. J. Appl. Crystallogr. 13(1):34-45.

Kolpak F., Blackwell J. (1976). Determination of the structure of cellulose II. Macromolecules 9(2):273-278.

Kong F., Engler C., Soltes E. (1992). Effects of cell-wall acetate, xylan backbone, and lignin on enzymatic hydrolysis of aspen wood. Appl. Biochem. Biotechnol. 34(1):23-35.

Konnerth J., Gierlinger N., Keckes J., Gindl W. (2009). Actual versus apparent within cell wall variability of nanoindentation results from wood cell walls related to cellulose microfibril angle. Journal of Materials science 44(16):4399-4406.

Kraessig H. 1993. Cellulose: structure, accessibility, and reactivity: CRC.

Krimm S., Tobolsky A. (1951). Quantitative X-Ray Studies of Order in Amorphous and Crystalline Polymers: Scattering from Various Polymers and a Study of the Glass Transition in Polystyrene and Polymethyl Methacrylate. Textile Research Journal 21(11):805.

Kroon-Batenburg L., Bouma B., Kroon J. (1996). Stability of cellulose structures studied by MD simulations. Could mercerized cellulose II Be parallel? Macromolecules 29(17):5695-5699.

Kumar P., Barrett D., Delwiche M., Stroeve P. (2009a). Methods for pretreatment of lignocellulosic biomass for efficient hydrolysis and biofuel production. Industrial & Engineering Chemistry 48(8):3713-3729.

Kumar R., Mago G., Balan V., Wyman C. (2009b). Physical and chemical characterizations of corn stover and poplar solids resulting from leading pretreatment technologies. Bioresour. Technol. 100(17):3948-3962.

Kumar R., Mago G., Balan V., Wyman C. E. (2009c). Physical and chemical characterizations of corn stover and poplar solids resulting from leading pretreatment technologies. Bioresour. Technol. 100(17):3948-3962.

Kumar S., Gupta R. B. (2009). Biocrude Production from Switchgrass Using Subcritical Water. Energy & Fuels 23(10):5151-5159.

Langford J., Wilson A. (1978). Scherrer after sixty years: a survey and some new results in the determination of crystallite size. J. Appl. Crystallogr. 11(2):102-113.

Larsson S., Cassland P., Jonsson L. (2001). Development of a Saccharomyces cerevisiae strain with enhanced resistance to phenolic fermentation inhibitors in lignocellulose hydrolysates by heterologous expression of laccase. Appl. Environ. Microbiol. 67(3):1163.

Lau M. W., Gunawan C., Balan V., Dale B. E. (2010). Comparing the fermentation performance of Escherichia coli KO11, Saccharomyces cerevisiae 424A (LNH-ST) and Zymomonas mobilis AX101 for cellulosic ethanol production. Biotechnology for biofuels 3(1):11.

Lee J. (1997). Biological conversion of lignocellulosic biomass to ethanol. J. Biotechnol. 56(1):1-24.

Lee J., Jameel H., Venditti R. (2010). A comparison of the autohydrolysis and ammonia fiber explosion (AFEX) pretreatments on the subsequent enzymatic hydrolysis of coastal Bermuda grass. Bioresour. Technol. 101(14):5449-5458.

Li C., Cheng G., Balan V., Kent M. S., Ong M., Chundawat S. P. S., daCosta Sousa L., Melnichenko Y. B., Dale B. E., Simmons B. A. (2011). Influence of Physico-Chemical Changes on Enzymatic Digestibility of Ionic Liquid and AFEX pretreated Corn Stover. Bioresour. Technol. 102(13):6928-6936.

Li C., Knierim B., Manisseri C., Arora R., Scheller H. V., Auer M., Vogel K. P., Simmons B. A., Singh S. (2010). Comparison of dilute acid and ionic liquid pretreatment of switchgrass: Biomass recalcitrance, delignification and enzymatic saccharification. Bioresour. Technol. 101(13):4900-4906.

Liang C., Marchessault R. (1959). Infrared spectra of crystalline polysaccharides. I. Hydrogen bonds in native celluloses. Journal of Polymer Science 37(132):385-395.

Lichtenegger H., Reiterer A., Stanzl-Tschegg S., Fratzl P. (1999). Variation of cellulose microfibril angles in softwoods and hardwoods--a possible strategy of mechanical optimization. Journal of Structural Biology 128(3):257-269.

Lin Y., Tanaka S. (2006). Ethanol fermentation from biomass resources: current state and prospects. Appl. Microbiol. Biotechnol. 69(6):627-642.

Liu Q., El Abedin S. Z., Endres F. (2006). Electroplating of mild steel by aluminium in a first generation ionic liquid: A green alternative to commercial Al-plating in organic solvents. Surf. Coat. Technol. 201(3-4):1352-1356.

Liu R., Yu H., Huang Y. (2005). Structure and morphology of cellulose in wheat straw. Cellulose 12(1):25-34.

Liu Z., Slininger P., Dien B., Berhow M., Kurtzman C., Gorsich S. (2004). Adaptive response of yeasts to furfural and 5-hydroxymethylfurfural and new chemical evidence for HMF conversion to 2, 5-bis-hydroxymethylfuran. J. Ind. Microbiol. Biotechnol. 31(8):345-352.

Lloyd T., Wyman C. (2005). Combined sugar yields for dilute sulfuric acid pretreatment of corn stover followed by enzymatic hydrolysis of the remaining solids. Bioresour. Technol. 96(18):1967-1977.

Ma H., Liu W., Chen X., Wu Y., Yu Z. (2009). Enhanced enzymatic saccharification of rice straw by microwave pretreatment. Bioresour. Technol. 100(3):1279-1284.

Maiorella B., Blanch H. W., Wilke C. R. (1983). By-product inhibition effects on ethanolic fermentation by <I>Saccharomyces cerevisiae</I>. Biotechnol. Bioeng. 25(1):103-121.

Maki-Arvela P., Anugwom I., Virtanen P., Sjoholm R., Mikkola J. (2010). Dissolution of lignocellulosic materials and its constituents using ionic liquids--A review. Ind. Crop Prod. 32(3):175-201.

Mansfield S., Mooney C., Saddler J. (1999a). Substrate and enzyme characteristics that limit cellulose hydrolysis. Biotechnology Progress 15(5):804-816.

Mansfield S. D., Mooney C., Saddler J. N. (1999b). Substrate and enzyme characteristics that limit cellulose hydrolysis. Biotechnol. Progr. 15(5):804-816.

Marchisio D. (2009). On the use of bi-variate population balance equations for modelling barium titanate nanoparticle precipitation. Chem. Eng. Sci. 64(4):697-708.

McCollum III T., McCuistion K., Bean B., Genotypes B. Brown Midrib and photoperiod-sensitive forage sorghums; 2005. p 36-46.

McCusker L., Von Dreele R., Cox D., Louer D., Scardi P. (1999). Rietveld refinement guidelines. J. Appl. Crystallogr. 32(1):36-50.

McMillan J. 1994. Pretreatment of lignocellulosic biomass. In: Michael E. Himmel JOB, Ralph P. Overend, editor. Enzymatic Conversion of Biomass for Fuels Production. Washington: ACS Publications. p 292-324.

Mielenz J. (2001). Ethanol production from biomass: technology and commercialization status. Current Opinion in Microbiology 4(3):324-329.

Monro J., Penny D., Bailey R. (1976). The organization and growth of primary cell walls of lupin hypocotyl. Phytochemistry 15(8):1193-1198.

Mosier N., Hendrickson R., Ho N., Sedlak M., Ladisch M. (2005a). Optimization of pH controlled liquid hot water pretreatment of corn stover. Bioresour. Technol. 96(18):1986-1993.

Mosier N., Ladisch C., Ladisch M. (2002). Characterization of acid catalytic domains for cellulose hydrolysis and glucose degradation. Biotechnol. Bioeng. 79(6):610-618.

Mosier N., Wyman C., Dale B., Elander R., Lee Y., Holtzapple M., Ladisch M. (2005b). Features of promising technologies for pretreatment of lignocellulosic biomass. Bioresour. Technol. 96(6):673-686.

Nishida M., Uraki Y., Sano Y. (2003). Lignin gel with unique swelling property. Bioresource technology 88(1):81-83.

Nishiyama Y., Kim U. J., Kim D. Y., Katsumata K. S., Roland P., Langan P. (2003). Periodic disorder along ramie cellulose microfibrils. Biomacromolecules 4(4):1013-1017.

Nishiyama Y., Langan P., Chanzy H. (2002). Crystal structure and hydrogen-bonding system in cellulose Iβ from synchrotron X-ray and neutron fiber diffraction. JACS 124(31):9074-9082.

Oh S., Yoo D., Shin Y., Kim H., Kim H., Chung Y., Park W., Youk J. (2005). Crystalline structure analysis of cellulose treated with sodium hydroxide and carbon dioxide by means of X-ray diffraction and FTIR spectroscopy. Carbohydr. Res. 340(15):2376-2391.

Öhgren K., Vehmaanperä J., Siika-Aho M., Galbe M., Viikari L., Zacchi G. (2007). High temperature enzymatic prehydrolysis prior to simultaneous saccharification and fermentation of steam pretreated corn stover for ethanol production. Enzyme Microb. Technol. 40(4):607-613.

Paakkari T., Serimaa R. (1984). A study of the structure of wood cells by X-ray diffraction. Wood Science and Technology 18(2):79-85.

Palmqvist E., Hahn-Hägerdal B., Galbe M., Zacchi G. (1996). The effect of water-soluble inhibitors from steam-pretreated willow on enzymatic hydrolysis and ethanol fermentation. Enzyme Microb. Technol. 19(6):470-476.

Park S., Baker J., Himmel M., Parilla P., Johnson D. (2010). Cellulose crystallinity index: measurement techniques and their impact on interpreting cellulase performance. Biotechnology for Biofuels 3(1):10.

Pasha C., Reddy G. (2005). Nutritional and medicinal improvement of black tea by yeast fermentation. Food Chem. 89(3):449-453.

Pavlostathis S., Gossett J. (1985). Alkaline treatment of wheat straw for increasing anaerobic biodegradability. Biotechnol. Bioeng. 27(3):334-344.

Perret R., Ruland W. (1969). Single and multiple x-ray small-angle scattering of carbon fibres. J. Appl. Crystallogr. 2(5):209-218.

Pingali S. V., Urban V. S., Heller W. T., McGaughey J., O'Neill H. M., Foston M., Myles D. A., Ragauskas A. J., Evans B. R. (2010a). SANS study of cellulose extracted from switchgrass. Acta Crystallogr., Sect D: Biol. Crystallogr. 66(11):1189-1193.

Pingali S. V., Urban V. S., Heller W. T., McGaughey J., O'Neill H., Foston M., Myles D. A., Ragauskas A., Evans B. R. (2010b). Breakdown of cell wall nanostructure in dilute acid pretreated biomass. Biomacromolecules 11(9):2329-2335.

Puri V. P. (1984). Effect of crystallinity and degree of polymerization of cellulose on enzymatic saccharification. Biotechnol. Bioeng. 26(10):1219-1222.

Puri V. P., Pearce G. R. (1986). Alkali-explosion pretreatment of straw and bagasse for enzymic hydrolysis. Biotechnol. Bioeng. 28(4):480-485.

Rai K., Murty D., Andrews D., Bramel-Cox P. (1999). Genetic enhancement of pearl millet and sorghum for the semi-arid tropics of Asia and Africa. Genome 42(4):617-628.

Ramos L., Nazhad M., Saddler J. (1993). Effect of enzymatic hydrolysis on the morphology and fine structure of pretreated cellulosic residues. Enzyme Microb. Technol. 15(10):821-831.

Ran S., Fang D., Zong X., Hsiao B., Chu B., Cunniff P. (2001). Structural changes during deformation of Kevlar fibers via on-line synchrotron SAXS/WAXD techniques. Polymer 42(4):1601-1612.

Ran S., Wang Z., Burger C., Chu B., Hsiao B. (2002). Mesophase as the precursor for strain-induced crystallization in amorphous poly (ethylene terephthalate) film. Macromolecules 35(27):10102-10107.

Rastogi N., Rashmi K. (1999). Optimisation of enzymatic liquefaction of mango pulp by response surface methodology. Eur. Food Res. Technol. 209(1):57-62.

Ray P., Green P., Cleland R. (1972). Role of turgor in plant growth. Nature 239:163-164.

Reddy N., Yang Y. (2005). Structure and properties of high quality natural cellulose fibers from cornstalks. Polymer 46(15):5494-5500.

Reiterer A., Jakob H., Stanzl-Tschegg S., Fratzl P. (1998). Spiral angle of elementary cellulose fibrils in cell walls ofPicea abies determined by small-angle x-ray scattering. Wood Science and Technology 32(5):335-345.

Rietveld H. (1967). Line profiles of neutron powder-diffraction peaks for structure refinement. Acta Crystallographica 22(1):151-152.

Rondeau-Mouro C., Bouchet B., Pontoire B., Robert P., Mazoyer J., Buléon A. (2003). Structural features and potential texturising properties of lemon and maize cellulose microfibrils. Carbohydr. Polym. 53(3):241-252.

Rosenow D., Quisenberry J., Wendt C., Clark L. (1983). Drought tolerant sorghum and cotton germplasm. Agricultural Water Management 7(1-3):207-222.

Roy C., Budtova T., Navard P. (2003). Rheological properties and gelation of aqueous cellulose-NaOH solutions. Biomacromolecules 4(2):259-264.

Rubin E. (2008). Genomics of cellulosic biofuels. Nature 454(7206):841-845.

Ruland W. (1961). X-ray determination of crystallinity and diffuse disorder scattering. Acta Crystallographica 14(11):1180-1185.

Ruland W. (1969). Small-angle scattering studies on carbonized cellulose fibers. Journal of Polymer Science Part C: Polymer Symposia 28(1):143-151.

Saha B., Bothast R. (1999). Pretreatment and enzymatic saccharification of corn fiber. Appl. Biochem. Biotechnol. 76(2):65-77.

Saha B., Iten L., Cotta M., Wu Y. (2005a). Dilute acid pretreatment, enzymatic saccharification and fermentation of wheat straw to ethanol. Process Biochem. 40(12):3693-3700.

Saha B. C., Iten L. B., Cotta M. A., Wu Y. V. (2005b). Dilute acid pretreatment, enzymatic saccharification and fermentation of wheat straw to ethanol. Process Biochem. 40(12):3693-3700.

Sassner P., Mårtensson C. G., Galbe M., Zacchi G. (2008). Steam pretreatment of H2SO4-impregnated Salix for the production of bioethanol. Bioresour. Technol. 99(1):137-145.

Schell D., Farmer J., Newman M., McMillan J. (2003). Dilute-sulfuric acid pretreatment of corn stover in pilot-scale reactor. Appl. Biochem. Biotechnol. 105(1):69-85.

Schmidt P. (1991). Small-angle scattering studies of disordered, porous and fractal systems. J. Appl. Crystallogr. 24(5):414-435.

Schultz T., Templeton M., McGinnis G. (1985). Rapid determination of lignocellulose by diffuse reflectance Fourier transform infrared spectrometry. Anal. Chem. 57(14):2867-2869.

Segal L., Creely J., Martin Jr A., Conrad C. (1959). An empirical method for estimating the degree of crystallinity of native cellulose using the X-ray diffractometer. Textile Research Journal 29(10):786.

Selig M. J., Viamajala S., Decker S. R., Tucker M. P., Himmel M. E., Vinzant T. B. (2007). Deposition of lignin droplets produced during dilute acid pretreatment of maize stems retards enzymatic hydrolysis of cellulose. Biotechnol. Progr. 23(6):1333-1339.

Shivakumara C., Bellakki M. (2009). Synthesis, structural and ferromagnetic properties of La 1-x K x MnO 3 (0· 0 x 0· 25) phases by solution combustion method. Bull. Mater. Sci. 32(4):443-449.

Silverstein R., Chen Y., Sharma-Shivappa R., Boyette M., Osborne J. (2007a). A comparison of chemical pretreatment methods for improving saccharification of cotton stalks. Bioresour. Technol. 98(16):3000-3011.

Silverstein R. A., Chen Y., Sharma-Shivappa R. R., Boyette M. D., Osborne J. (2007b). A comparison of chemical pretreatment methods for improving saccharification of cotton stalks. Bioresour. Technol. 98(16):3000-3011.

Sinitsyn A., Gusakov A., Vlasenko E. (1991). Effect of structural and physico-chemical features of cellulosic substrates on the efficiency of enzymatic hydrolysis. Appl. Biochem. Biotechnol. 30(1):43-59.

Sisson W. (1935). X-Ray Studies of Crystallite Orientation in Cellulose Fibers Natural Fibers. Industrial & Engineering Chemistry 27(1):51-56.

Sivakesava S., Irudayaraj J., Demirci A. (2001). Monitoring a bioprocess for ethanol production using FT-MIR and FT-Raman spectroscopy. J. Ind. Microbiol. Biotechnol. 26(4):185-190.

Sluiter A., Hames B., Ruiz R., Scarlata C., Sluiter J., Templeton D., Crocker D. (2004). Determination of structural carbohydrates and lignin in biomass. NREL, Golden, CO.

Somerville C., Bauer S., Brininstool G., Facette M., Hamann T., Milne J., Osborne E., Paredez A., Persson S., Raab T. (2004). Toward a systems approach to understanding plant cell walls. Science 306(5705):2206-2211.

Stephens P. (1999). Phenomenological model of anisotropic peak broadening in powder diffraction. J. Appl. Crystallogr. 32(2):281-289.

Sun F., Chen H. (2008). Enhanced enzymatic hydrolysis of wheat straw by aqueous glycerol pretreatment. Bioresour. Technol. 99(14):6156-6161.

Sun R., Tomkinson J., Ma P., Liang S. (2000). Comparative study of hemicelluloses from rice straw by alkali and hydrogen peroxide treatments. Carbohydr. Polym. 42(2):111-122.

Sun Y., Cheng J. (2002). Hydrolysis of lignocellulosic materials for ethanol production: a review. Bioresour. Technol. 83(1):1-11.

Suryawati L., Wilkins M., Bellmer D., Huhnke R., Maness N., Banat I. (2008). Simultaneous saccharification and fermentation of Kanlow switchgrass pretreated by hydrothermolysis using Kluyveromyces marxianus IMB 4. Biotechnol. Bioeng. 101(5):894-902.

Swatloski R. P., Spear S. K., Holbrey J. D., Rogers R. D. (2002). Dissolution of cellose with ionic liquids. JACS 124(18):4974-4975.

Tanahashi M., Takada S., Higuchi T., Hanai S. (1983). Characterization of Explosion Wood: 1. Structure and Physical Properties. Wood research 69:36-51.

Tang L. G., Hon D. N. S., Pan S. H., Zhu Y. Q., Wang Z., Wang Z. Z. (1996). Evaluation of microcrystalline cellulose. I. Changes in ultrastructural characteristics during preliminary acid hydrolysis. J. Appl. Polym. Sci. 59(3):483-488.

Teixeira L. (1999). Optimizing peracetic acid pretreatment conditions for improved simultaneous saccharification and co-fermentation (SSCF) of sugar cane bagasse to ethanol fuel. Renewable energy 16(1-4):1070-1073.

Teleman A., Larsson P., Iversen T. (2001). On the accessibility and structure of xylan in birch kraft pulp. Cellulose 8(3):209-215.

Theerarattananoon K., Wu X., Staggenborg S., Propheter J., Madl R., Wang D. (2010). Evaluation and Characterization of Sorghum Biomass as Feedstock for Sugar Production. Transactions of the ASABE 53(2):509-525.

Thompson D. N., Chen H.-C., Grethlein H. E. (1992). Comparison of pretreatment methods on the basis of available surface area. Bioresour. Technol. 39(2):155-163.

Tilman D., Hill J., Lehman C. (2006). Carbon-negative biofuels from low-input high-diversity grassland biomass. Science 314(5805):1598.

Tolbert N. (1980). Plant Cells.(Book Reviews: The Biochemistry of Plants). Science 210:1119.

Torget R., Walter P., Himmel M., Grohmann K. (1991). Dilute-acid pretreatment of corn residues and short-rotation woody crops. Appl. Biochem. Biotechnol. 28(1):75-86.

Vainio U., Maximova N., Hortling B., Laine J., Stenius P., Simola L., Gravitis J., Serimaa R. (2004). Morphology of dry lignins and size and shape of dissolved kraft lignin particles by x-ray scattering. Langmuir 20(22):9736-9744.

Vickers M., Briggs N., Ibbett R., Payne J., Smith S. (2001). Small angle X-ray scattering studies on lyocell cellulosic fibres: the effects of drying, re-wetting and changing coagulation temperature. Polymer 42(19):8241-8248.

Wadehra I., Manley R. (1965). Recrystallization of amorphous cellulose. J. Appl. Polym. Sci. 9(7):2627-2630.

Waigh T., Donald A., Heidelbach F., Riekel C., Gidley M. (1999). Analysis of the native structure of starch granules with small angle X-ray microfocus scattering. Biopolymers 49(1):91-105.

Wei C., Cheng C. (1985). Effect of hydrogen peroxide pretreatment on the structural features and the enzymatic hydrolysis of rice straw. Biotechnol. Bioeng. 27(10):1418-1426.

Weil J., Sarikaya A., Rau S., Goetz J., Ladisch C., Brewer M., Hendrickson R., Ladisch M. (1997). Pretreatment of yellow poplar sawdust by pressure cooking in water. Appl. Biochem. Biotechnol. 68(1):21-40.

Whetten R., MacKay J., Sederoff R. (1998). Recent advances in understanding lignin biosynthesis. Annual Review of Plant Biology 49(1):585-609.

Wright J., Wyman C., Grohmann K. (1988). Simultaneous saccharification and fermentation of lignocellulose. Appl. Biochem. Biotechnol. 18(1):75-90.

Wu H., Mora Pale M., Miao J., Doherty T. V., Linhardt R. J., Dordick J. S. (2011). Facile pretreatment of lignocellulosic biomass at high loadings in room temperature ionic liquids. Biotechnol. Bioeng. 108(12):2865-2875.

Wu X., Staggenborg S., Propheter J., Rooney W., Yu J., Wang D. (2010). Features of sweet sorghum juice and their performance in ethanol fermentation. Ind. Crop Prod. 31(1):164-170.

Wyman C. E. (2003). Potential Synergies and Challenges in Refining Cellulosic Biomass to Fuels, Chemicals, and Power. Biotechnol. Progr. 19(2):254-262.

Xiang Q., Lee Y., Torget R. (2004). Kinetics of glucose decomposition during dilute-acid hydrolysis of lignocellulosic biomass. Appl. Biochem. Biotechnol. 115(1):1127-1138.

Xu F., Shi Y.-C., Wang D. (2012). Structural features and changes of lignocellulosic biomass during thermochemical pretreatments: A synchrotron X-ray scattering study on photoperiod-sensitive sorghum. Carbohydr. Polym. 88(4):1149-1156.

Xu F., Shi Y.-C., Wu X., Theerarattananoon K., Staggenborg S., Wang D. (2011a). Sulfuric acid pretreatment and enzymatic hydrolysis of photoperiod sensitive sorghum for ethanol production. Bioprocess and Biosystems Engineering 34(4):485-492.

Xu F., Theerarattananoon K., Wu X., Pena L., Shi Y. C., Staggenborg S., Wang D. (2011b). Process optimization for ethanol production from photoperiod-sensitive sorghum: Focus on cellulose conversion. Ind. Crop Prod. 34(1):1212-1218.

Xu J., Cheng J., Sharma-Shivappa R., Burns J. (2010). Lime pretreatment of switchgrass at mild temperatures for ethanol production. Bioresour. Technol. 101(8):2900-2903.

Yazdani S., Gonzalez R. (2007). Anaerobic fermentation of glycerol: a path to economic viability for the biofuels industry. Curr. Opin. Biotechnol. 18(3):213-219.

Yu P., McKinnon J., Christensen C., Christensen D., Marinkovic N., Miller L. (2003). Chemical imaging of microstructures of plant tissues within cellular dimension using synchrotron infrared microspectroscopy. J. Agric. Food Chem 51(20):6062-6067.

Zeng M. (2007). Microscopic examination of changes of plant cell structure in corn stover due to hot water pretreatment and enzymatic hydrolysis. Biotechnol. Bioeng. 97(2):265.

Zeng M., Mosier N., Huang C., Sherman D., Ladisch M. (2007). Microscopic examination of changes of plant cell structure in corn stover due to hot water pretreatment and enzymatic hydrolysis. Biotechnol. Bioeng. 97(2):265-278.

Zhang Y., Ding S., Mielenz J., Cui J., Elander R., Laser M., Himmel M., McMillan J., Lynd L. (2007). Fractionating recalcitrant lignocellulose at modest reaction conditions. Biotechnol. Bioeng. 97(2):214-223.

Zhao H., Kwak J. H., Wang Y., Franz J. A., White J. M., Holladay J. E. (2006). Effects of crystallinity on dilute acid hydrolysis of cellulose by cellulose ball-milling study. Energy & fuels 20(2):807-811.

Zhao Y., Lu W., Wang H., Yang J. (2009). Fermentable hexose production from corn stalks and wheat straw with combined supercritical and subcritical hydrothermal technology. Bioresour. Technol. 100(23):5884-5889.

Zhao Y., Wang Y., Zhu J., Ragauskas A., Deng Y. (2008). Enhanced enzymatic hydrolysis of spruce by alkaline pretreatment at low temperature. Biotechnol. Bioeng. 99(6):1320-1328.

Zheng Y., Pan Z., Zhang R., Wang D., Jenkins B. (2008). Non-ionic Surfactants and Non-Catalytic Protein Treatment on Enzymatic Hydrolysis of Pretreated Creeping Wild Ryegrass. Appl. Biochem. Biotechnol. 146(1):231-248.

Zhu S., Wu Y., Chen Q., Yu Z., Wang C., Jin S., Ding Y., Wu G. (2006a). Dissolution of cellulose with ionic liquids and its application: a mini-review. Green Chem. 8(4):325-327.

Zhu S., Wu Y., Yu Z., Zhang X., Wang C., Yu F., Jin S. (2006b). Production of ethanol from microwave-assisted alkali pretreated wheat straw. Process Biochem. 41(4):869-873.

Zhu Y., Lee Y., Elander R. (2004). Dilute-acid pretreatment of corn stover using a high-solids percolation reactor. Appl. Biochem. Biotechnol. 117(2):103-114.

Zhu Z., Sathitsuksanoh N., Vinzant T., Schell D., McMillan J., Zhang Y. (2009). Comparative study of corn stover pretreated by dilute acid and cellulose solvent-based lignocellulose fractionation: Enzymatic hydrolysis, supramolecular structure, and substrate accessibility. Biotechnol. Bioeng. 103(4):715-724.